

Electronic structures and magnetic orders of iron- pnictides or chalcogenides

What have we learnt about iron-pnictides from electronic
structure calculations?

LU, Zhong-Yi
卢仲毅

Department of Physics
Renmin University of China
Beijing 100872, China
zlu@ruc.edu.cn

In collaboration with

Ma, Fengjie (马锋杰)

Yan, Xun-Wang (闫循旺)

Gao, Miao (高淼)

Renmin University of China

and Xiang, Tao (向涛)

Institute of Physics, CAS

Financial support by CNSF and MOST

量子力学与电子结构计算

- **电子与原子核是组成材料的基本粒子：原子、分子、凝聚态物质、以及人造结构；**
 - **电子**：1896-1897 Thomson、Zeeman, Nobel Prize (1902, 1906)
 - **玻尔的氢原子模型** 1913
 - **Stern-Gerlach 实验** -----**电子自旋** 1921, proposed by Compton
 - **量子力学**：de Broglie、Schrodinger, Heisenberg (1923-1925)
 - **Pauli不相容原理** 1925
 - **Fermi-Dirac统计** 1926
- **Pauli和Sommerfeld的金属自由电子气模型 (1926-1928)**
 - **遵守Fermi统计的费米气体**
 - **没有考虑原子核和晶体结构**
- **自由电子的能带理论**
 - **Bloch于1928提出Bloch定理**
 - **Move freely through the perfect lattice, resistance due to deviation from perfection**
 - **Prediction of semiconductors**

电子结构是凝聚态物理核心问题之一

- 什么是凝聚态物质
- 电子是“量子胶”-----把原子核粘织成原子、分子、固体、液体以及各种凝聚态物质
- 电子激发-----确定材料的电、光、磁性质
- 量子力学支配电子行为
- 多电子的相互作用

The many-body problem

- **Electronic terms:**

$$-\frac{\hbar^2}{2m_e} \sum_i \nabla_i^2 + \sum_{i,l} \frac{Z_l e^2}{|\mathbf{r}_i - \mathbf{R}_l|} + \frac{1}{2} \sum_{i \neq j} \frac{e^2}{|\mathbf{r}_i - \mathbf{r}_j|}$$

- **Nuclear terms:**

$$-\sum_l \frac{\hbar^2}{2M_l} \nabla_l^2 + \frac{1}{2} \sum_{l \neq j} \frac{e^2}{|\mathbf{R}_l - \mathbf{R}_j|}$$

- **Electrons are fast (small mass, 10^{-31} Kg) - nuclei are slow (heavy mass, 10^{-27} Kg) → natural separation of variables**
- **In the expression above we can ignore the kinetic energy of the nuclei, since it is a small term, given the inverse mass of the nuclei**
- **If we omit this term then the nuclei are just a fixed potential (sum of point charges potentials) acting on the electrons: this is called the**
Born-Oppenheimer approximation
- **The last terms remains to insure charge neutrality, but it is just a classical term (Ewald energy)**

Many-Body Schrödinger Equation

$$\hat{H}\Psi(\mathbf{r}_1, \mathbf{r}_2, \dots, \mathbf{r}_N) = E\Psi(\mathbf{r}_1, \mathbf{r}_2, \dots, \mathbf{r}_N)$$

$$\hat{H} = \hat{T} + \hat{V} + \hat{W}$$

$$\hat{V} = \sum_{j=1}^N v(\mathbf{r}_j)$$

$$\hat{T} = \sum_{j=1}^N -\frac{\hbar^2 \nabla_j^2}{2m}$$

$$\hat{W} = \frac{1}{2} \sum_{\substack{j,k=1 \\ j \neq k}}^N \frac{e^2}{|\mathbf{r}_j - \mathbf{r}_k|}$$

Hartree-Fock approach

Hartree product is

$$\Psi_{HP}(\mathbf{x}_1, \mathbf{x}_2, \dots, \mathbf{x}_N) = \chi_1(\mathbf{x}_1)\chi_2(\mathbf{x}_2)\cdots\chi_N(\mathbf{x}_N).$$

Problem: This wavefunction does *not* satisfy the antisymmetry principle!

Considering two-electron case with antisymmetry:

$$\Psi(\mathbf{x}_1, \mathbf{x}_2) = \frac{1}{\sqrt{2}} [\chi_1(\mathbf{x}_1)\chi_2(\mathbf{x}_2) - \chi_1(\mathbf{x}_2)\chi_2(\mathbf{x}_1)].$$

Namely, a Slater determinant

$$\Psi(\mathbf{x}_1, \mathbf{x}_2)$$

=

$$\frac{1}{\sqrt{2}} \begin{vmatrix} \chi_1(\mathbf{x}_1) & \chi_2(\mathbf{x}_1) \\ \chi_1(\mathbf{x}_2) & \chi_2(\mathbf{x}_2) \end{vmatrix}$$

Hartree-Fock approach

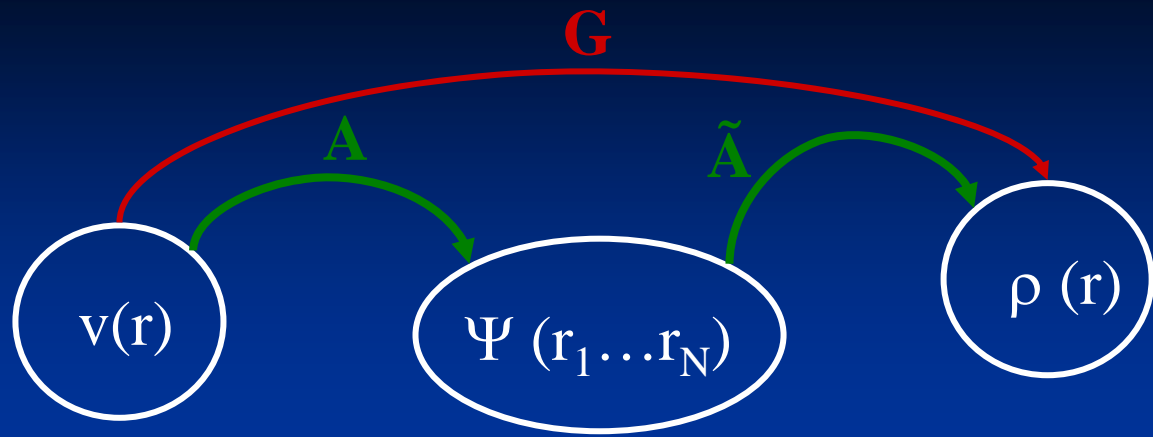
- The basic equations that define the Hartree-Fock method are obtained plugging the Slater determinant into the electronic Hamiltonian to derive a compact expression for its expectation value

$$\begin{aligned}
 \langle \Psi | \hat{H} | \Psi \rangle = & \sum_{i,s} \int d\mathbf{r} \psi_i^{s*}(\mathbf{r}) \left[-\frac{1}{2} \nabla^2 + V_{\text{ext}}(\mathbf{r}) \right] \psi_i^s(\mathbf{r}) \\
 & + \frac{1}{2} \sum_{i,j,s_i,s_j} \int d\mathbf{r} d\mathbf{r}' \psi_i^{s_i*}(\mathbf{r}) \psi_j^{s_j*}(\mathbf{r}') \frac{1}{|\mathbf{r} - \mathbf{r}'|} \psi_i^{s_i}(\mathbf{r}) \psi_j^{s_j}(\mathbf{r}') \quad J_{ij} \text{ Direct term} \\
 & - \sum_{i,j,s} \int d\mathbf{r} d\mathbf{r}' \psi_i^{s*}(\mathbf{r}) \psi_j^{s*}(\mathbf{r}') \frac{1}{|\mathbf{r} - \mathbf{r}'|} \psi_j^s(\mathbf{r}) \psi_i^s(\mathbf{r}') \quad K_{ij} \text{ Exchange term}
 \end{aligned}$$

- Direct term is essentially the classical Hartree energy (acts between electrons with different spin states ($i=j$ terms cancel out in the direct and exchange terms))
- Exchange term acts only between same spin electrons, and takes care of the energy that is involved in having electron pairs with parallel or anti-parallel spins together with the obedience of the Pauli exclusion principle

“Exchange” and “Correlation”

- Exchange term is a two-body interaction term: it takes care of the many-body interactions at the level of two single electrons;
- In this respect it includes also correlation effects at the two-body level: it neglects all correlations but the one required by the Pauli exclusion principle;
- Since the interaction always involve pairs of electrons, a two-body correlation term is often sufficient to determine many physical properties of the system;
- In general terms it measures the joint probability of finding electrons of spin s at point r and of spin s' at point r'
- Beyond the two-body treatment of Hartree-Fock, we introduce extra degrees of freedom in the wavefunctions whose net effect is the reduction of the total energy of any state;
- This additional energy is termed the “correlation” energy, E_c and is a key quantity for the solution of the electronic structure problem for an interacting many-body system.



single-particle potentials having nondegenerate ground state

ground-state wavefunction s

ground-state densities

Hohenberg-Kohn-Theorem (1964)

$G: v(\mathbf{r}) \rightarrow \rho(\mathbf{r})$ is invertible

Use Rayleigh-Ritz principle:

$$\begin{aligned} \blacktriangle \quad E &= \langle \Psi | \hat{H} | \Psi \rangle < \langle \Psi' | \hat{H} | \Psi' \rangle = \langle \Psi' | H' + V - V' | \Psi' \rangle \\ &= E' + \int d^3r \rho'(r) [v(r) - v'(r)] \end{aligned}$$

$$\begin{aligned} \star \quad E' &= \langle \Psi' | \hat{H}' | \Psi' \rangle < \langle \Psi | \hat{H}' | \Psi \rangle \\ &= E + \int d^3r \rho(r) [v'(r) - v(r)] \end{aligned}$$

Reductio ad absurdum:

Assumption $\rho = \rho'$. Add \blacktriangle and $\star \Rightarrow E + E' < E + E'$



Kohn-Sham Theorem (1965)

The ground state density of the interacting system of interest can be calculated as ground state density of non-interacting particles moving in an effective potential $v_s(\mathbf{r})$:

$$\left(-\frac{\hbar^2 \nabla^2}{2m} + v_s[\rho](\mathbf{r}) \right) \phi_i(\mathbf{r}) = \epsilon_i \phi_i(\mathbf{r})$$

$$\rho(\mathbf{r}) = \sum_{N \text{ lowest } \epsilon_j} |\phi_j(\mathbf{r})|^2$$

$$v_s[\rho](\mathbf{r}) = v_0(\mathbf{r}) + \int \frac{\rho(\mathbf{r}')}{|\mathbf{r}-\mathbf{r}'|} d^3r' + v_{xc}[\rho](\mathbf{r})$$

Coulomb potential of nuclei

Hartree potential

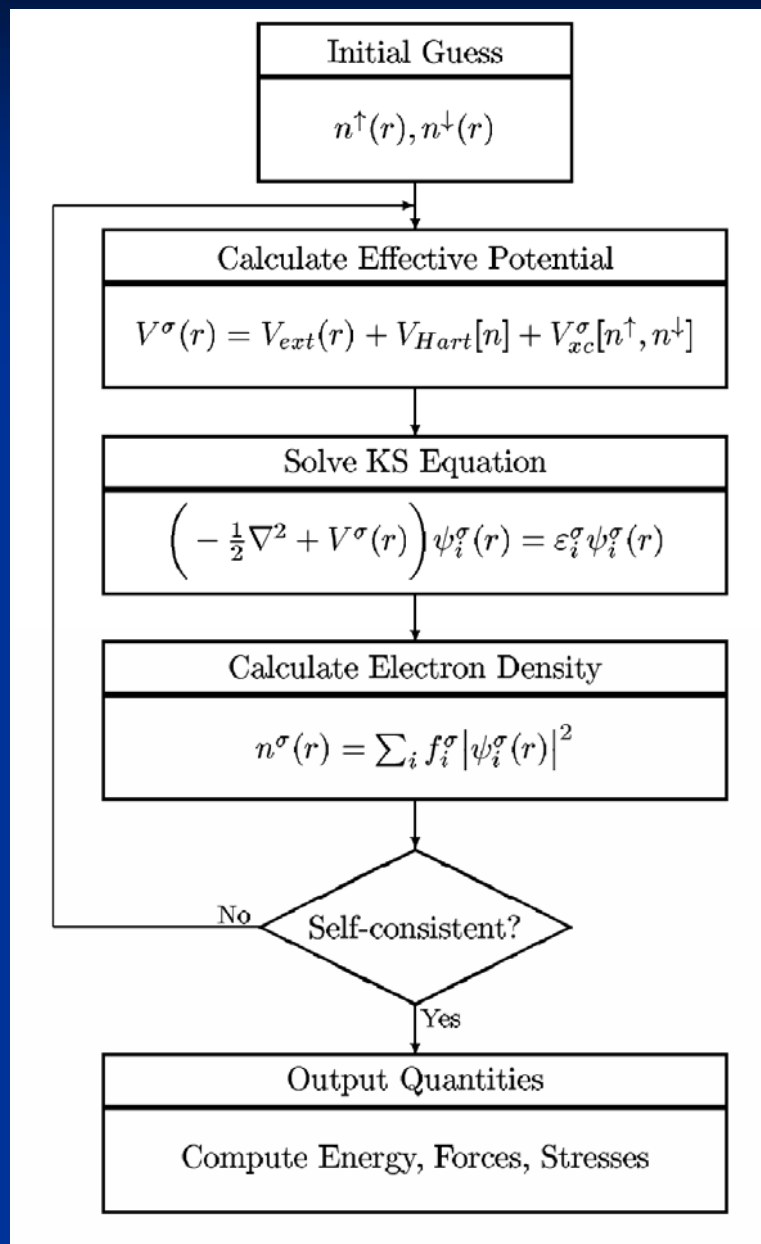
exchange-correlation potential

$$E_{xc}[\rho] = T[\rho] - T_S[\rho] + V_{ee}[\rho] - J[\rho]$$

$$v_{xc}(\mathbf{r}) = \frac{\delta E_{xc}[\rho]}{\delta \rho(\mathbf{r})}$$

universal

自洽求解流程图

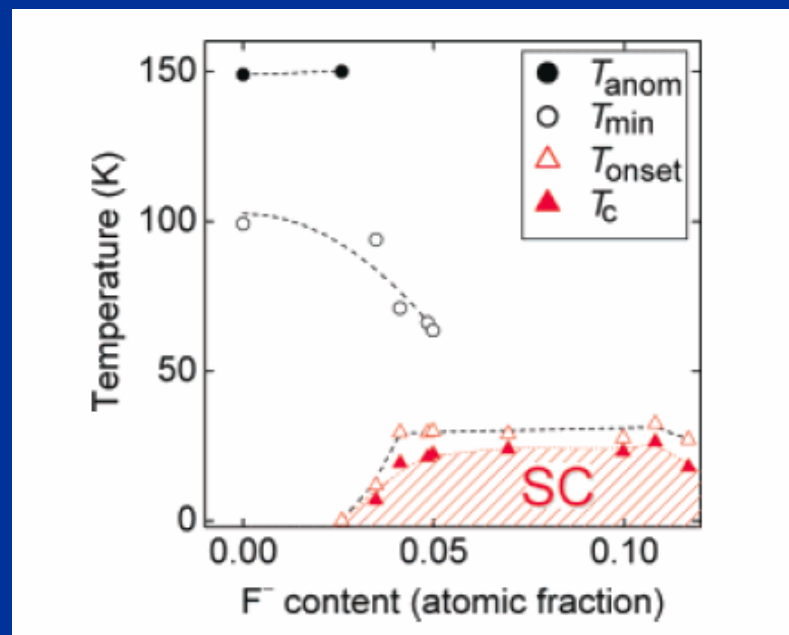
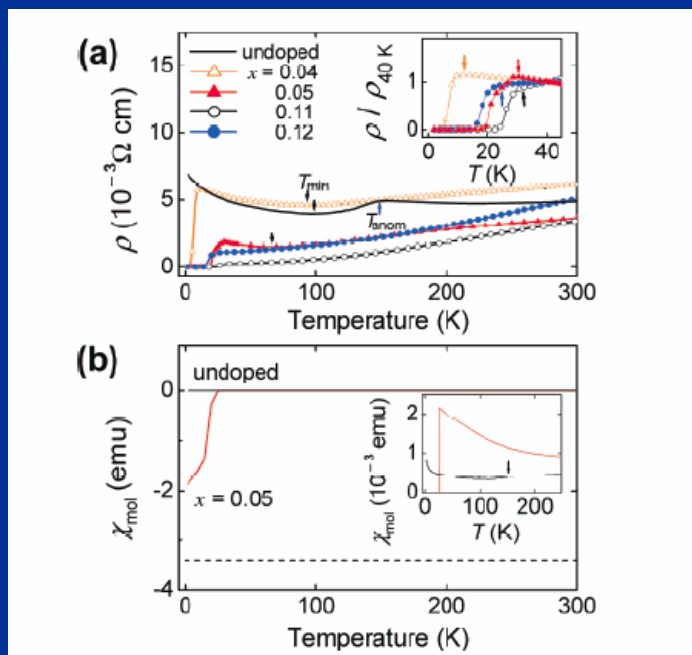


**Iron-Based Layered Superconductor La[O_{1-x}F_x]FeAs ($x = 0.05-0.12$)
with $T_c = 26$ K**

Yoichi Kamihara,^{*,†} Takumi Watanabe,[‡] Masahiro Hirano,^{†,§} and Hideo Hosono^{†,‡,§}

ERATO-SORST, JST, Frontier Research Center, Tokyo Institute of Technology, Mail Box S2-13, Materials and Structures Laboratory, Tokyo Institute of Technology, Mail Box R3-1, and Frontier Research Center, Tokyo Institute of Technology, Mail Box S2-13, 4259 Nagatsuta, Midori-ku, Yokohama 226-8503, Japan

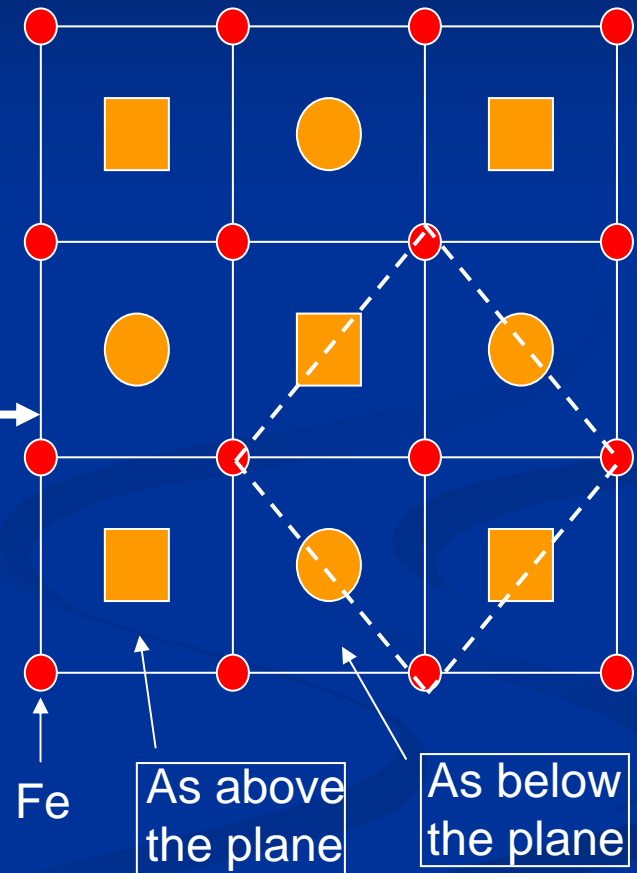
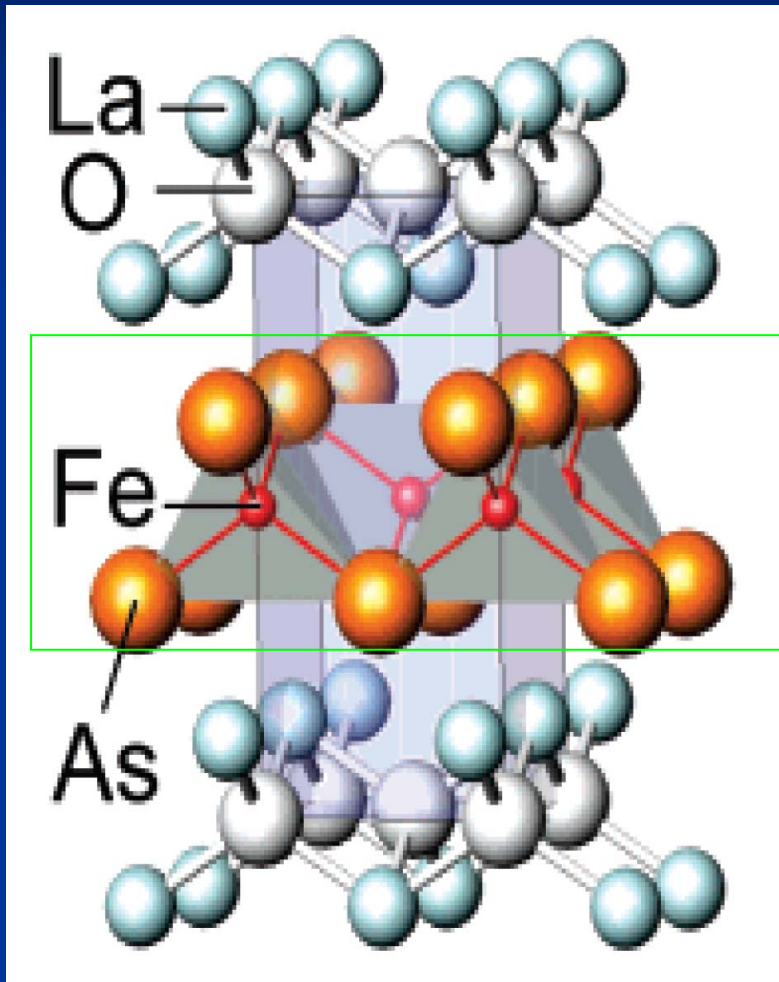
Received January 9, 2008; E-mail: hosono@msl.titech.ac.jp



Y. Kamihara et al., JACS, 130, 3296 (2008).

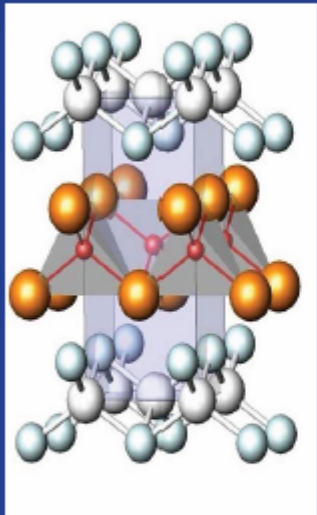
Looks like a not bad metal without magnetism

Structure of LaOFeAs

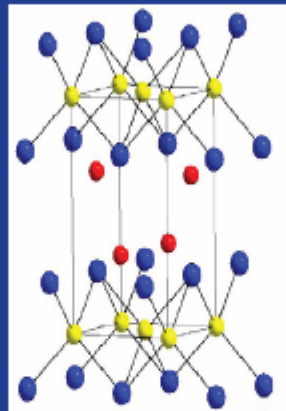


Experimental background

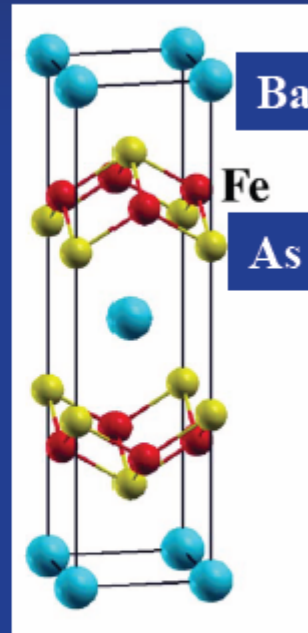
iron pnictide



1111
LaOFeAs
 $T_c \sim 55\text{K}$

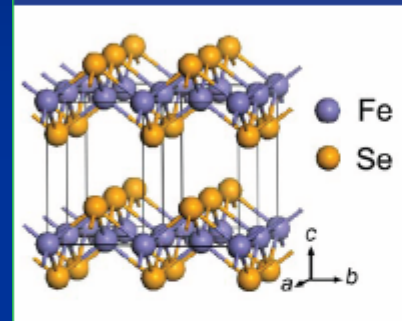


111
LiFeAs
 $T_c \sim 18\text{K}$



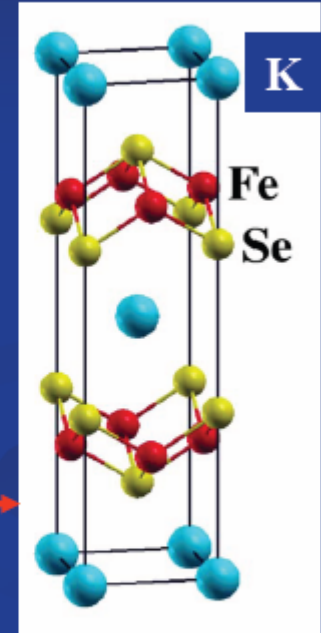
122
BaFe₂As₂
 $T_c \sim 38\text{K}$

iron chalcogenide



11
FeSe
 $T_c \sim 9\text{K}$

K intercalating →



122
KFe_{2-x}Se₂
 $T_c \sim 33\text{K}$

1. Y. Kamihara, T. Watanabe, M. Hirano, and H. Hosono, *J. Am. Chem. Soc.* **130**, 3296 (2008).
2. M. Rotter, M. Tegel, and D. Johrendt, *Phys. Rev. Lett.* **101**, 107006 (2008).
3. X. C. Wang, Q. Q. Liu, Y. X. Lv, W. B. Gao, L. X. Yang, R. C. Yu, F. Y. Li, and C. Q. Jin, *Solid State Commun.* **148**, 538 (2008).
4. F.-C. Hsu, J.-Y. Luo, K.-W. Yeh, T.-K. Chen, T.-W. Huang, P. M. Wu, Y.-C. Lee, Y.-L. Huang, Y.-Y. Chu, D.-C. Yan, and M.-

Questions to address in this talk

1. Origin of a local moment around Fe atom?

Answer: The Hund's rule coupling among the five Fe-3d orbitals.

2. The mechanism underlying magnetic structures?

Answer: As(Se, Te)-bridged superexchange antiferromagnetic interactions.

We are going to show that these two answers are universal to all the iron- pnictides or chalcogenides

Outline

- Electronic structures and Magnetism in iron-pnictides;
- Mechanism underlying magnetism and structural transition in iron-pnictides;
- Bi-collinear antiferromagnetic order in alpha-FeTe;
- Intercalated FeSe;
- Surface states of iron-pnictides;
- Conclusion.

1.

Electronic structures and Magnetism
in iron-pnictides?

Unlike in case of cuprates, the electronic structure calculations provide a substantial help and influence on study of iron-pnictides

- **Nonmagnetic band structure with ferromagnetic fluctuations; (Singh and Du, arXiv:0803.0429, PRL 100, 237003(2008))**
- **Possible SDW instability induced by Fermi surface nesting; (Mazin, Singh, Johannes, and Du, arXiv:0803.2740, PRL 101, 057003 (2008))**
- **Antiferromagnetic semimetal; (Ma and Lu, arXiv:0803.3286, PRB 78, 033111 (2008))**
- **Antiferromagnetic stripe-order due to the Fermi surface nesting. (Deng, et al., arXiv:0803.3426, EPL 83, 27006 (2008))**

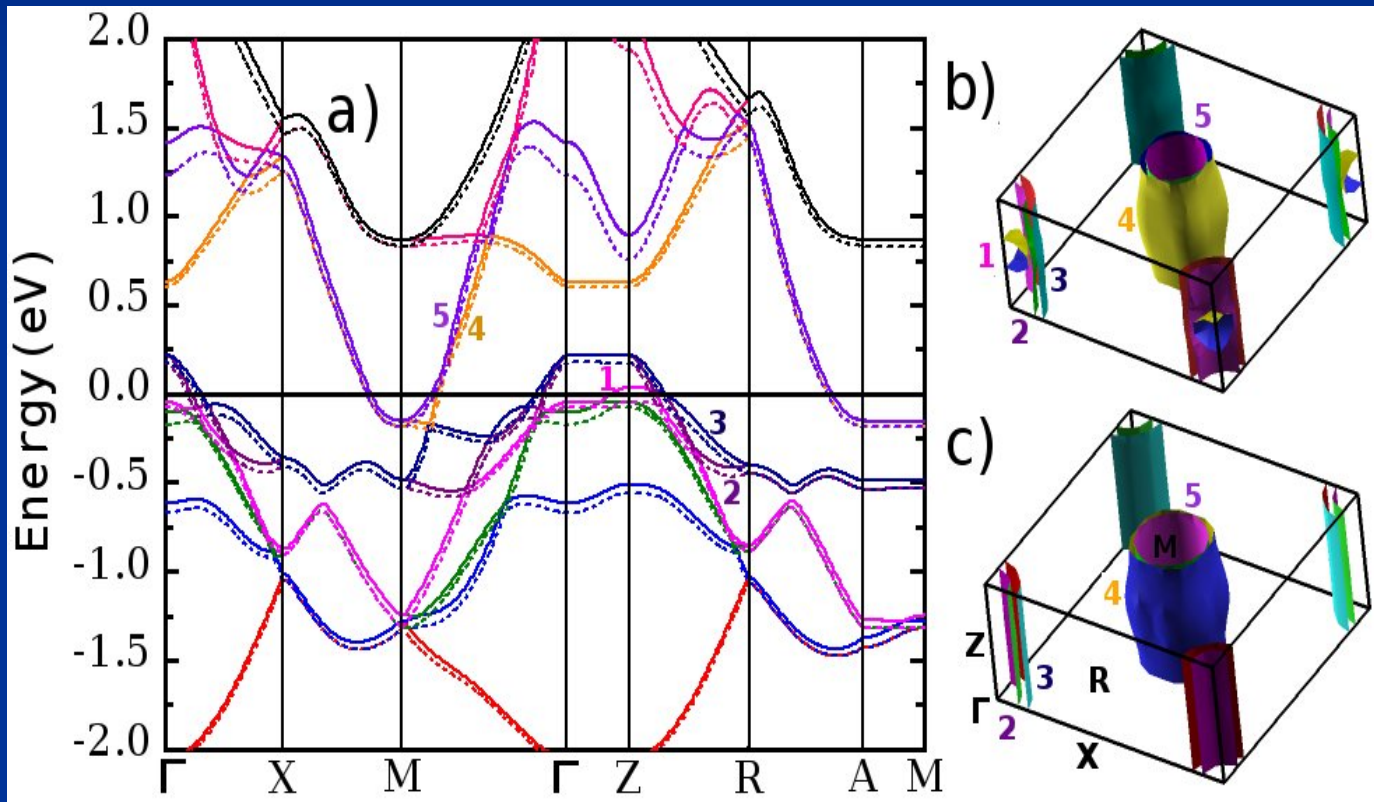
However, like cuprates, anything related to high T_c superconductivity eventually becomes complicated.

Iron-based layered compound LaFeAsO is an antiferromagnetic semimetal

Fengjie Ma¹ and Zhong-Yi Lu^{2,*}

¹Institute of Theoretical Physics, Chinese Academy of Sciences, Beijing 100080, People's Republic of China

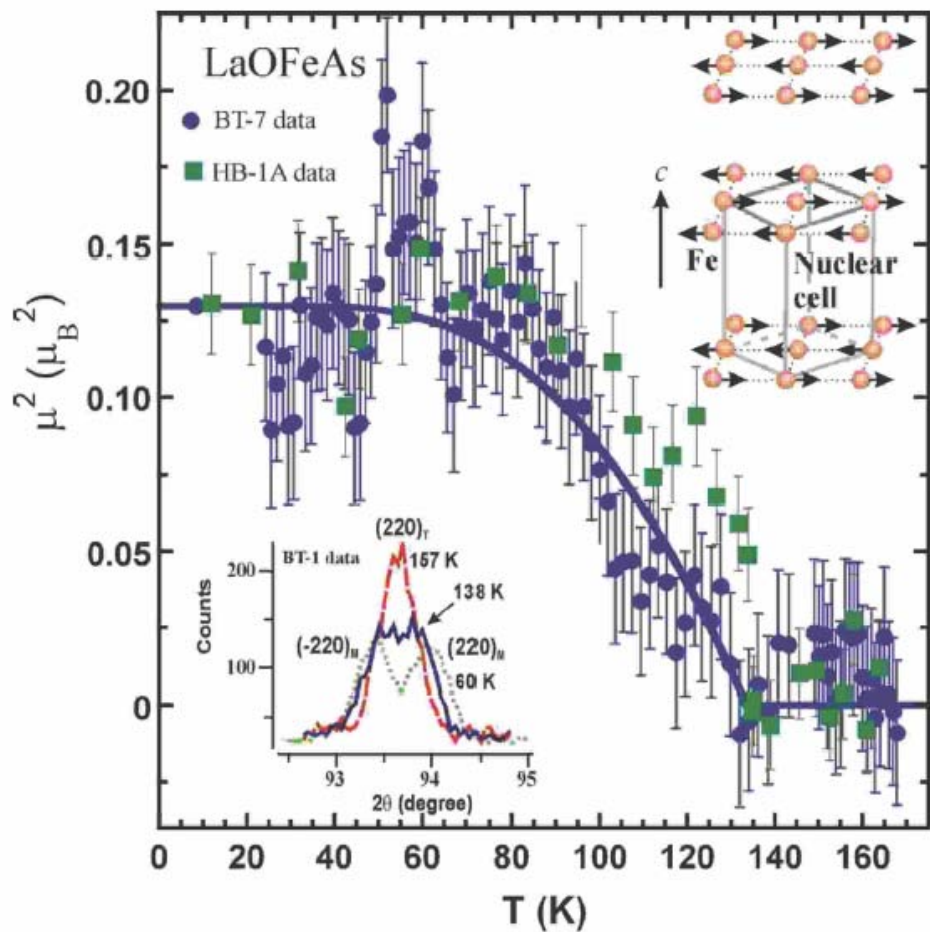
²Department of Physics, Renmin University of China, Beijing 100872, People's Republic of China



Carriers 0.28 electrons/cell
0.28 holes/cell

$9.97 \times 10^{21} / \text{cm}^3$ 出

Neutron scattering clarifies LaOFeAs is an antiferromagnetic semimetal with two transitions



About 150K, a structural transition from tetragonal to orthorhombic

About 135K, a collinear antiferromagnetic ordering observed with 0.38 Bohr moment

Fe-based Superconductors

- 1111 Series:

Electron doped:

$\text{CeO}_{1-x}\text{F}_x\text{FeAs}$: **41K** $\text{SmO}_{1-x}\text{F}_x\text{FeAs}$: **55K**

$\text{PrO}_{0.89}\text{F}_{0.11}\text{FeAs}$: **52K** SmFeAsO_{1-x} **55k**

CaFFeAs: 36K

Hole Doped: $\text{La}_{[1-x]}\text{Sr}_x\text{OFeAs}$

- 122 Series: (both Hole and Electron Doped)

BaFe_2As_2 , **38K**

- 11 Series:

FeSe , **8k - 37k (with pressure)**

- 111 Series: LiFeAs **16k**

- 42622: $\text{Sr}_4\text{V}_2\text{O}_6\text{Fe}_2\text{As}_2$ **37K**

Issues raised by the neutron observation

The microscopic origin of magnetic state in iron-based superconductors?

and its relation to tetragonal-orthorhombic structural transition?

two contradictive views upon these questions as follows

- (1) no local moments and the antiferromagnetic order is induced by the Fermi surface nesting.
Mazin, Singh, Johannes, and Du, arXiv:0803.2740, PRL 101, 057003 (2008)
- (2) (Se, Te, or As)-bridged superexchange antiferromagnetic interactions between the Fe-Fe fluctuating local moments.
arXiv:0804.3370, PRB 78, 224517 (2008); arXiv:0804.2252. PRL 101, 057010 (2008)

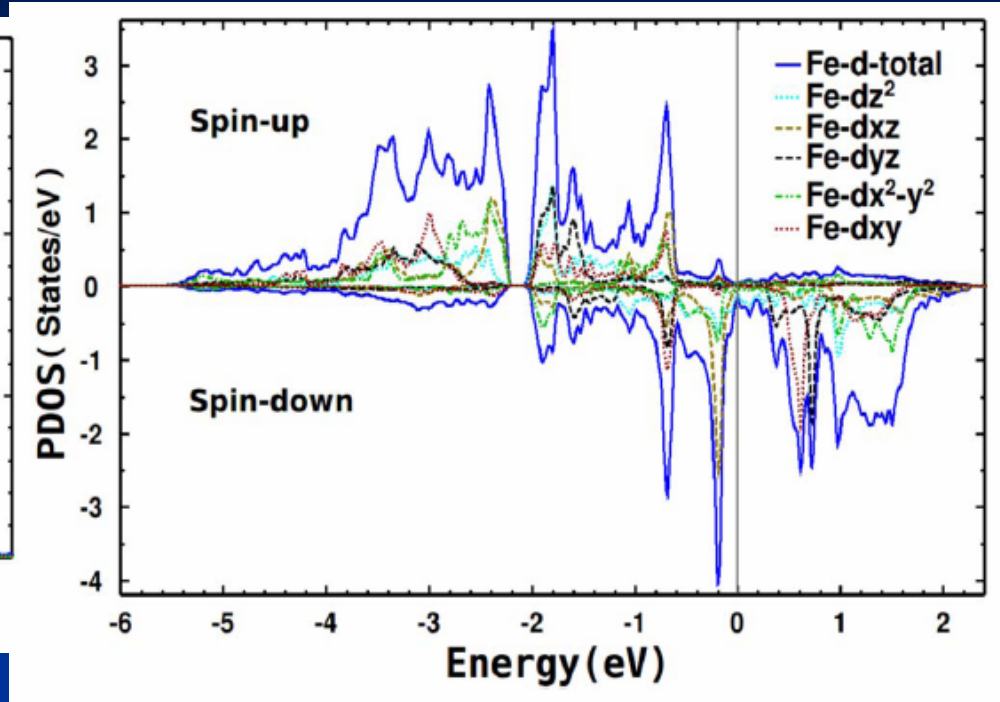
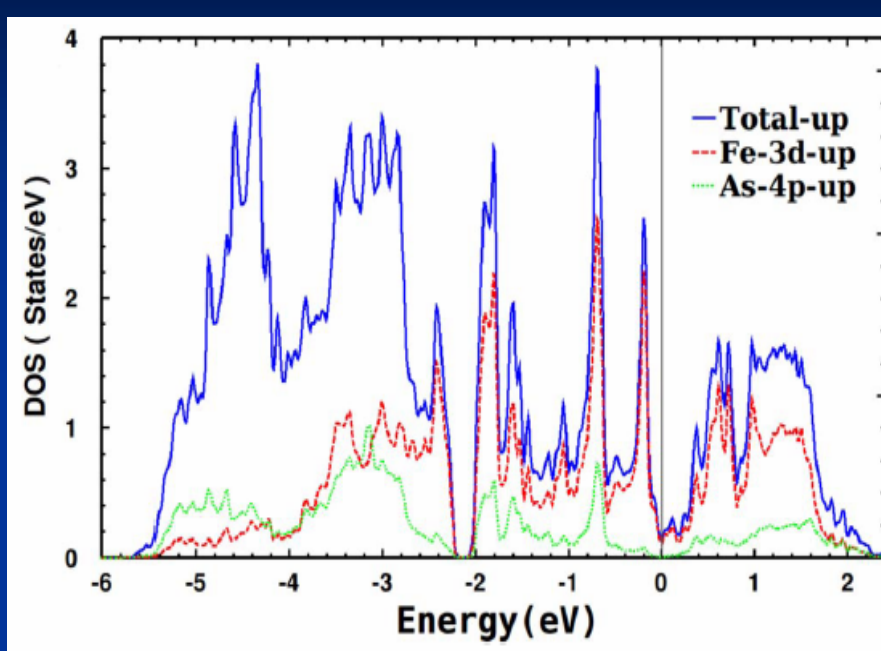
2.

Mechanism underlying magnetism and structural transition in iron-pnictides?

What we found

- The calculations on iron-pnictides without spin degree exclude any structural transition;
- The two transitions observed by neutron scattering share the same origin: the next nearest neighbor Fe-Fe antiferromagnetic superexchange interaction bridged by As atoms.

Analyzing electronic structure of collinear AFM state



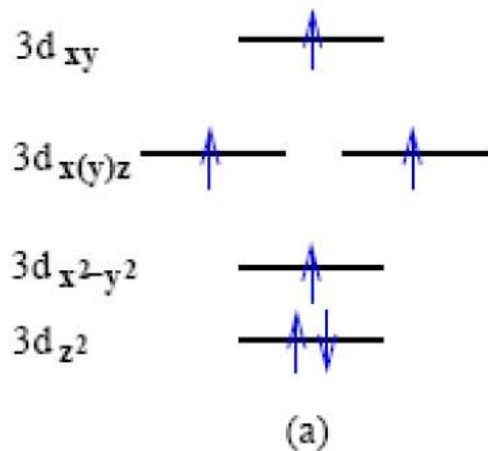
The peaks of As 4p-resolved DOS coincide with the ones of Fe 3d-resolved DOS between -2eV-0eV

arXiv:0804.3370,
PRB 78, 224517 (2008)

- ✓ five up-spin orbitals ~ almost filled
- ✓ five down-spin orbitals ~ nearly uniformly half filled
- ✓ small crystal field splitting imposed by As atoms
- ✓ Fe 3d orbitals hybridize with As 4p orbitals
- ✓ The Hund's rule coupling is strong, which would lead to a magnetic moment formed around each Fe atom.

Origin of Local moment: Hund's rule coupling

Bare $\text{Fe}^{2+} : S = 2$



$$H_{Hund} = -J_H \sum_{\alpha < \beta} S_{i\alpha} \cdot S_{i\beta}$$

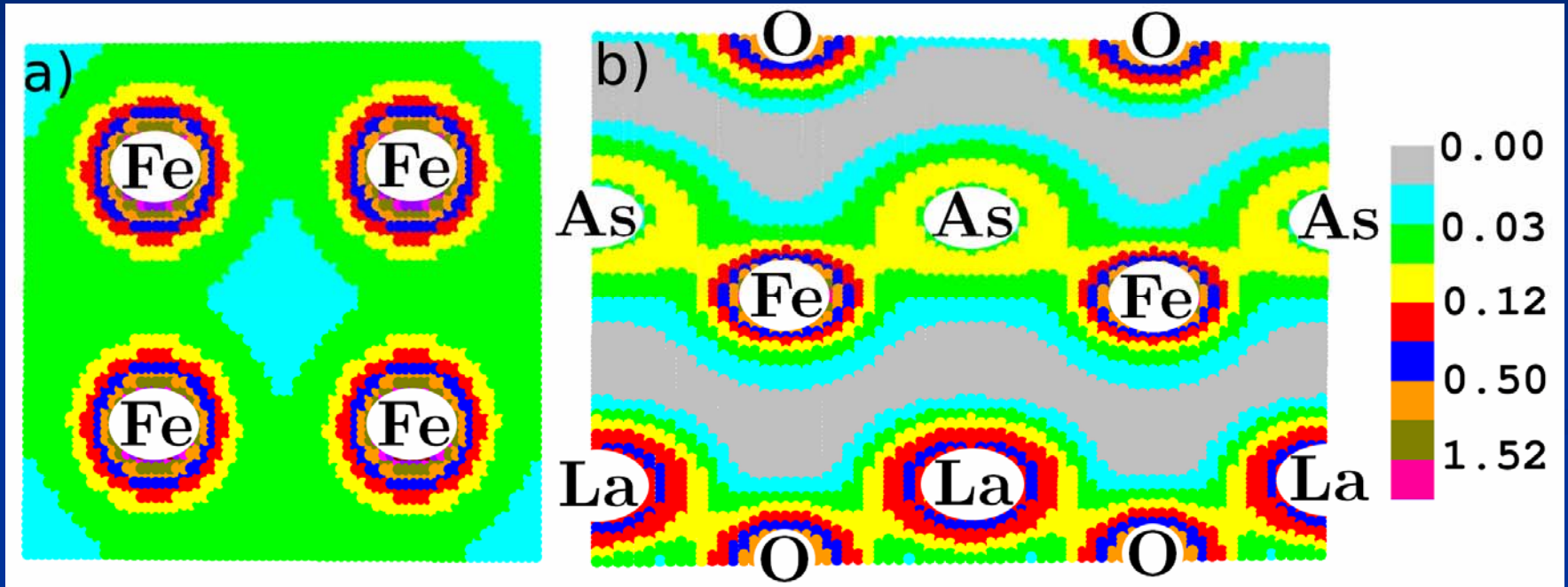
$$J_H \sim 0.6-1 \text{ eV}$$

This is also the main interaction which couples itinerant electrons with local moments on each Fe site

Crystal splitting between e_g and t_{2g} is very small

No evidence for the orbit selective Mott transition

Charge density distribution

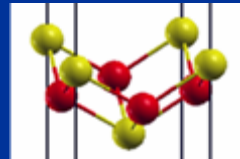
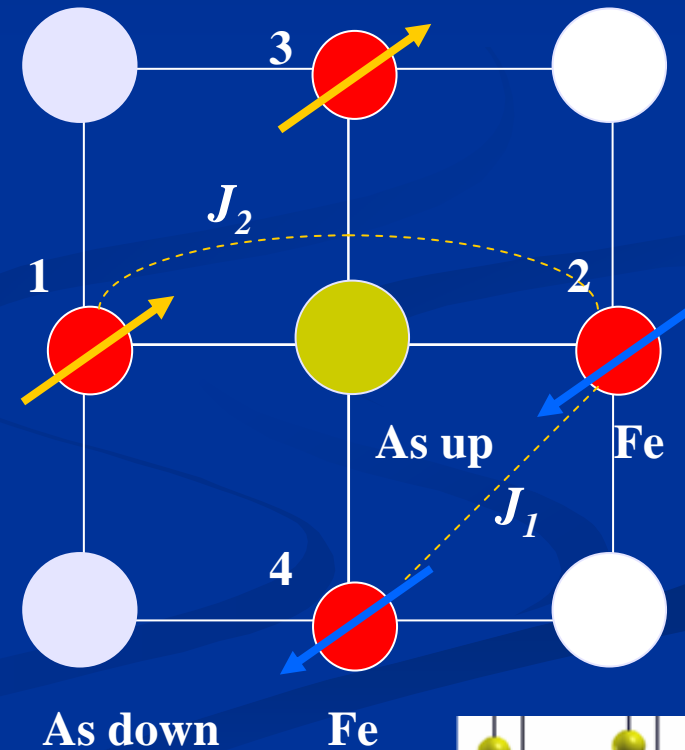


Covalence between Fe and As atoms

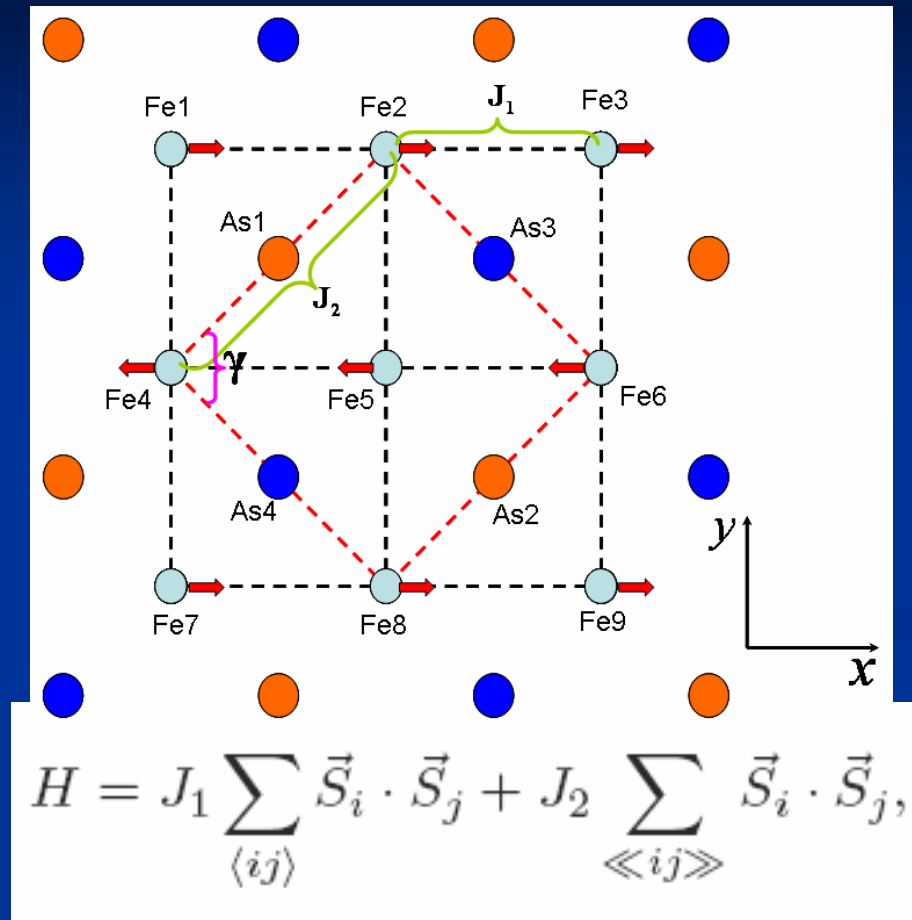
Fe-Fe Direct or superexchange interaction
Fe-As-Fe Superexchange interaction

The features of As-bridged superexchange interactions

- Mainly between the second nearest Fe atoms, namely J_2 ;
- Antiferromagnetic;
- Each pair of the next next nearest Fe moments in anti-parallel orientation if J_2 dominates;
- In a square lattice, a collinear antiferromagnetic order is of each pair of the next next nearest Fe moments in anti-parallel.



Schematic top view of LaFeAsO or BaFe₂As₂ in the collinear antiferromagnetic order



For $J_2 > J_1/2$, the collinear antiferromagnetic order replaces the Neel order

Angle γ increases to 90.5 with an energy gain of $\sim 6\text{meV}$,
 correspondingly, the unit cell transform from a square to a rhombus.

The origin of magnetic moment on Fe atom and the magnetic orders

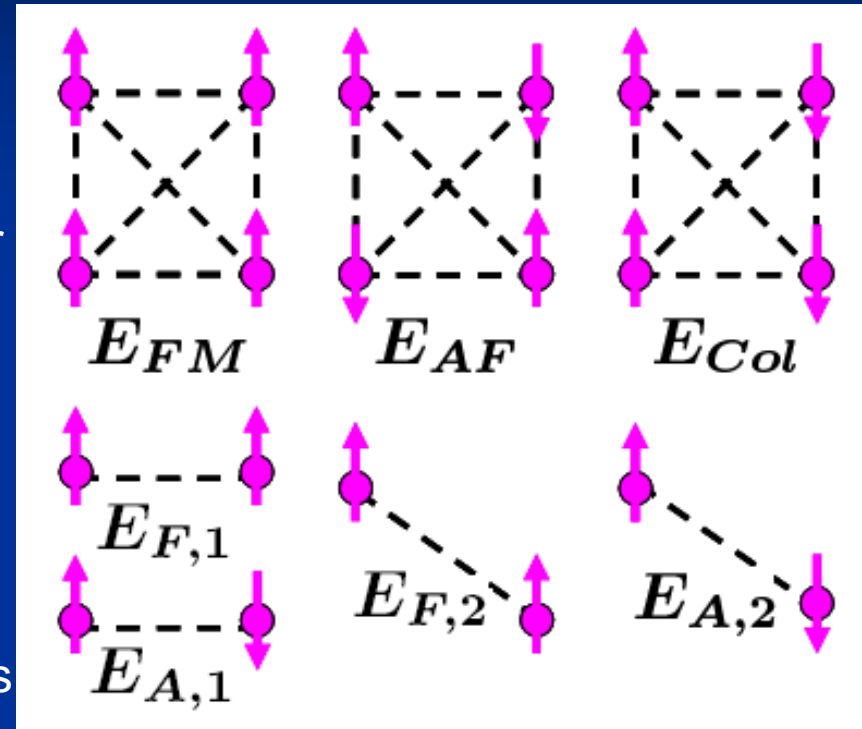
- Local magnetic moment is formed on Fe atom due to the strong Hund's rule coupling
- As(Se,Te)-bridged antiferromagnetic superexchange interaction
- The structural transition is driven by this superexchange interaction through the spin-lattice coupling.

Mapping into J1-J2 Heisenberg model

Set the nonmagnetic state energy =0,
Then the energies of ferromagnetic,
checkerboard antiferromagnetic, and collinear
antiferromagnetic states are

(0.0905, -0.10875, -0.21475) eV/Fe

Any magnetic structure may be described by
a combination of $E_{F,1}$ and $E_{A,1}$, $E_{F,2}$ and $E_{A,2}$,
equivalent to J_1 and J_2 with constant energies



$$H = J_1 \sum_{\langle ij \rangle} \vec{S}_i \cdot \vec{S}_j + J_2 \sum_{\langle\langle ij \rangle\rangle} \vec{S}_i \cdot \vec{S}_j,$$

$$J_1 = (E_{F,1} - E_{A,1}) / (2S^2),$$

$$J_2 = (E_{F,2} - E_{A,2}) / (2S^2).$$

Energy ordering on different magnetic states I

LaFeAsO:

$$E_{\text{FM}} > E_{\text{NM}} > E_{\text{Bi}} > E_{\text{AFM}} > E_{\text{Col}}$$

$$0.0905 \text{ eV/Fe}, 0.0, -0.1005 \text{ eV/Fe}, -0.1088 \text{ eV/Fe}, -0.2148 \text{ eV/Fe}$$

==>

$$J1 = 50 \text{ meV/Fe}, J2 = 51 \text{ meV/Fe}, J3 \sim 0.$$

(Ma, Lu, and Xiang, arXiv:0804.3370, PRB 78, 224517 (2008))

BaFe₂As₂:

$$E_{\text{FM}} > E_{\text{NM}} > E_{\text{AFM}} > E_{\text{Bi}} > E_{\text{Col}}$$

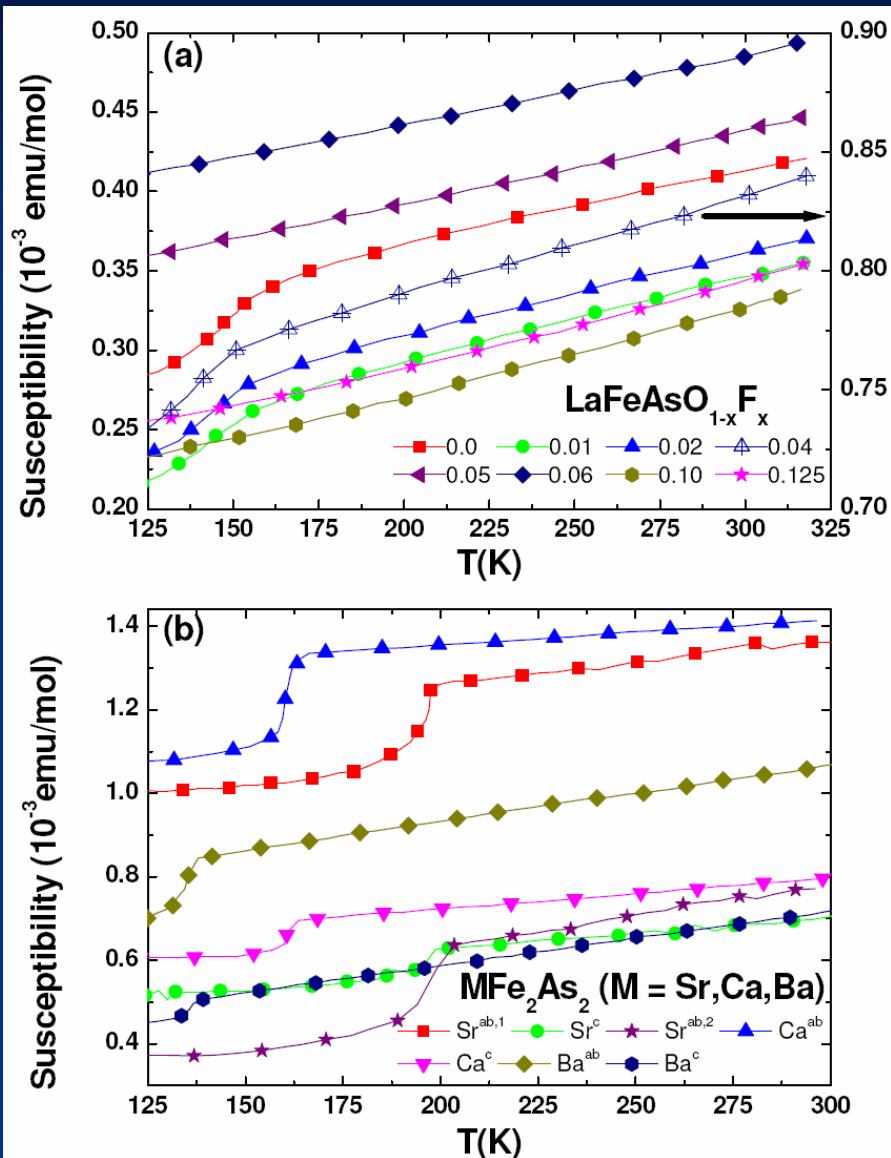
$$0.0113 \text{ eV/Fe}, 0.0, -0.116 \text{ eV/Fe}, -0.135 \text{ eV/Fe}, -0.194 \text{ eV/Fe}$$

==>

$$J1 = 32 \text{ meV/Fe}, J2 = 35 \text{ meV/Fe}, J3 \sim 0.$$

(arXiv:0806.3526, Front. Phys. China, 2010, 5(2): 150)

Strong AFM Fluctuation: universal linear susceptibility



Quantum spin fluctuation of the J_1 - J_2 model leads to the linear magnetic susceptibility

This linear susceptibility was observed in all iron pnictides

Zhang et al., EPL 86 (2009) 37006, arXiv:0809.3874

More comments on local magnetic moment in iron-pnictides

- There are localized moments around Fe atoms in real space;
- It is those bands far from the Fermi energy rather than the bands nearby the Fermi energy that determine the magnetic behavior of pnictides, namely the hybridization of Fe with the neighbor As atoms to play a substantial role;
- The local moments embedded in itinerant electrons;
- The Hund's rule coupling is the main interaction which couples itinerant electrons with local moments on each Fe site;
- The above is why we call the fluctuating Fe local moments with the As-bridged superexchange antiferromagnetic interaction (the Hund's rule correlation picture).

We emphasize that As atoms play a substantial role.

(PHYSICAL REVIEW B 78, 224517 (2008)).

Front. Phys. China, 2010, 5(2): 150

Main Interactions in Iron-based Superconductors

1. FM Hund's rule coupling:

it leads to the formation of local moments and the coupling between itinerant electrons and more localized orbitals

2. AFM exchange interaction between neighboring spins

$$H = \sum_{ij\alpha\beta} t_{ij}^{\alpha\beta} c_{i\alpha}^\dagger c_{j\beta} - J_H \sum_{i\alpha \neq \beta} \vec{S}_{i\alpha} \cdot \vec{S}_{i\beta} \\ + J_1 \sum_{\langle ij \rangle \alpha\beta} \vec{S}_{i\alpha} \cdot \vec{S}_{j\beta} + J_2 \sum_{\langle\langle ij \rangle\rangle \alpha\beta} \vec{S}_{i\alpha} \cdot \vec{S}_{j\beta}$$

$$\vec{S}_{i\alpha} = c_{i\alpha}^\dagger \frac{\vec{\sigma}}{2} c_{i\alpha}$$

F. Ma, Z. Y. Lu, T. Xiang, *Front Phys. China* **5**, 150 (2010); arXiv:0806.3526v2
S.P. Kou, T. Li, Z.Y. Weng, *EPL* **88**, 17010 (2009).

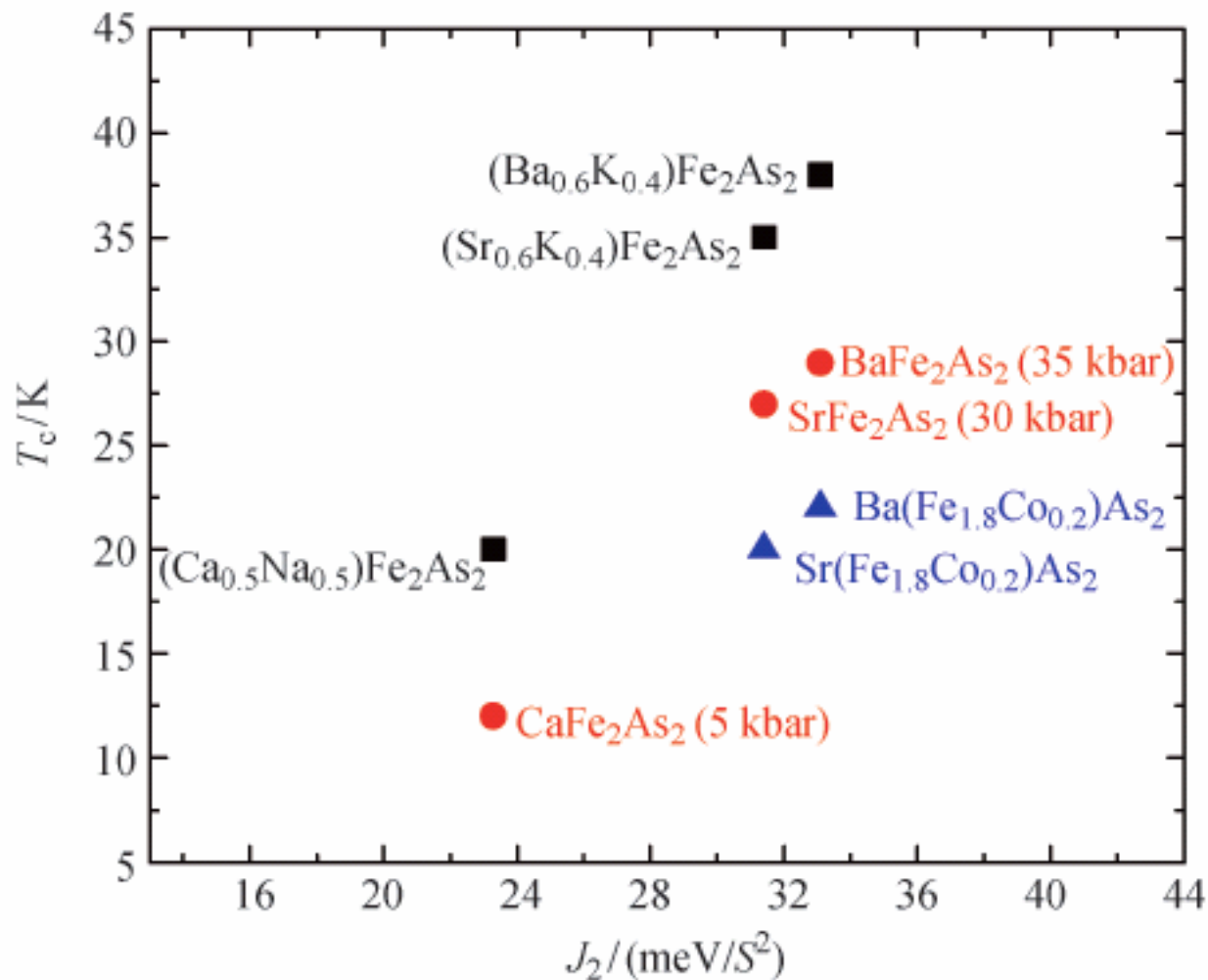


Fig. 13 Various critical superconductivity temperature T_c versus exchange interaction J_2 for $A\text{Fe}_2\text{As}_2$ ($A=\text{Ba}$, Ca , or Sr) with doping or under high pressures. T_c are taken from Refs. [3, 5, 13, 25, 34, 35].

3.

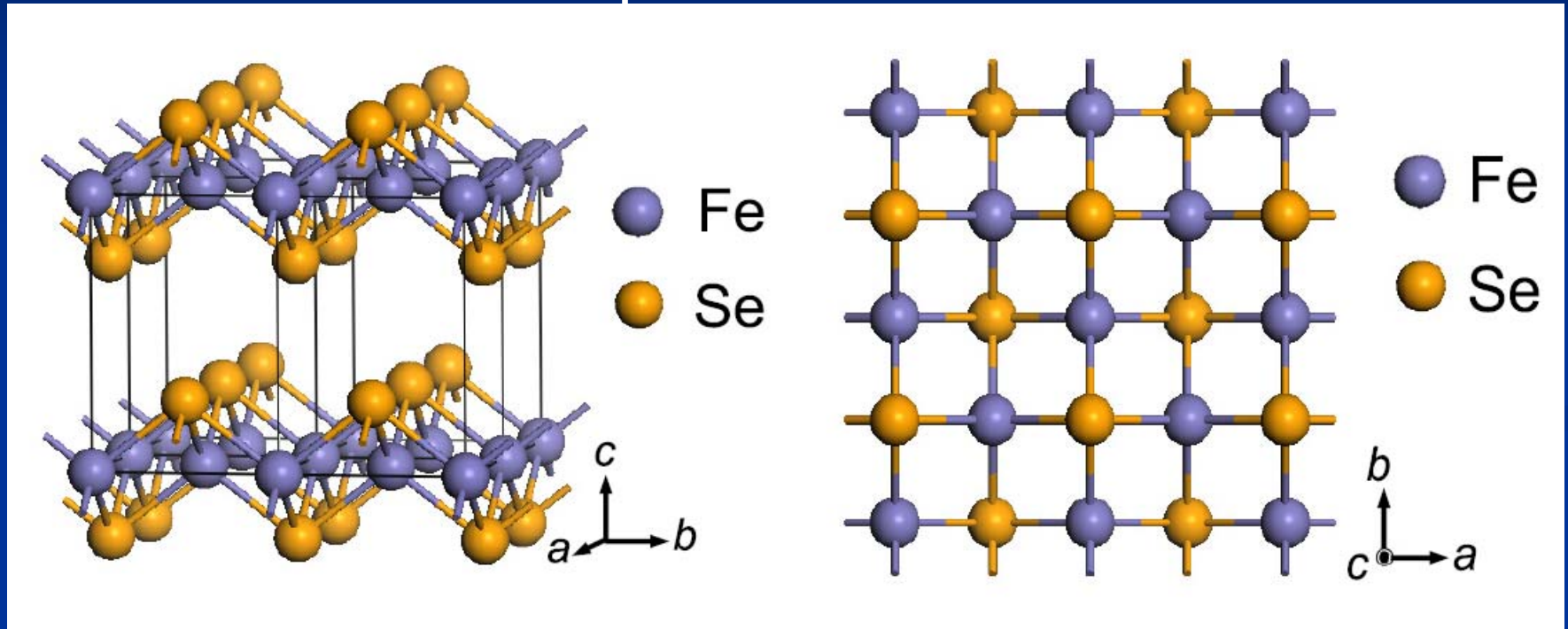
Bi-collinear AFM order in alpha-FeTe

versus

Collinear AFM order in alpha-FeSe

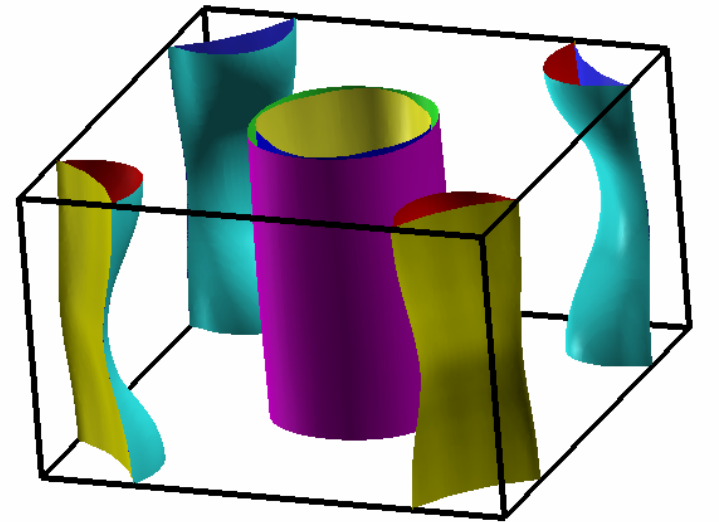
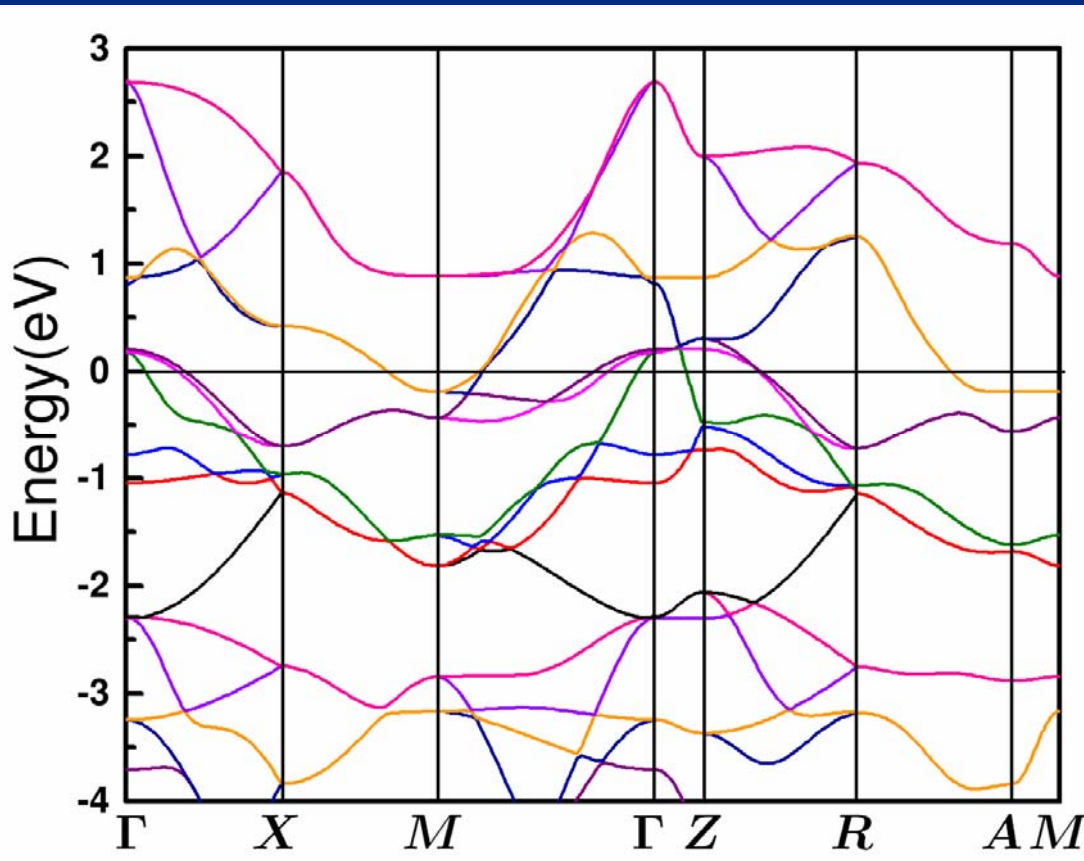
'11' iron-chalcogenides

alpha-FeSe

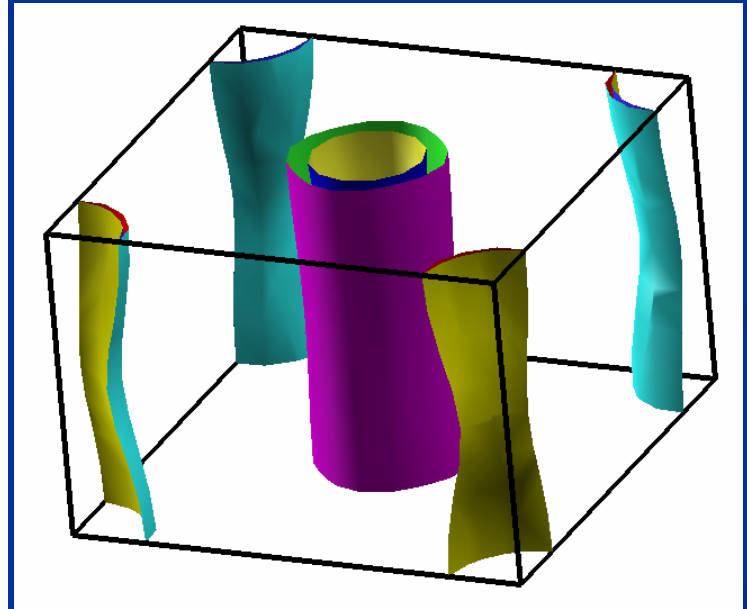
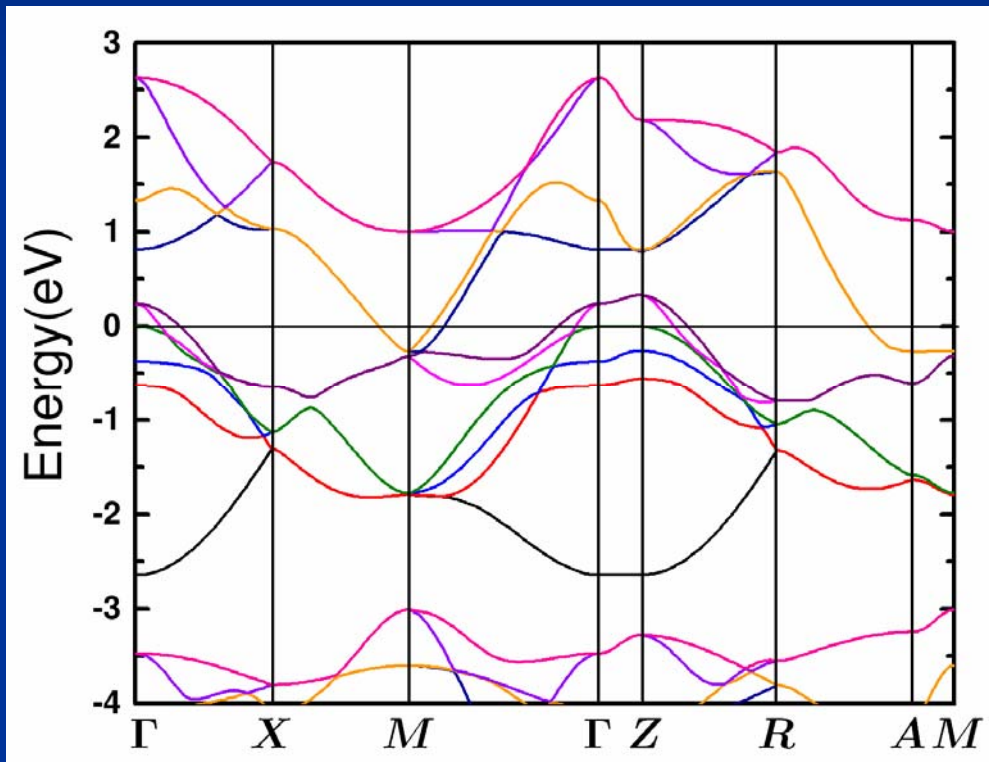


Replacing Se by Te: alpha-FeTe

Electronic structure of alpha-FeTe in nonmagnetic state



Electronic structure of alpha-FeSe in nonmagnetic state

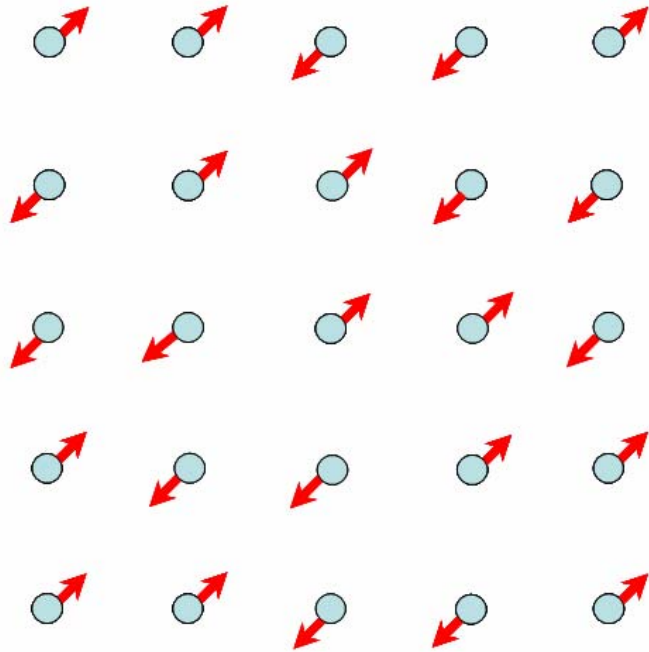


Fermi surface nesting?

- If the magnetic order is induced by the Fermi surface nesting, we expect that all these materials would adopt the similar magnetic order as the one in LaFeAsO, namely collinear antiferromagnetic order;
- What we find is that the ground state of alpha-FeTe is in a novel bi-collinear antiferromagnetic order, while that of alpha-FeSe is in a conventional collinear antiferromagnetic order.

Global view on (bi)-collinear antiferromagnetic order on a square lattice

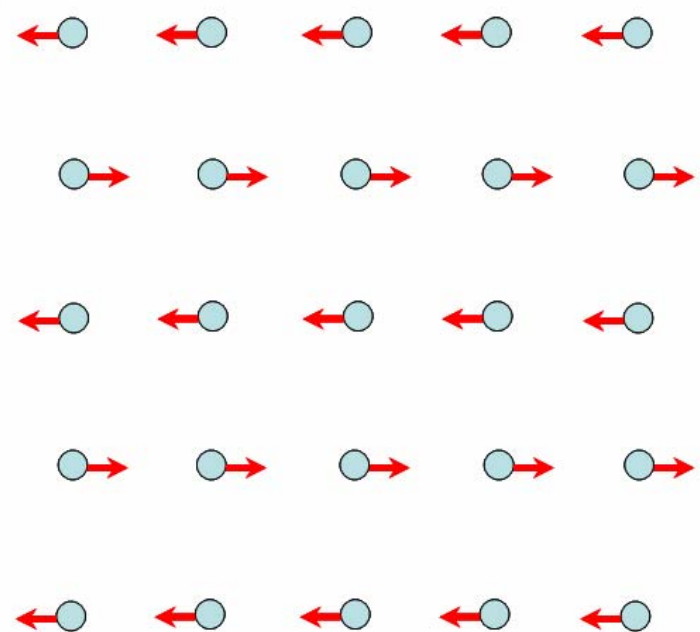
a)



Bi-Collinear

Alpha-FeTe

b)



Collinear

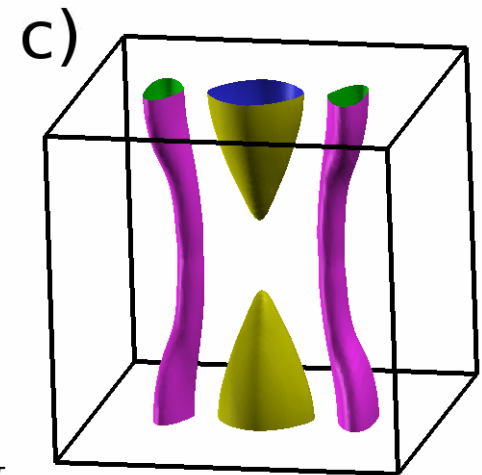
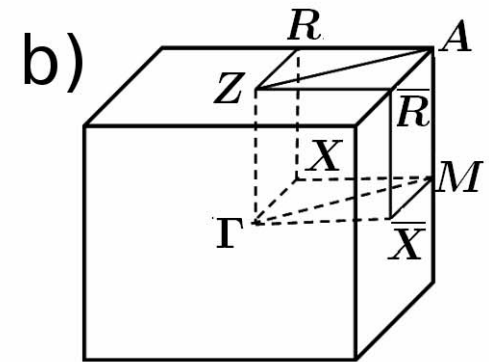
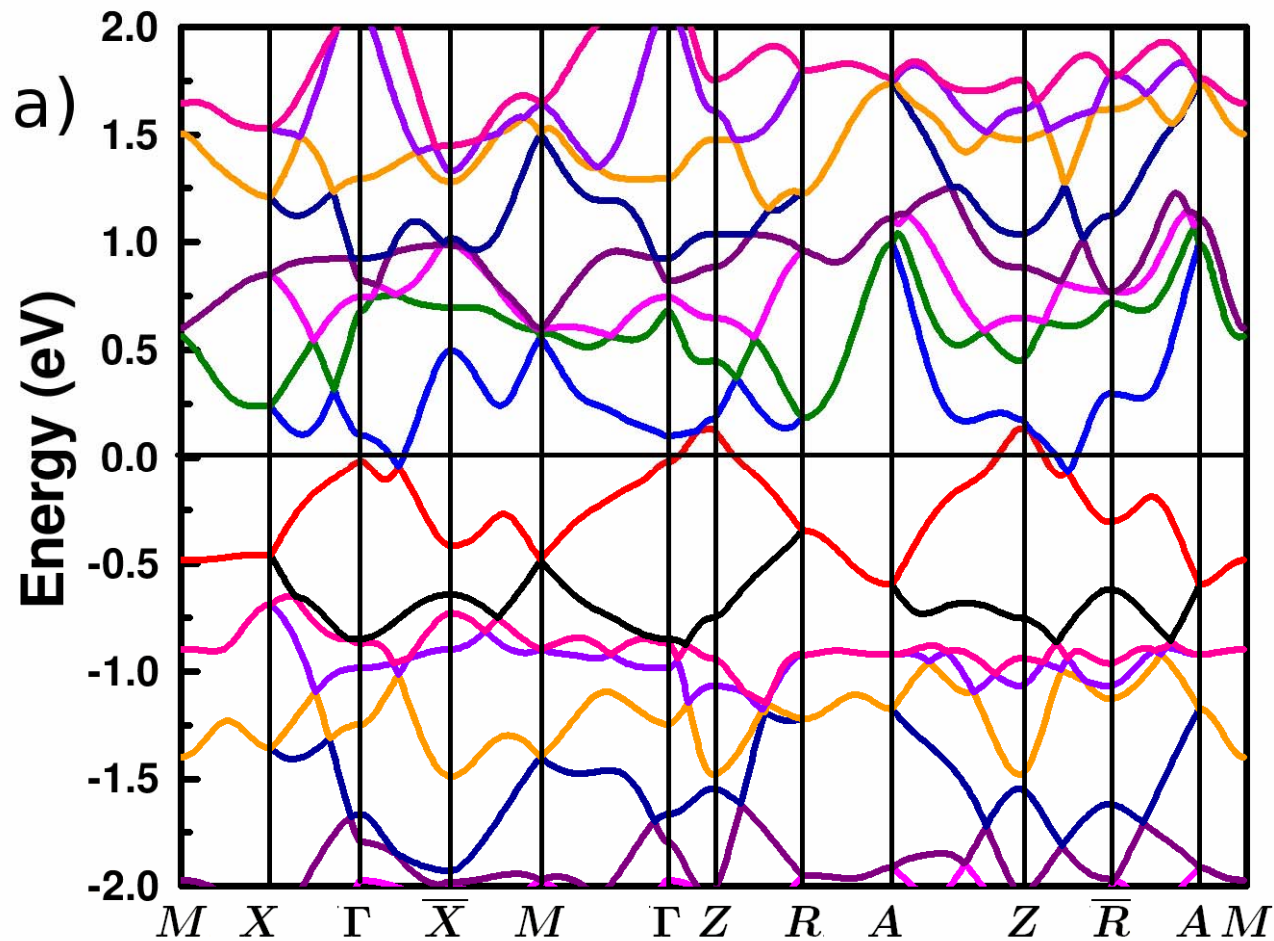
The others

The combination of magnetic orders in the two square sublattices A and B

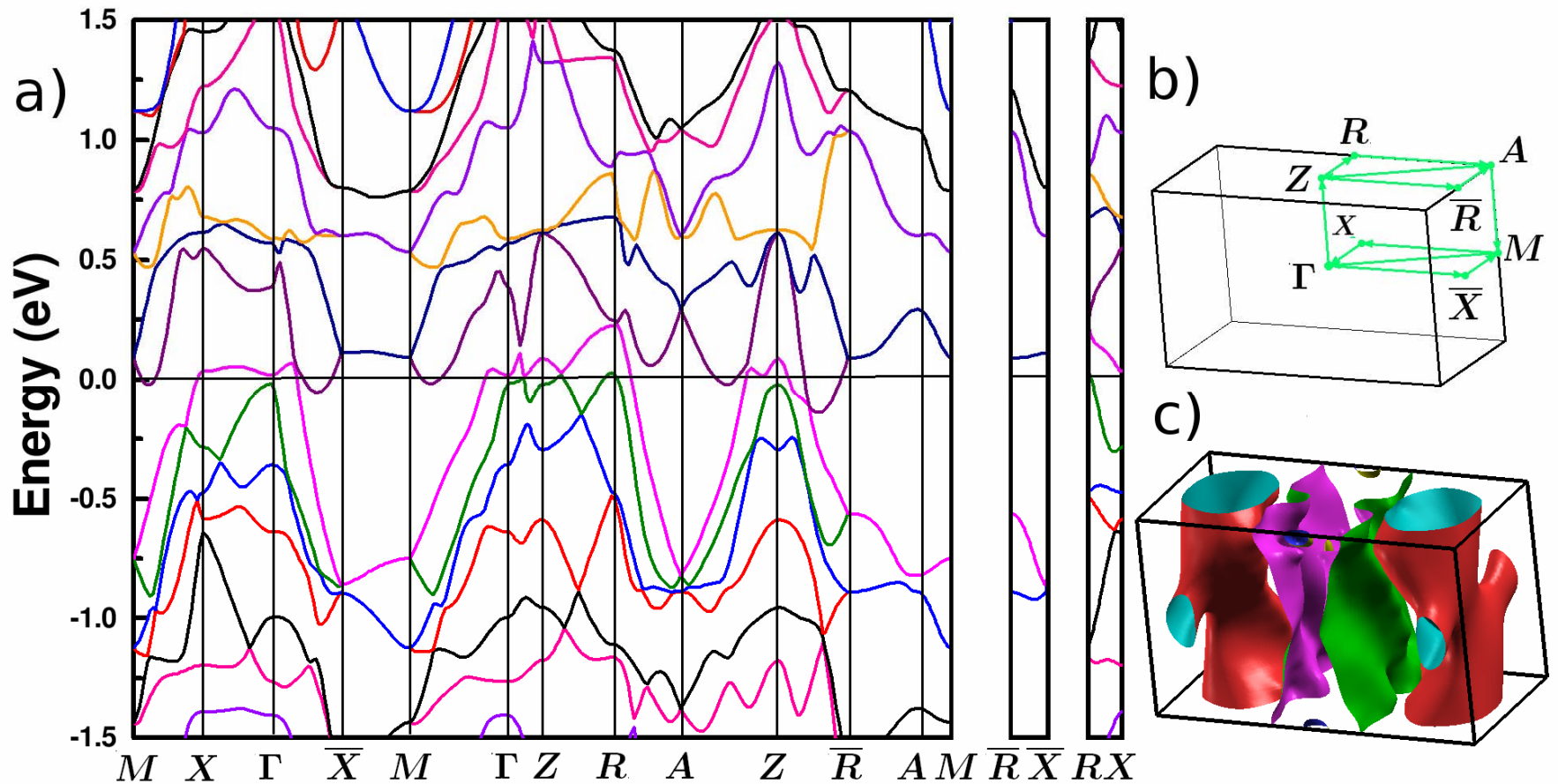
A \ B	FM	AFM (Neel)	Collinear
FM	AFM (Neel) or FM		
AFM (Neel)		Collinear	
Collinear			Bi-collinear

These rich magnetic orders are impossible to understand by the Fermi surface nesting. They can be well described by the Heisenberg model on the square lattice.

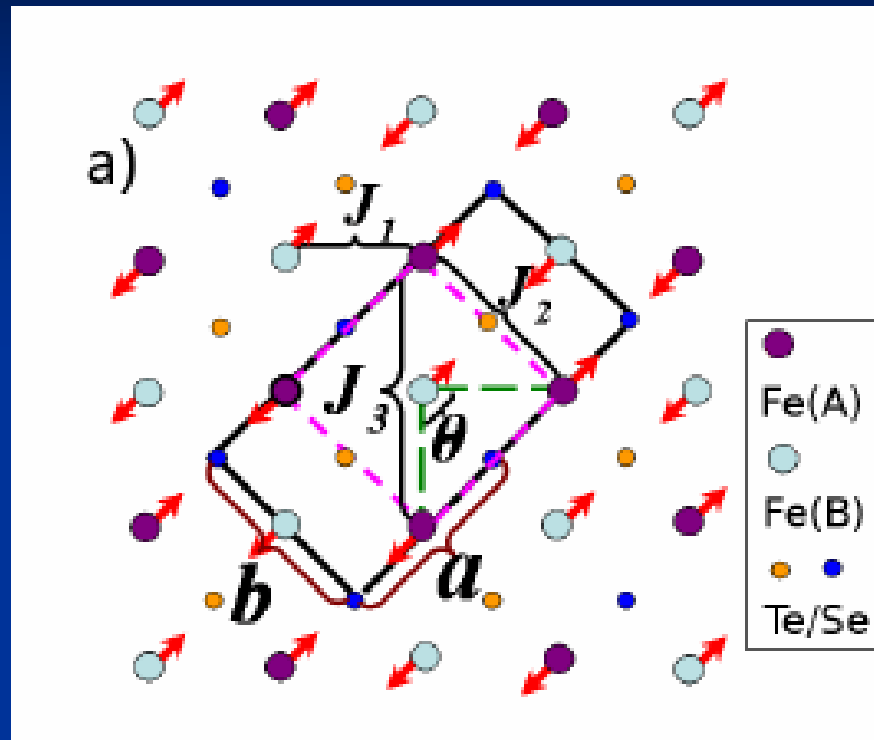
Electronic band structure of Alpha-FeSe in collinear antiferromagnetic order



Electronic band structure of Alpha-FeTe in bi-collinear antiferromagnetic order



Schematic top view of alpha-FeTe in the bi-collinear antiferromagnetic order

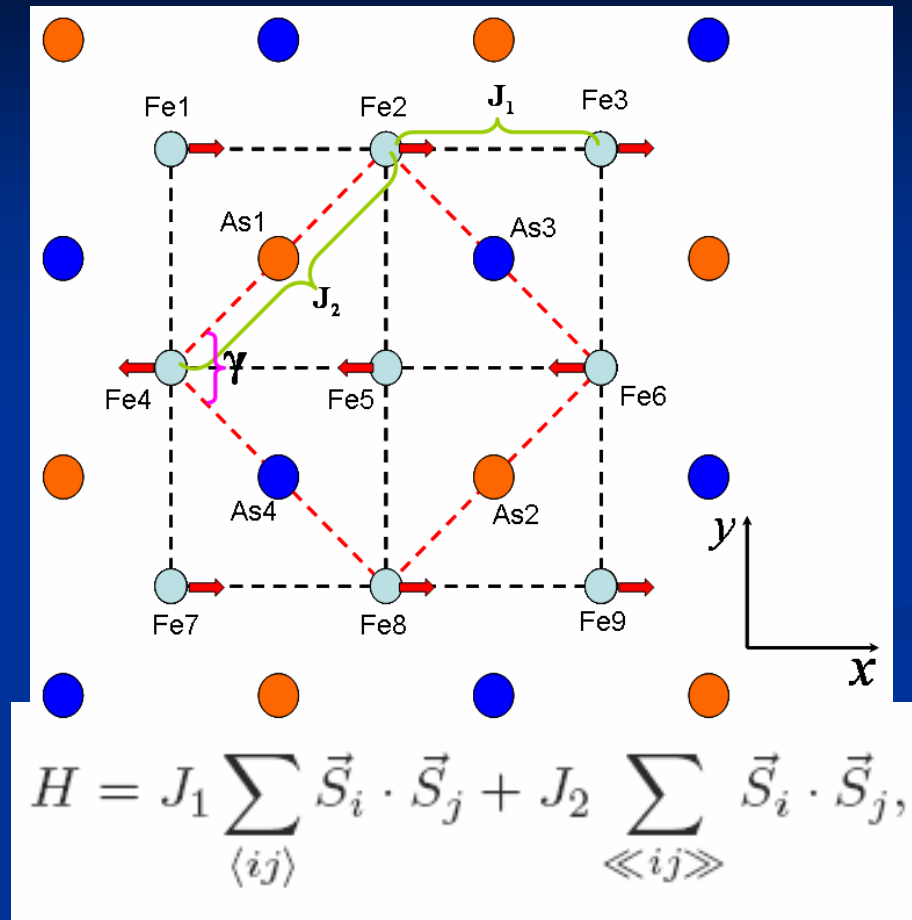


$$H = J_1 \sum_{\langle ij \rangle} \vec{S}_i \cdot \vec{S}_j + J_2 \sum_{\langle\langle ij \rangle\rangle} \vec{S}_i \cdot \vec{S}_j + J_3 \sum_{\langle\langle\langle ij \rangle\rangle\rangle} \vec{S}_i \cdot \vec{S}_j,$$

For $J_2 > J_1/2$ and $J_3 > J_2/2$, the bi-collinear antiferromagnetic order is lower in energy than the collinear antiferromagnetic order.

angle θ increases to 90.7, a square to a rectangle

Schematic top view of LaFeAsO or BaFe₂As₂ in the collinear antiferromagnetic order



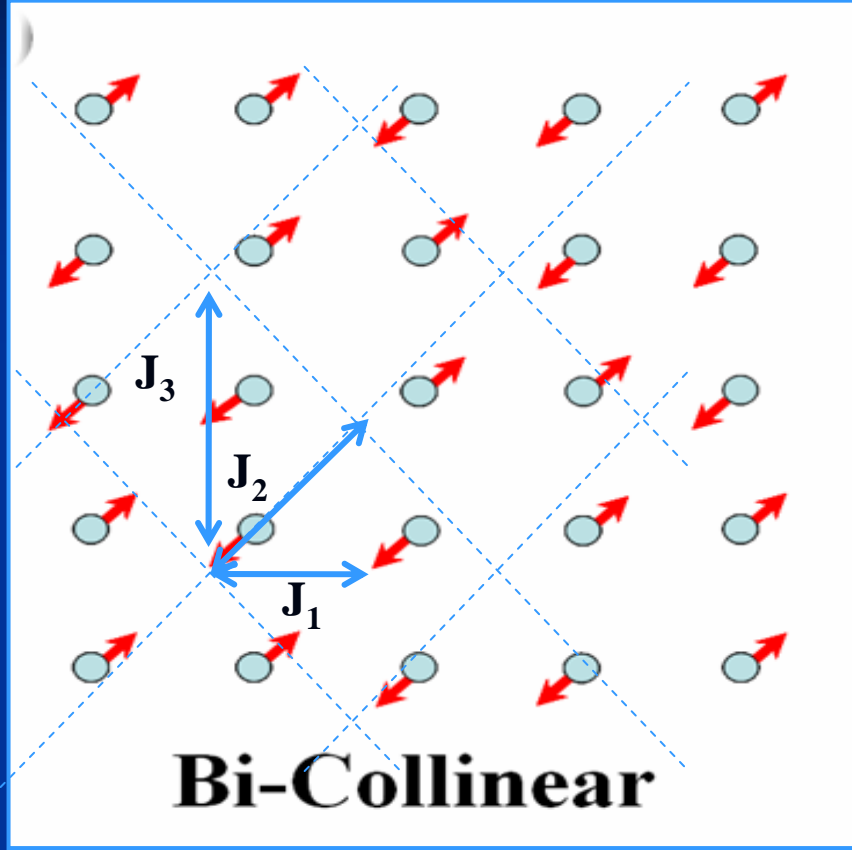
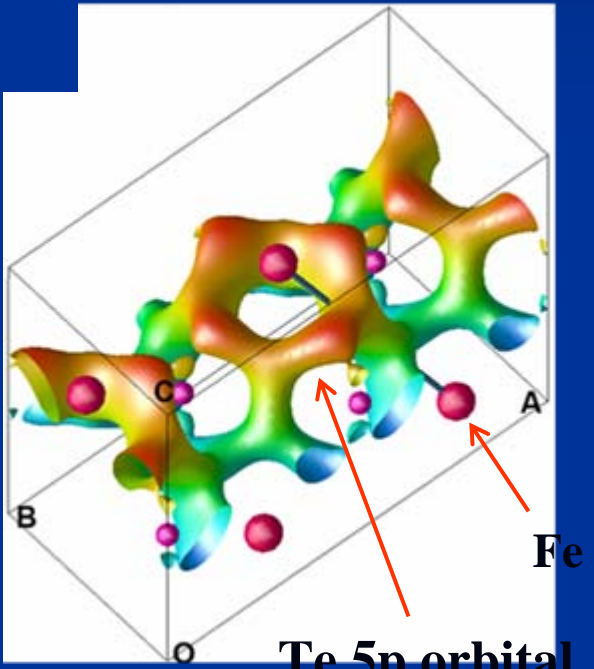
For $J_2 > J_1/2$, the collinear antiferromagnetic order replaces the Neel order

Angle γ increases to 90.5 with an energy gain of $\sim 6\text{meV}$,
 correspondingly, the unit cell transform from a square to a rhombus.

Origin of J_3 -Term: AFM Interaction Mediated by Te/Se p Orbitals

$$H = J_1 \sum_{\langle ij \rangle} \vec{S}_i \cdot \vec{S}_j + J_2 \sum_{\langle\langle ij \rangle\rangle} \vec{S}_i \cdot \vec{S}_j + J_3 \sum_{\langle\langle\langle ij \rangle\rangle\rangle} \vec{S}_i \cdot \vec{S}_j,$$

Te 5p orbital has a significant contribution at the Fermi level



5p electron in Te is more itinerant.
It mediates a RKKY-like interactions between Fe moments

Energy ordering on different magnetic states II

Alpha-FeTe:

$$E_{\text{NM}} > E_{\text{FM}} > E_{\text{AFM}} > E_{\text{Col}} > E_{\text{Bi}}$$

$$0.0, -0.0897\text{eV/Fe}, -0.0980\text{ eV/Fe}, -0.156\text{ eV/Fe}, -0.166\text{eV/Fe}$$

==>

$$J1 = 2.1\text{meV/Fe}, J2 = 15.8\text{ meV/Fe}, J3 = 10.1\text{ meV/Fe}$$

alpha-FeSe:

$$E_{\text{FM}} > E_{\text{NM}} > E_{\text{Bi}} > E_{\text{AFM}} > E_{\text{Col}}$$

$$0.183\text{ eV/Fe}, 0.0, -0.089\text{ eV/Fe}, -0.101\text{ eV/Fe}, -0.0152\text{ eV/Fe}$$

==>

$$J1 = 71\text{ meV/Fe}, J2 = 48\text{ meV/Fe}, J3 = 8.5\text{ meV/Fe}$$

Alpha-FeTe versus alpha-FeSe

The ground state of alpha-FeTe is in a novel bi-collinear antiferromagnetic order, while that of alpha-FeSe is in a conventional collinear antiferromagnetic order, which cannot be understood by the Fermi surface nesting picture

Problem of the Local Moment Scenario

The local moment picture can explain the magnetic structure of the ground state, but there is not a clear energy scale separating the localized and conducting orbitals in iron pnictides --- the definition of local moment is not so clean!

$$H = \sum_{ij\alpha\beta} t_{ij}^{\alpha\beta} c_{i\alpha}^\dagger c_{j\beta} - J_H \sum_{i\alpha\neq\beta} \vec{S}_{i\alpha} \cdot \vec{S}_{i\beta} \\ + J_1 \sum_{\langle ij \rangle \alpha\beta} \vec{S}_{i\alpha} \cdot \vec{S}_{j\beta} + J_2 \sum_{\langle\langle ij \rangle\rangle \alpha\beta} \vec{S}_{i\alpha} \cdot \vec{S}_{j\beta}$$

$$\vec{S}_{i\alpha} = c_{i\alpha}^\dagger \frac{\vec{\sigma}}{2} c_{i\alpha}$$

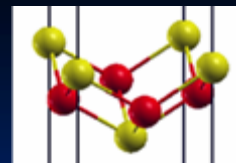
4.

Intercalated FeSe:

$A_y\text{Fe}_{2-x}\text{Se}_2$ (A=K, Rb, Cs, or Tl)

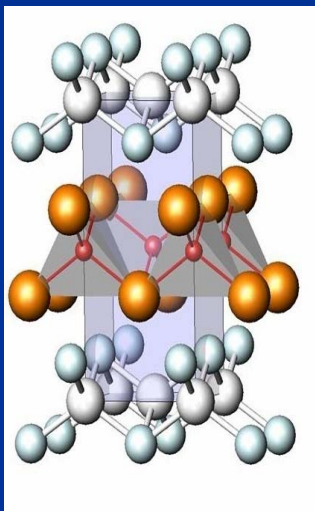
newly found Fe-based superconductors

Iron-based superconductors

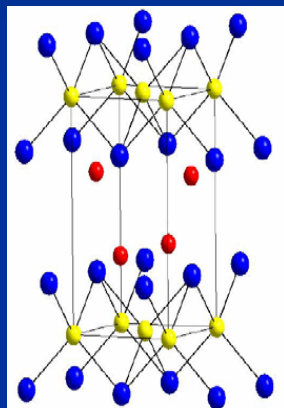


FeAs layer

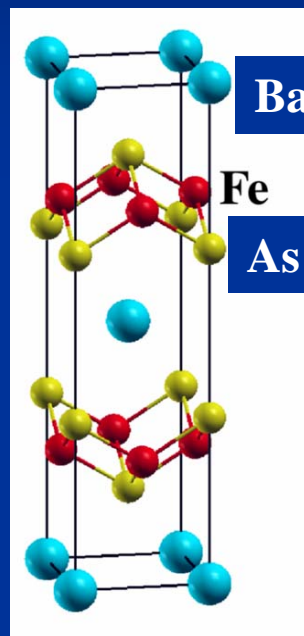
iron pnictide



1111
LaOFeAs
 $T_c \sim 55\text{K}$



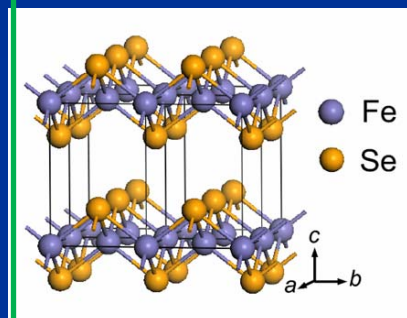
111
LiFeAs
 $T_c \sim 18\text{K}$



122
BaFe₂As₂
 $T_c \sim 38\text{K}$

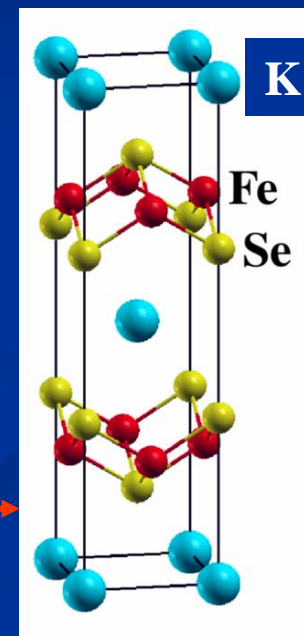
As^{-3}

iron chalcogenide



11
FeSe
 $T_c \sim 9\text{K}$

K intercalating
→



122
KFe_{2-x}Se₂
 $T_c \sim 33\text{K}$

Se^{-2}

New Features Revealed by (K,Rb,Cs,Tl) intercalated FeSe

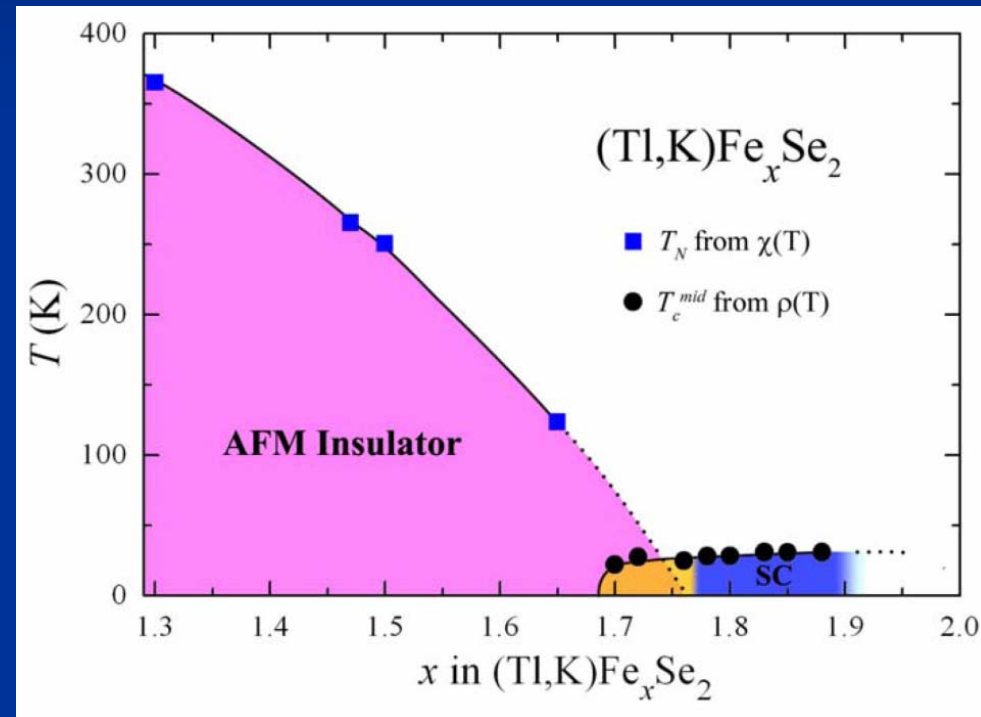
The superconductivity is proximity to an AFM insulating phase, similar to the high- T_c cuprates.

- ✓ The ordered Fe vacancies were found in stable phases, in which either one quarter or one fifth Fe atoms are missing;
- ✓ Possible coexistence of strong AFM order with SC.

Questions:

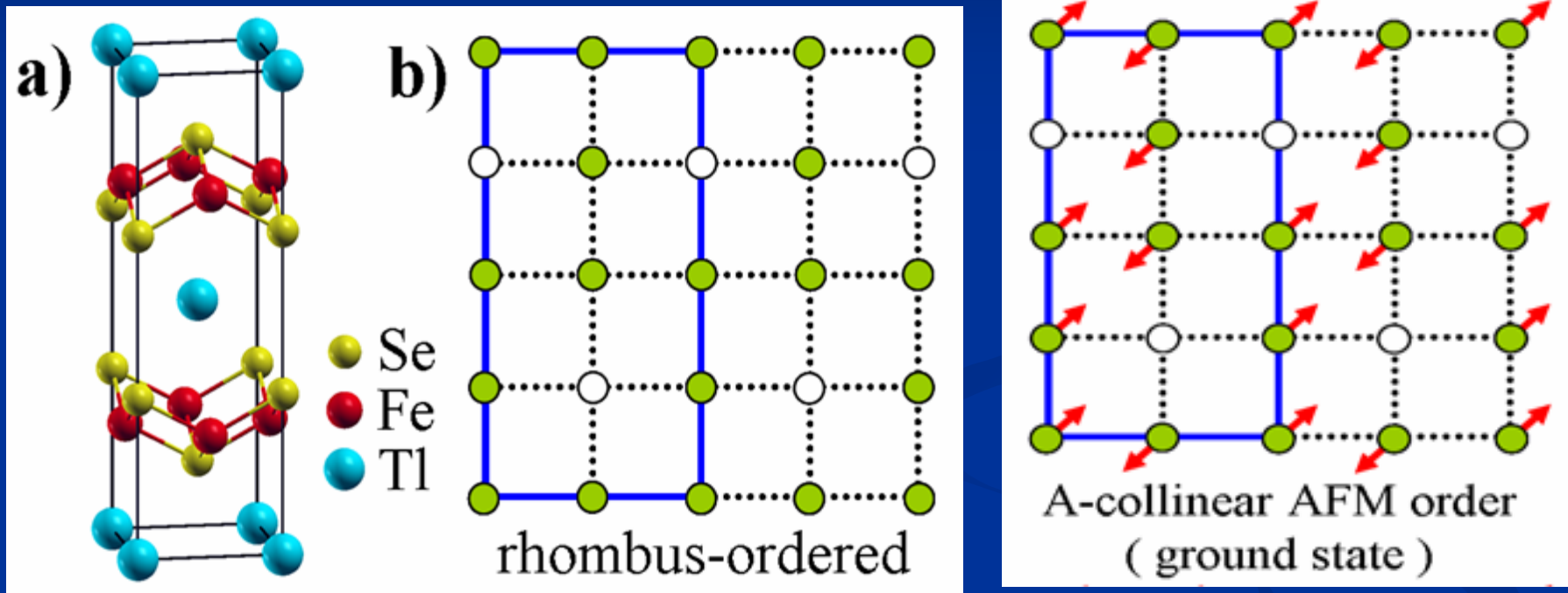
Fe vacancies or electron correlation effect matters?

Valence counting

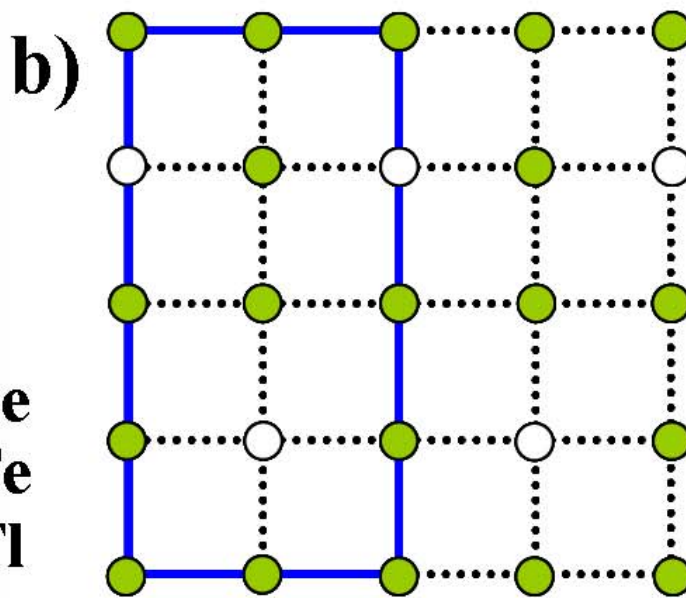
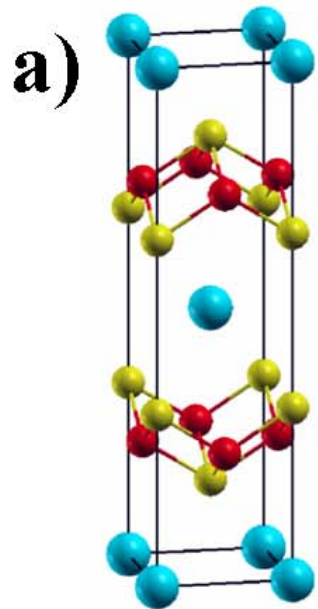


M. Fang *et al.* arXiv:1012.5236

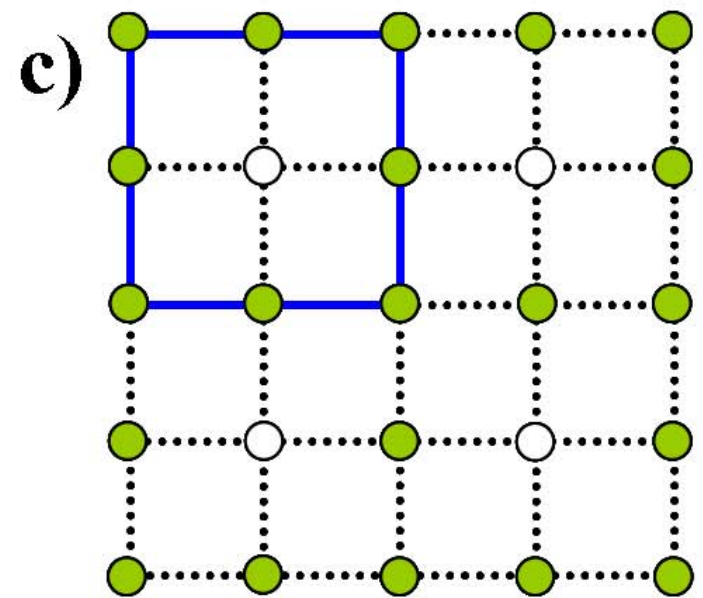
Magnetic Order in Fe-vacancies ordered $\text{TlFe}_{1.5}\text{Se}_2$



One-quarter Fe vacancies $A\text{Fe}_{1.5}\text{Se}_2$: there are two ordered vacancy structures

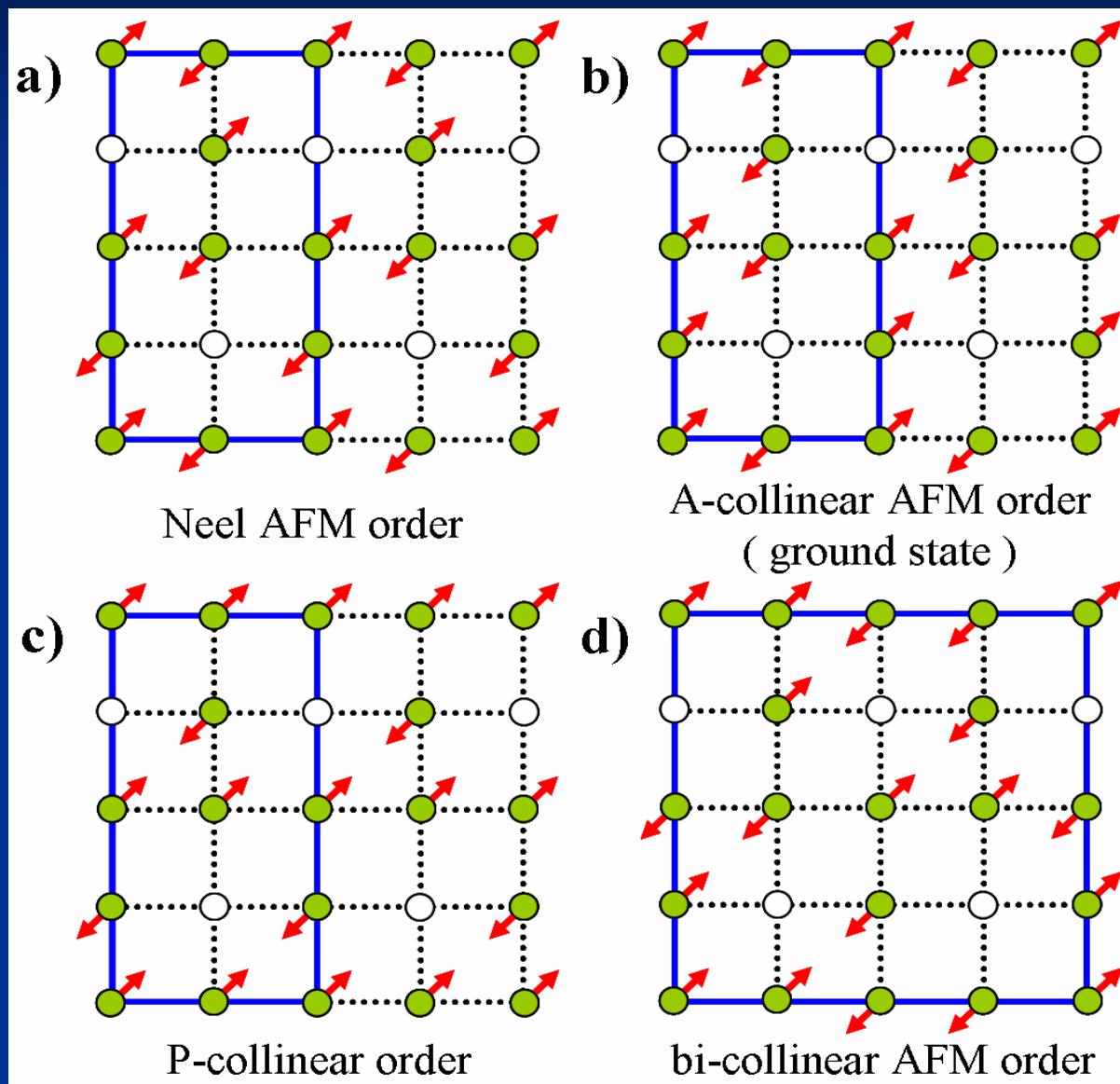


rhombus-ordered

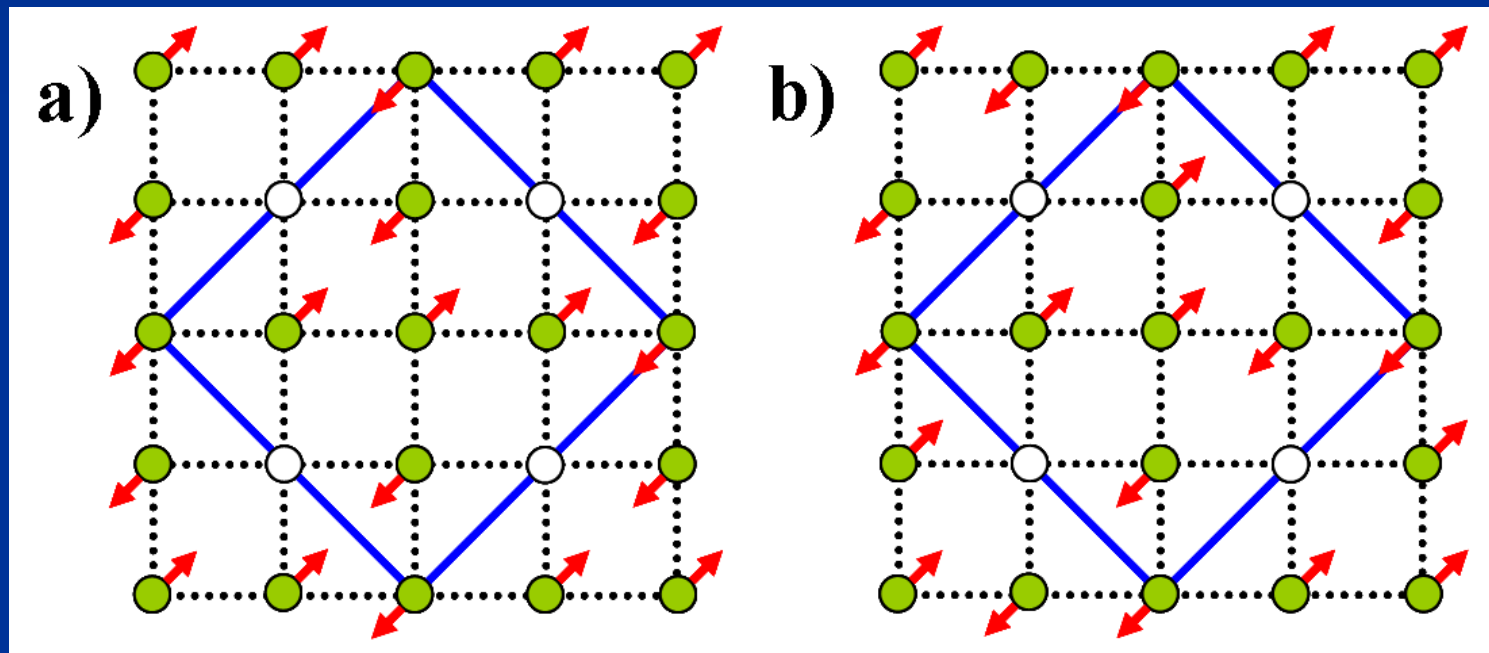


square-ordered

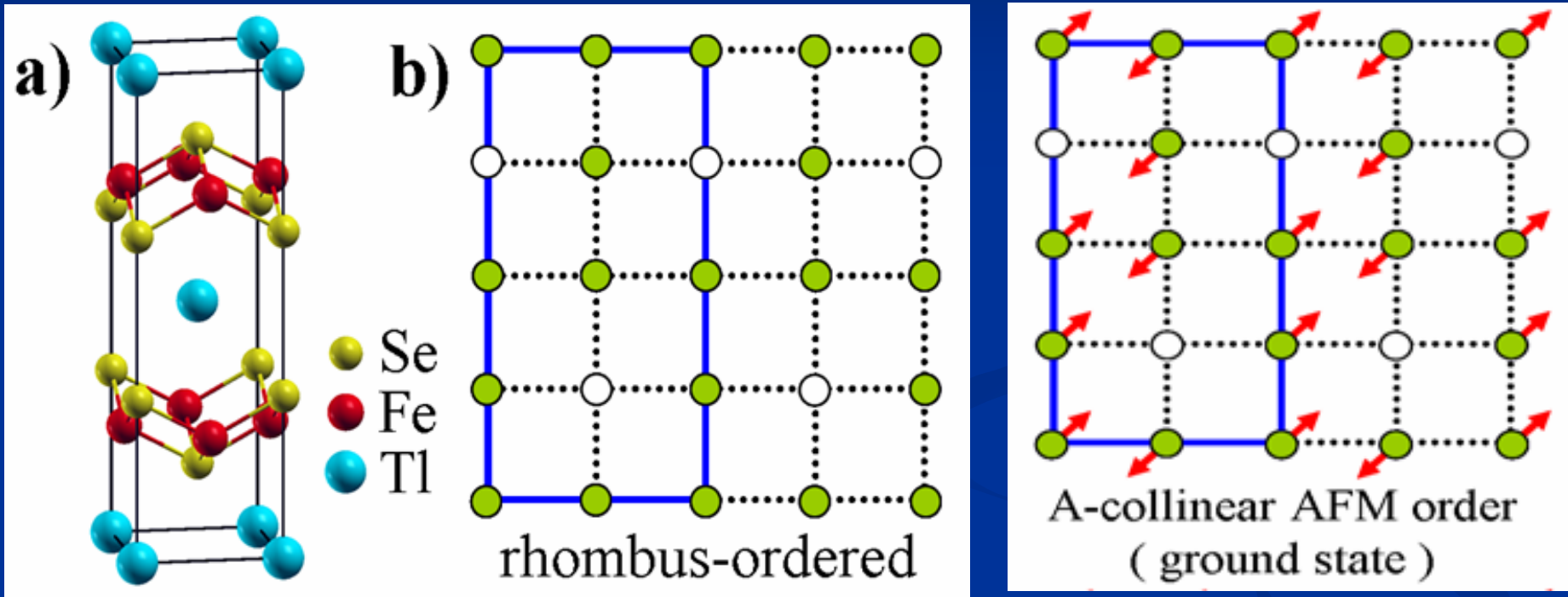
Possible magnetic orders for Fe-vacancies in rhombus-ordering



Possible magnetic orders for Fe-vacancies in square-ordering

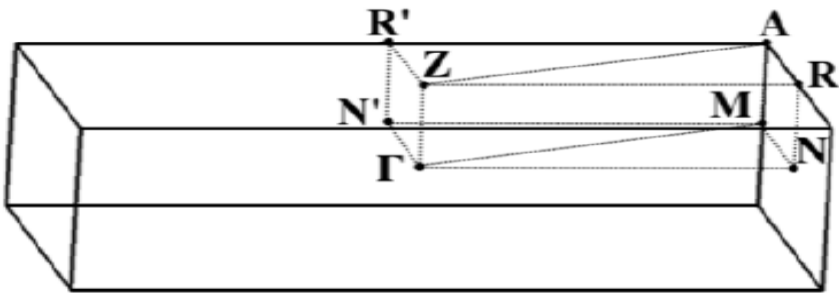
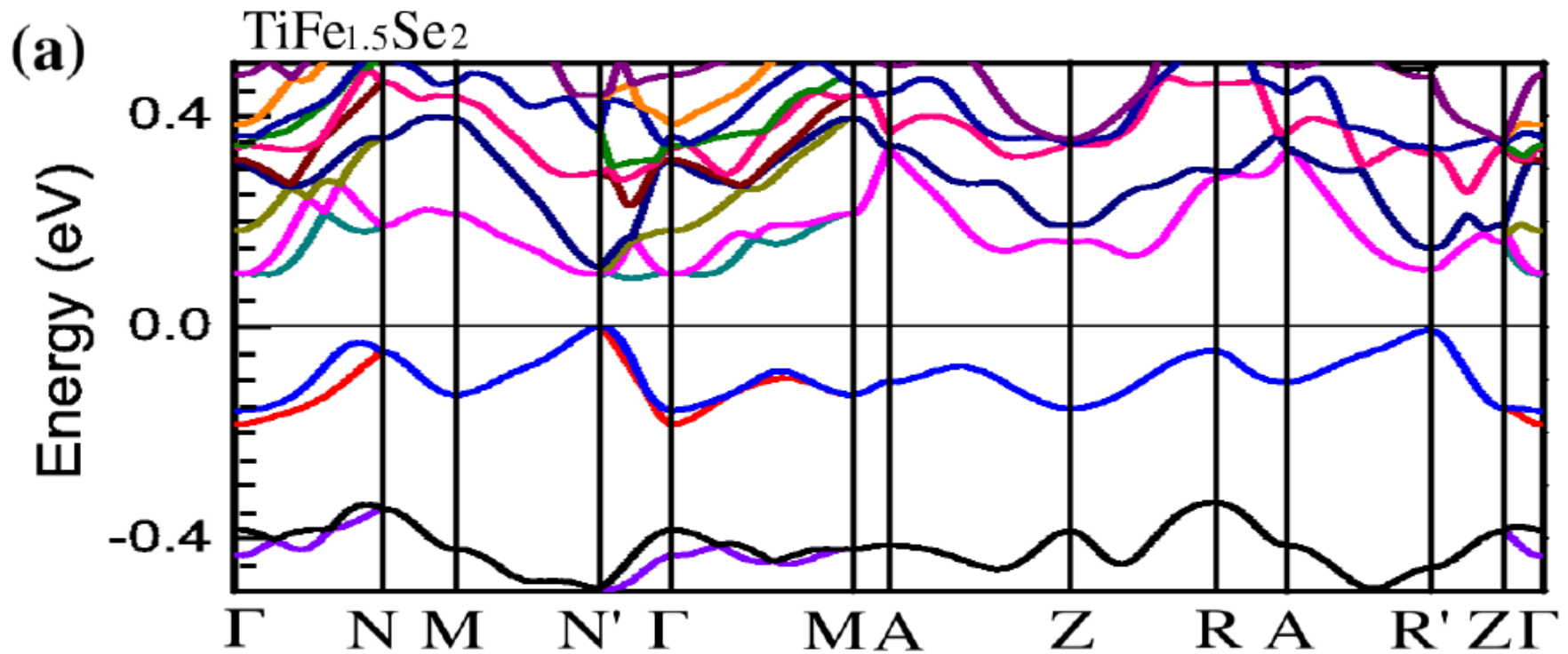


Magnetic Order in the ground state of Fe-vacancies ordered $\text{TlFe}_{1.5}\text{Se}_2$



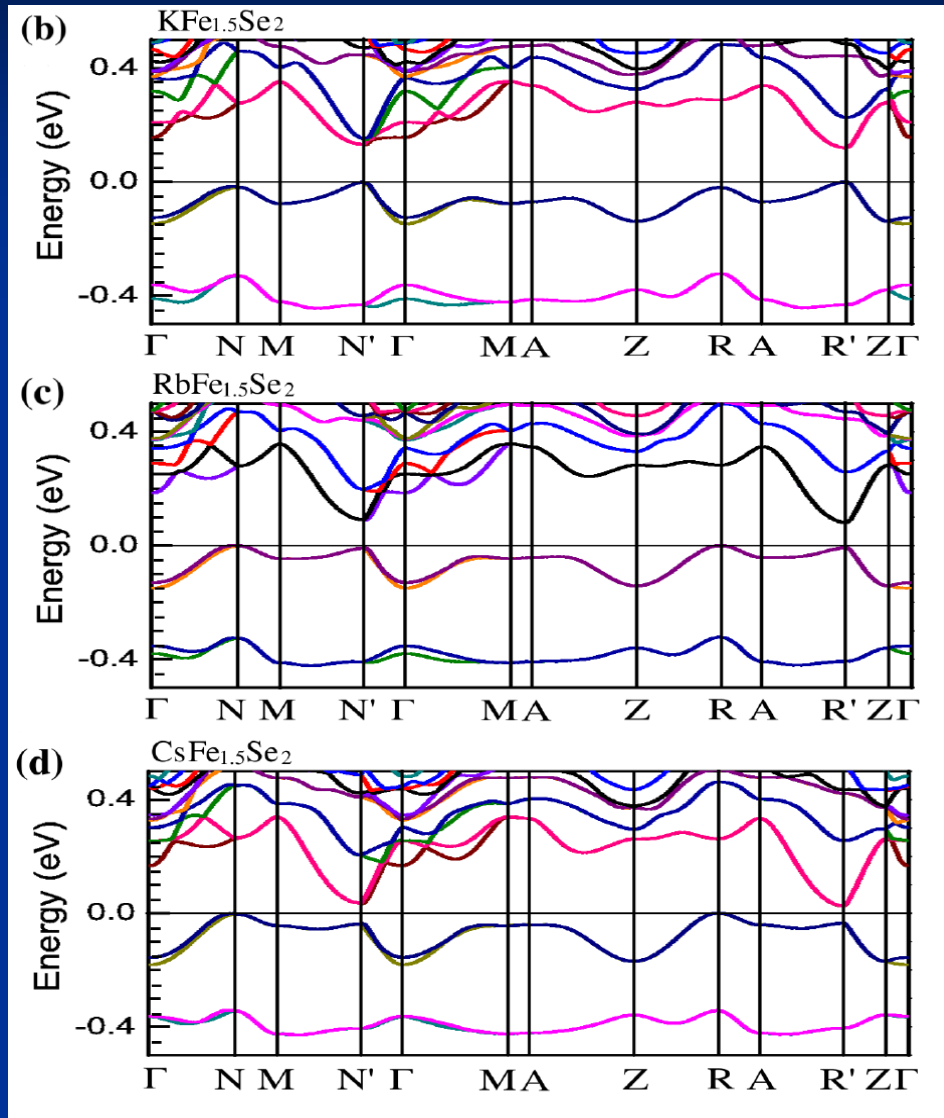
The A-collinear AFM order is with each pair of the next next nearest Fe spins orientated in anti-parallel, due to the Se-bridged superexchange interactions.

Band structure of $\text{TiFe}_{1.5}\text{Se}_2$ in the ground state with collinear AFM order



It is an antiferromagnetic semiconductor with an energy gap of 94 meV, in good agreement of measured value of 56 meV.

Band structures of $A\text{Fe}_{1.5}\text{Se}_2$ ($A=\text{K}, \text{Rb}, \text{or Cs}$) in the ground state, antiferromagnetic semiconductors

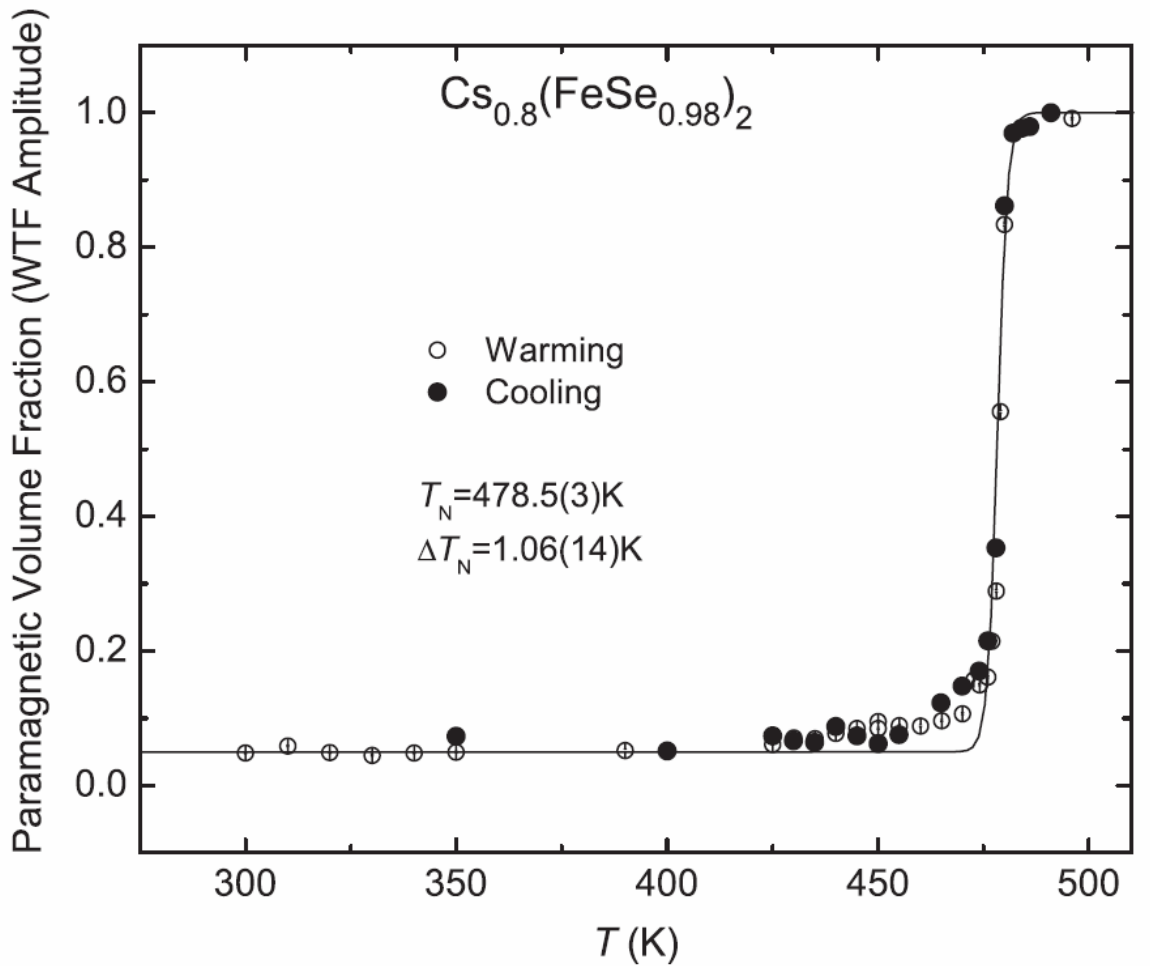


Gap=121 meV

Gap=69 meV

Gap= 26 meV

Coexistence of AFM and SC Orders: μ SR

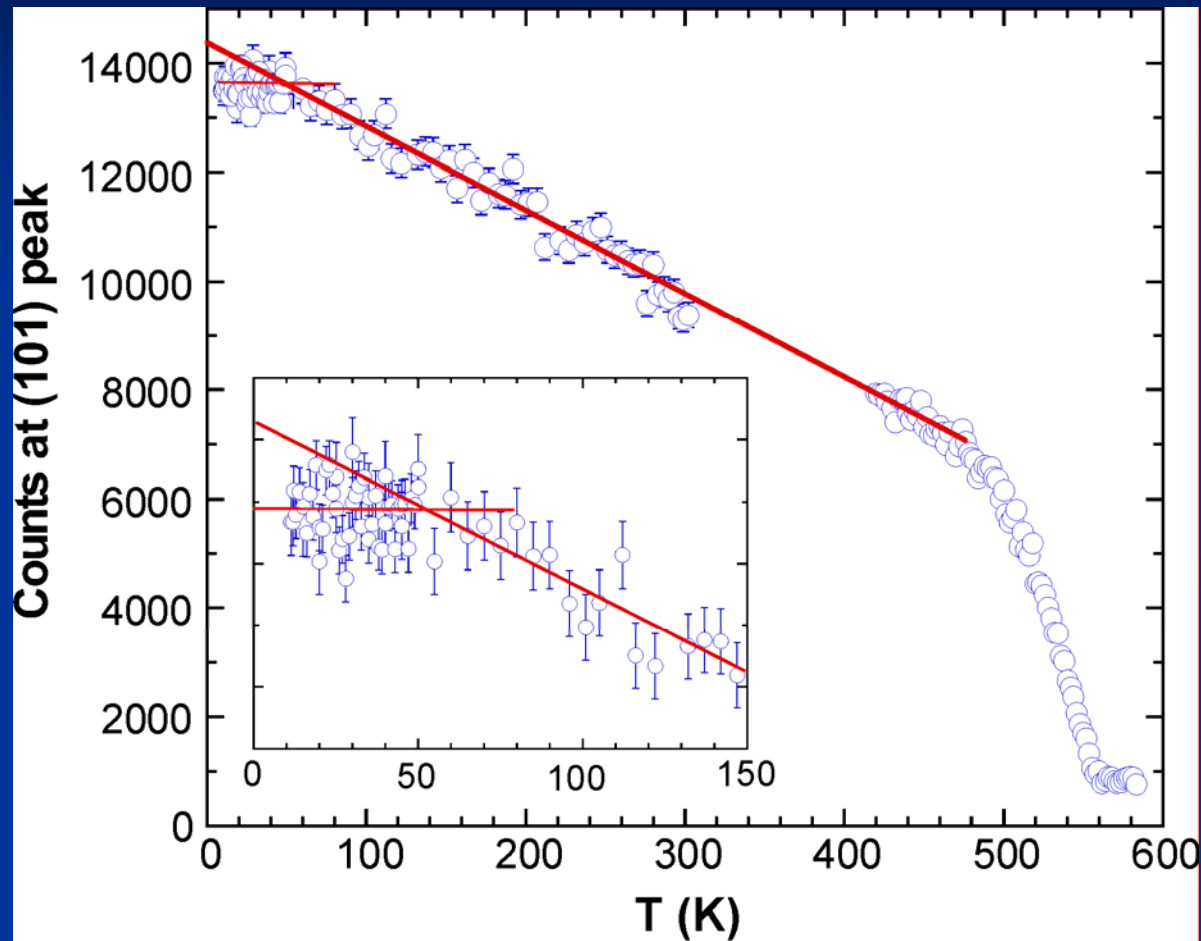


$\text{Cs}_{0.8}(\text{FeSe}_{0.98})_2$

$T_c = 29.6 \text{ K}$

$T_N = 478.5 \text{ K}$

Coexistence of AFM and SC Orders: neutron scattering



$\text{K}_{0.82}\text{Fe}_{1.626}\text{Se}_2$

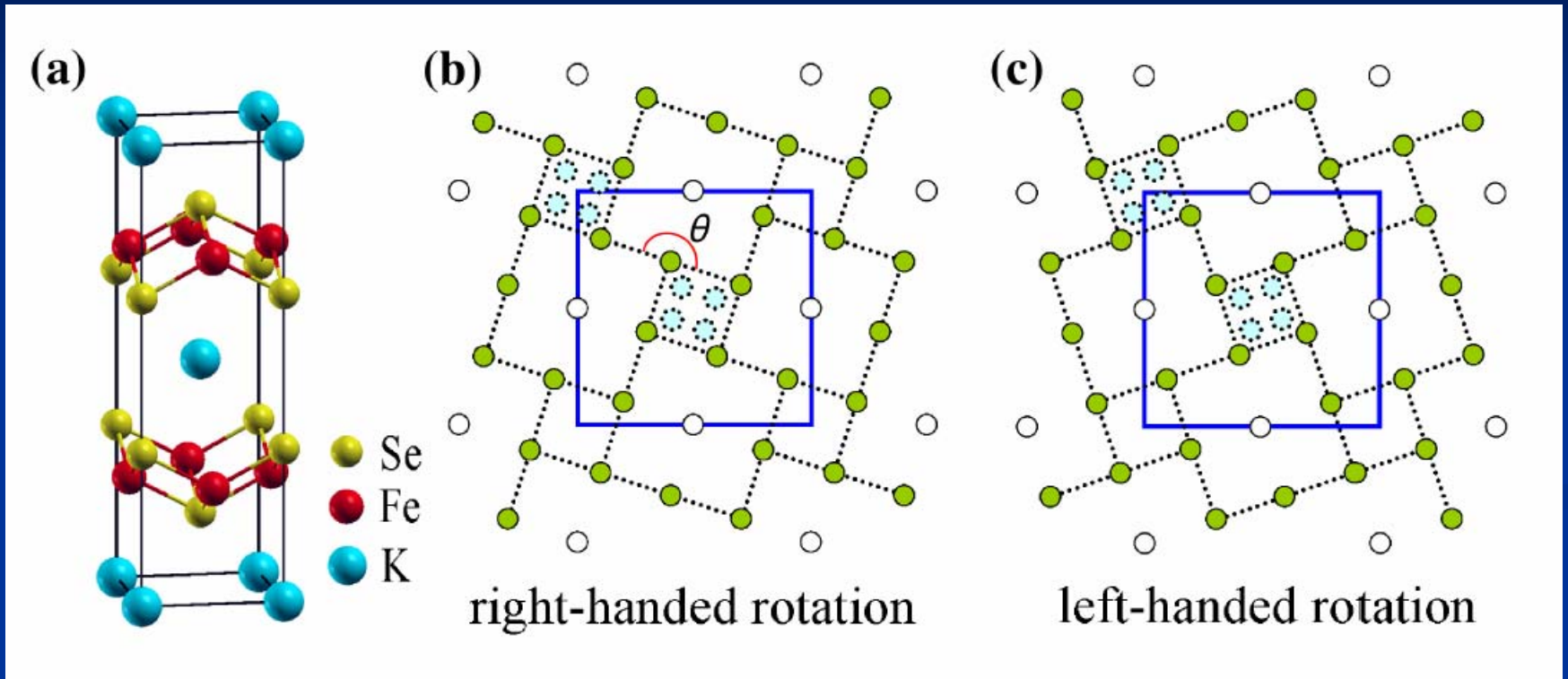
$T_c = 32\text{K}$

$T_N = 559\text{K}$

$m = 3.31 \mu_B / \text{Fe}$

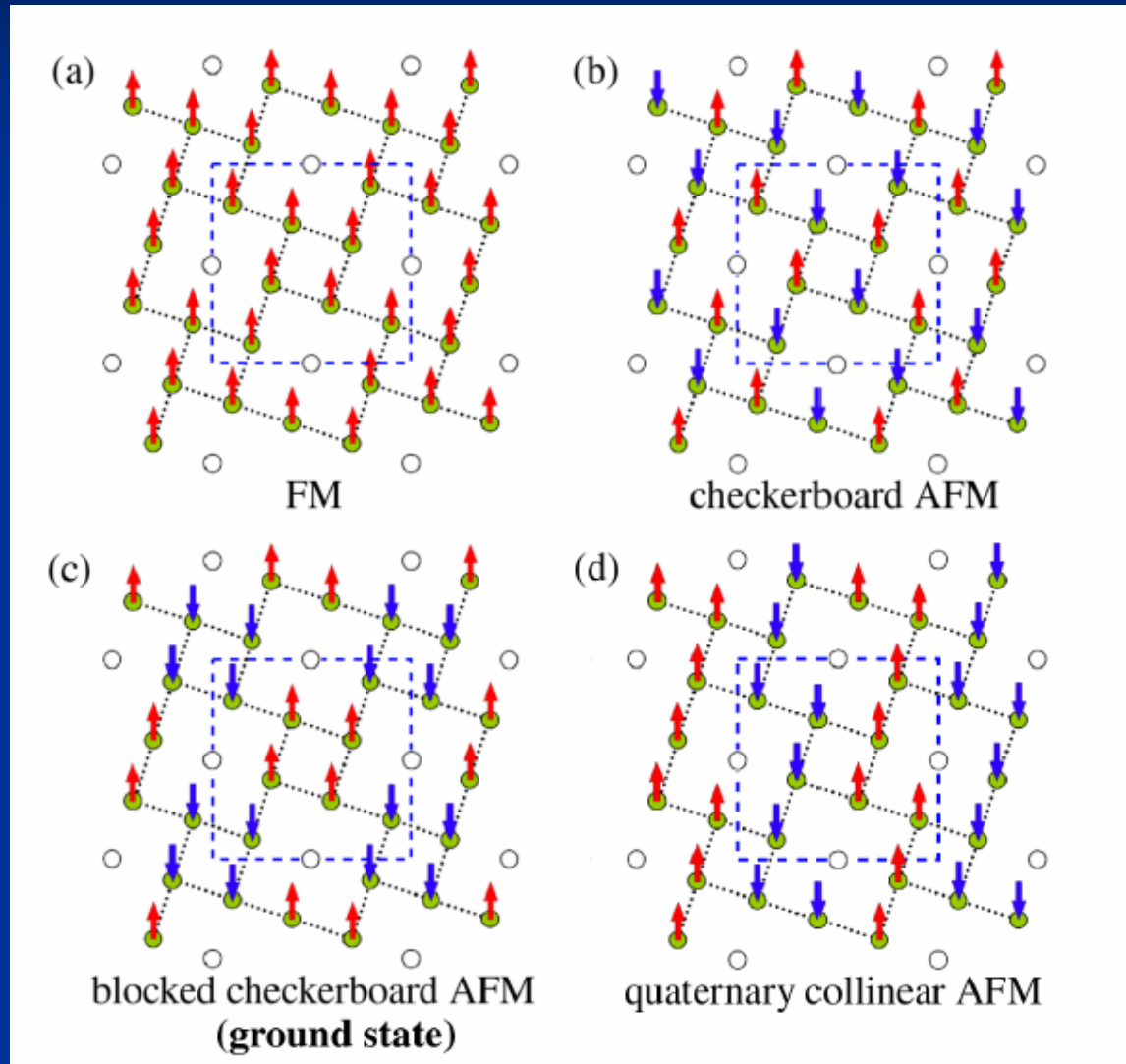
SC shielding 100%

One-fifth Fe vacancies $A_{0.8}Fe_{1.6}Se_2$: there is only one ordered vacancy structure but with left/right chirality

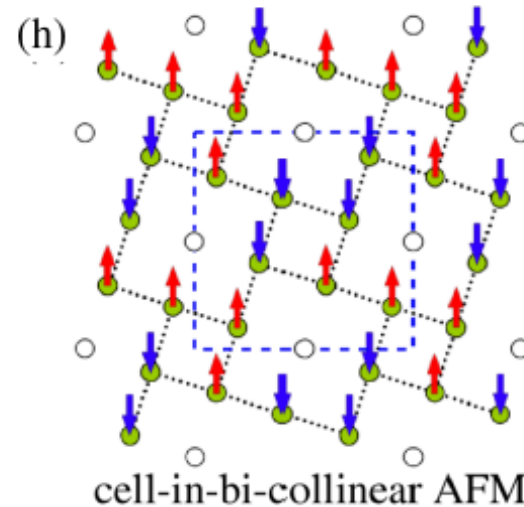
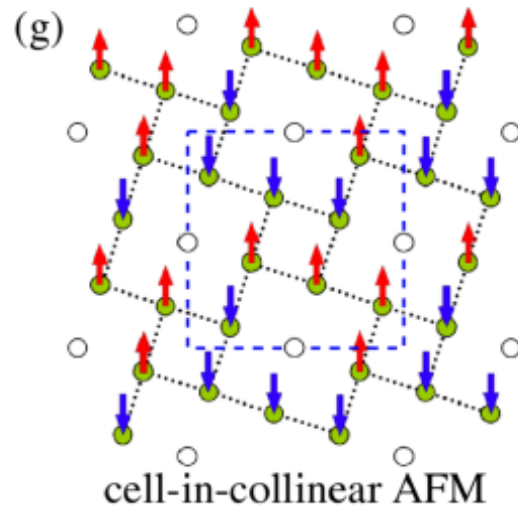
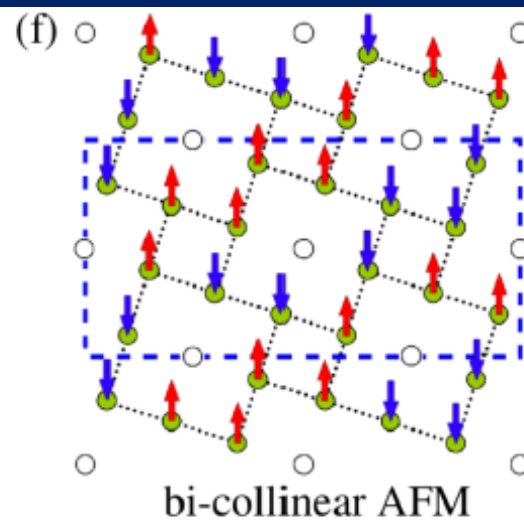
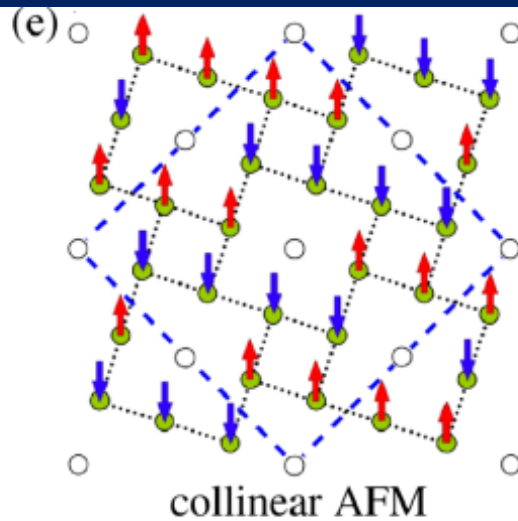


In this $\sqrt{5} \times \sqrt{5}$ lattice, the Fe atoms go into a blocked distribution from a uniform square distribution, in which the four closest Fe atoms form a block, whose bond distance is shorter than that of the uniform Fe square lattice, the chemical-bonding-driven tetramer lattice distortion.

Possible magnetic orders I



Possible magnetic orders II



Energies for different magnetic orders without structural distortions

■ nonmag :	0 meV/Fe	
■ fm:	-148 meV/Fe	
■ checkerboard :	-323 meV/Fe	
■ quaternary collinear:	-328 meV/Fe	
■ bi-collinear:	-335 meV/Fe	
■ cell-in-collinear:	-374 meV/Fe	
■ cell-in-bicollinear:	-378 meV/Fe	
■ Blocked checkerboard:	-416 meV/Fe	
■ collinear:	-431 meV/Fe	lowest

This shows the Se-bridged superexchange interaction J_2 plays a major role.

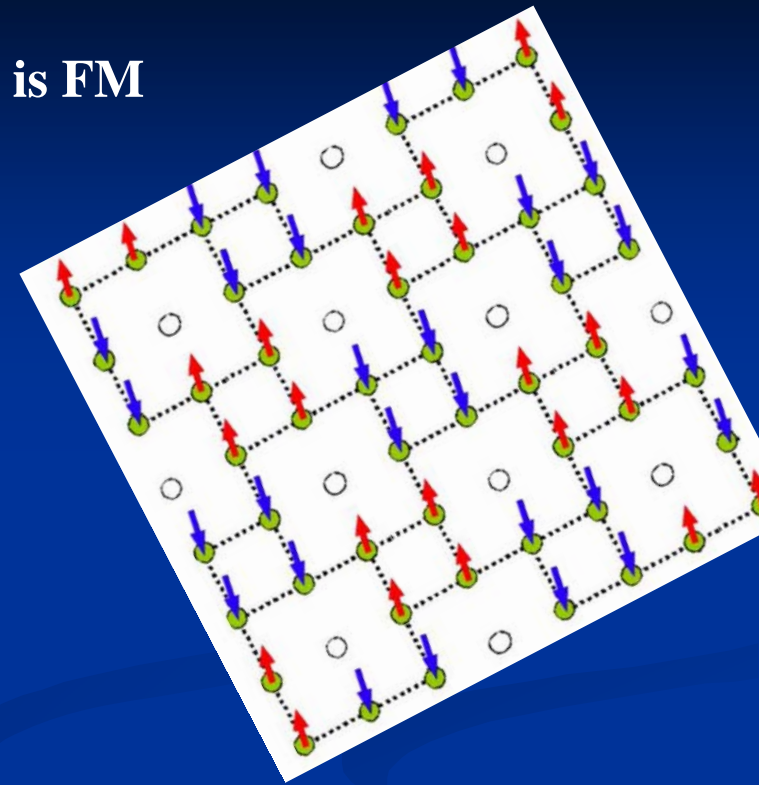
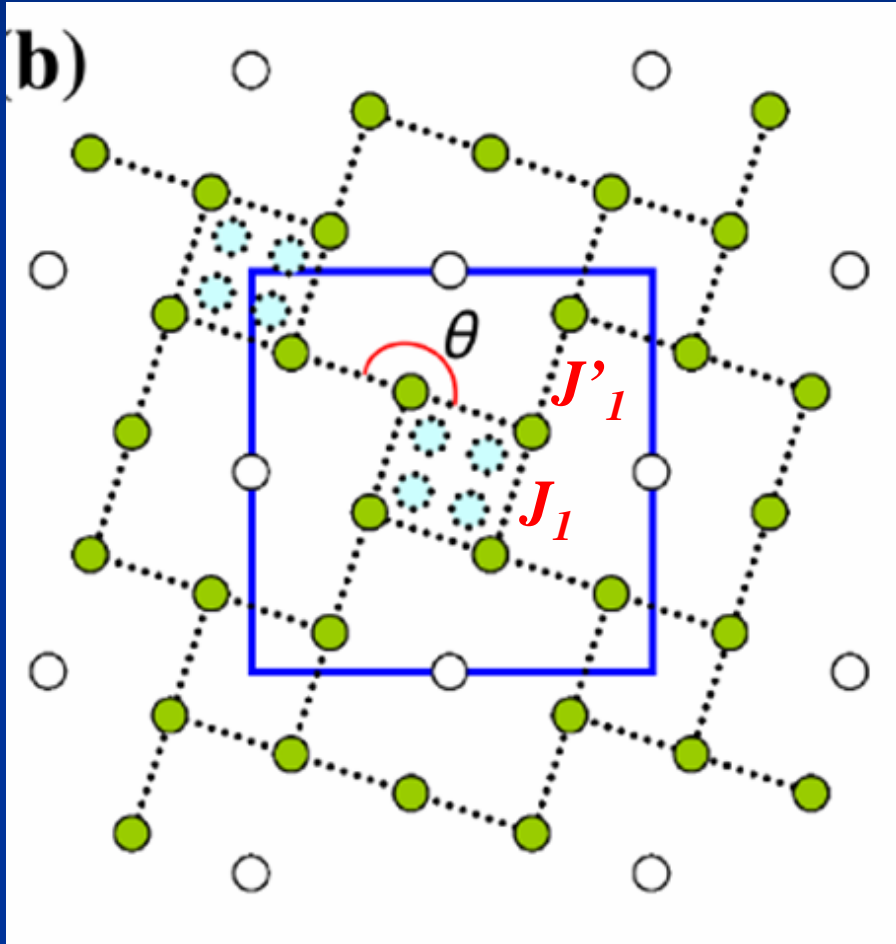
Energies for different magnetic orders after tetramer lattice distortion

■ nonmag :	0 meV/Fe	
■ fm:	-70 meV/Fe	
■ checkerboard :	-189 meV/Fe	
■ quaternary collinear:	-232 meV/Fe	
■ bi-collinear:	-229 meV/Fe	
■ cell-in-collinear:	-254 meV/Fe	
■ cell-in-bicollinear:	-267 meV/Fe	
■ Blocked checkerboard:	-342 meV/Fe	lowest
■ collinear:	-293 meV/Fe	

The chemical-bonding-driven effect, namely tetramer lattice distortion, competes over J_2

The blocked Neel order can be modeled by J_1 - J_2 - J_H -type interaction

Fe bond distance within a block is shortened, J_1 is FM



$$J_{1\text{intra}} = -0.0078 \text{ eV/S}^2$$

$$J_{2\text{intra}} = 0.0032 \text{ eV/S}^2$$

$$J_{1\text{inter}} = 0.0658 \text{ eV/S}^2$$

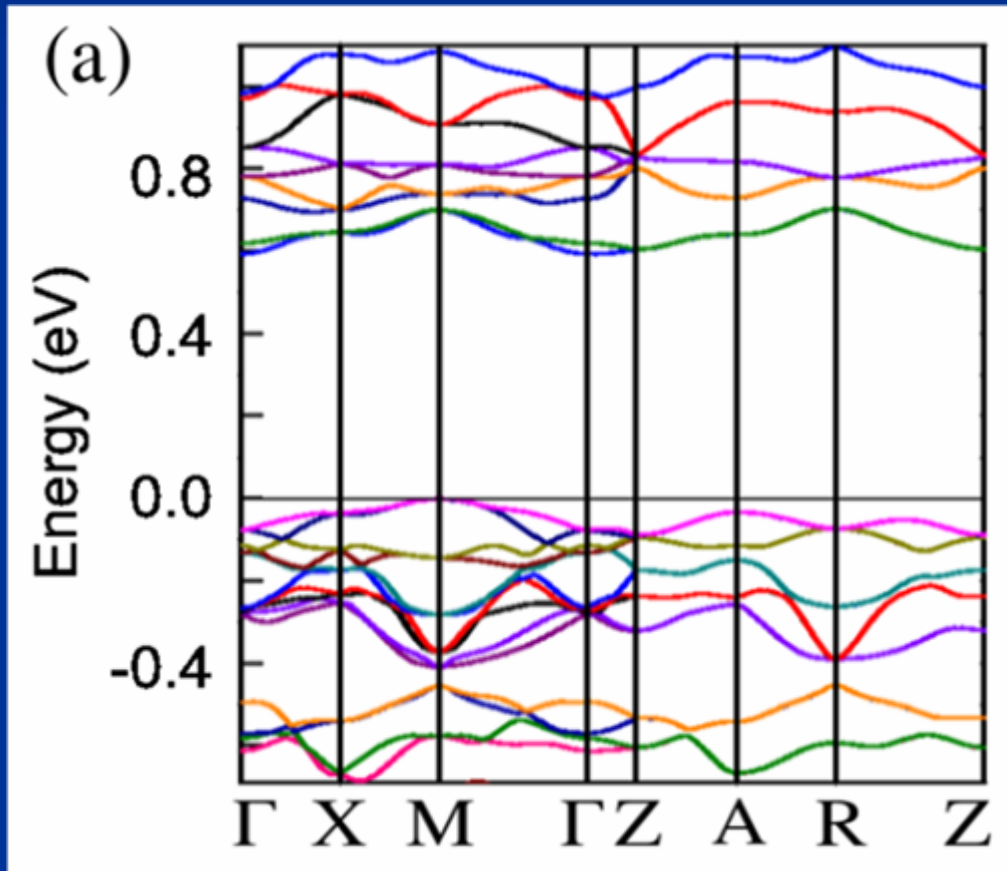
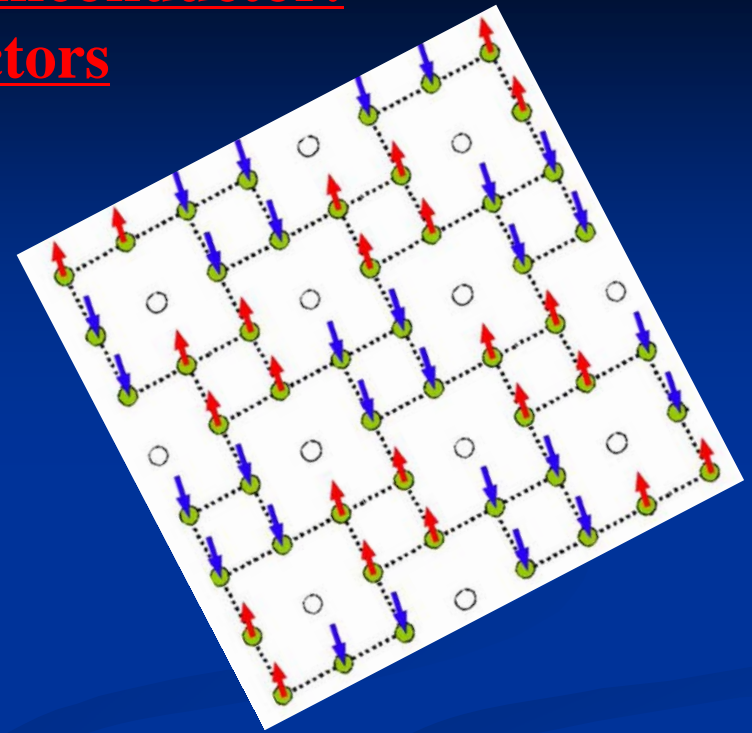
$$J_{2\text{inter}} = 0.10337 \text{ eV/S}^2$$

$\text{K}_{0.8}\text{Fe}_{1.6}\text{Se}_2$ is an antiferromagnetic semiconductor: an essential parent of the superconductors

Ordering moment:

DFT: $m = 3.37 \mu_B / \text{Fe}$

Neutron: $m = 3.31 \mu_B / \text{Fe}$



Gap Δ	$\text{A}_{0.8}\text{Fe}_{1.6}\text{Se}_2$
594 meV	K
571 meV	Rb
548 meV	Cs
440 meV	Tl

Formation energies

We have calculated the formation energy of $\text{K}_{0.8+x}\text{Fe}_{1.6-x/2}\text{Se}_2$, defined by $(0.8 + x)E_K + (1.6 - x/2)E_{Fe} + 2E_{Se} - E_x$, where E_K , E_{Fe} , and E_{Se} are the atomic energies of K, Fe, and Se, respectively, and E_x is the total energy of $\text{K}_{0.8+x}\text{Fe}_{1.6-x/2}\text{Se}_2$. For $x = 0$, 0.2 and -0.4 , corresponding to $\text{K}_{0.8}\text{Fe}_{1.6}\text{Se}_2$, $\text{KFe}_{1.5}\text{Se}_2$, and $\text{K}_{0.4}\text{Fe}_{1.8}\text{Se}_2$, we find that the formation energies are 16.652, 16.564, and 16.632 eV, respectively. Here

$\text{K}_{0.8}\text{Fe}_{1.6}\text{Se}_2$: 16.652 eV

$\text{KFe}_{1.5}\text{Se}_2$: 16.564 eV

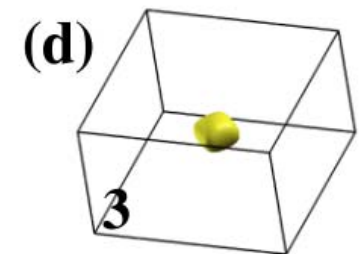
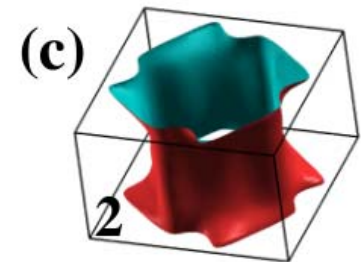
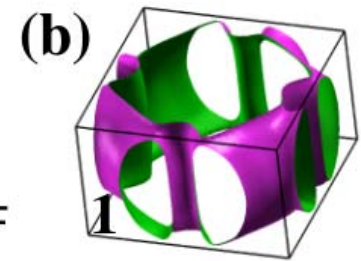
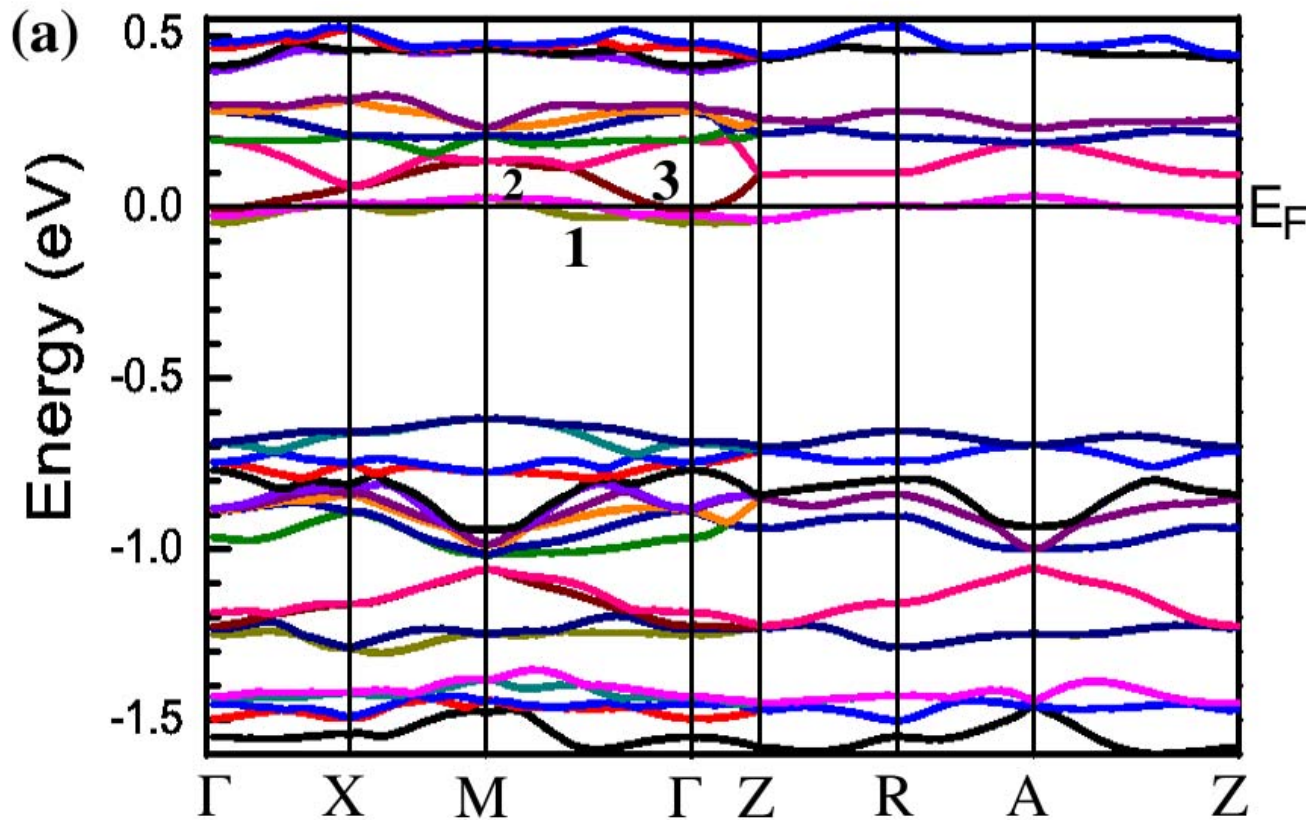
$\text{K}_{0.4}\text{Fe}_{1.8}\text{Se}_2$: 16.632 eV

Fe_2Se_2 : 16.611 eV

$\text{TlFe}_{1.5}\text{Se}_2$: 16.334 eV

$\text{Tl}_{0.8}\text{Fe}_{1.6}\text{Se}_2$: 16.442 eV

KFe_{1.6}Se₂ is electron doped antiferromagnetic semiconductor



Electronic structure of KFe_{1.6}Se₂

Fermi surface in the folded Brillouin zone

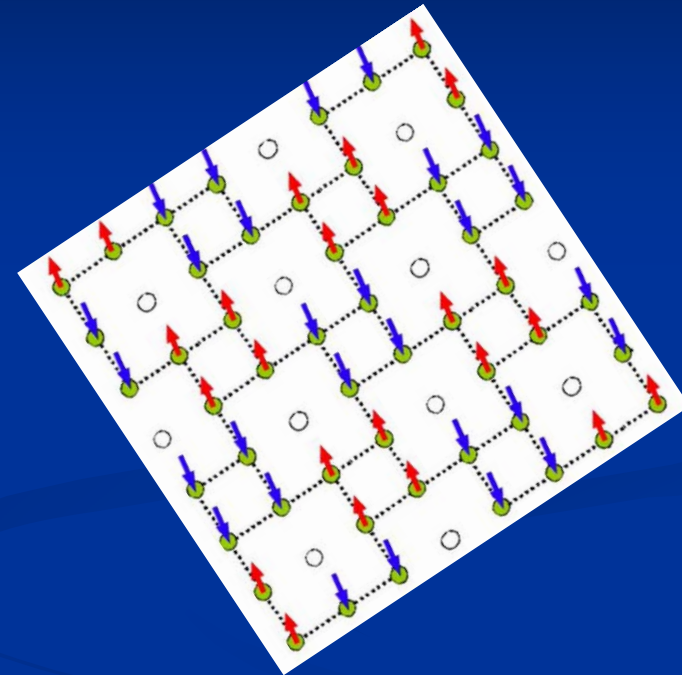
Minimal Model:

The moments contributed from the valence bands are charge fluctuation free (localized) due to the band gap

Effective AFM interaction
between block spins

Block spin

$$H = \sum_{k\alpha} \varepsilon_{\alpha k} c_{\alpha k}^\dagger c_{\alpha k} + J \sum_{\langle ij \rangle} \mathbf{S}_i \cdot \mathbf{S}_j + \sum_{ij\alpha} (J' \delta_{\langle ij \rangle} - K \delta_{i,j}) c_{\alpha,i}^\dagger \frac{\sigma}{2} c_{\alpha,i} \cdot \mathbf{S}_j,$$



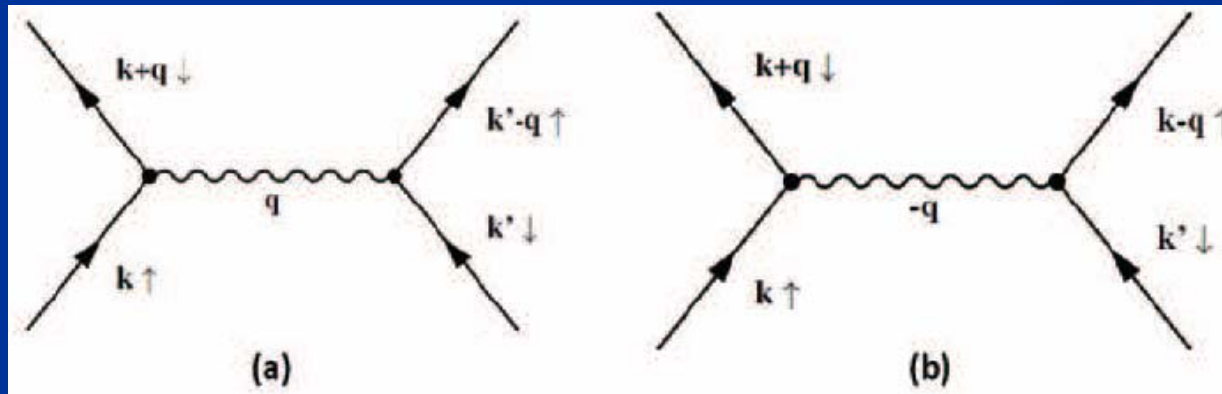
AFM coupling between local
spin and itinerant electrons
on neighboring blocks

FM coupling between local spin and
itinerant electrons within each block

Superconducting Pairing in $\text{KFe}_{2-x}\text{Se}_2$:

If a strong AFM ordered state coexists with a SC state microscopically

- the superconducting pairs are most likely to be formed just by mediating coherent spin wave (like phonon)
- The staggered moments provide a background periodic potential above the crystal periodic potential



The next key issue in iron-pnictides

- **Orbital degrees:** characterize the role of 5 Fe-3d orbitals and 3 As-4p orbitals in iron-pnictides;
- **Microscopic model including orbital-characterization.**

5.

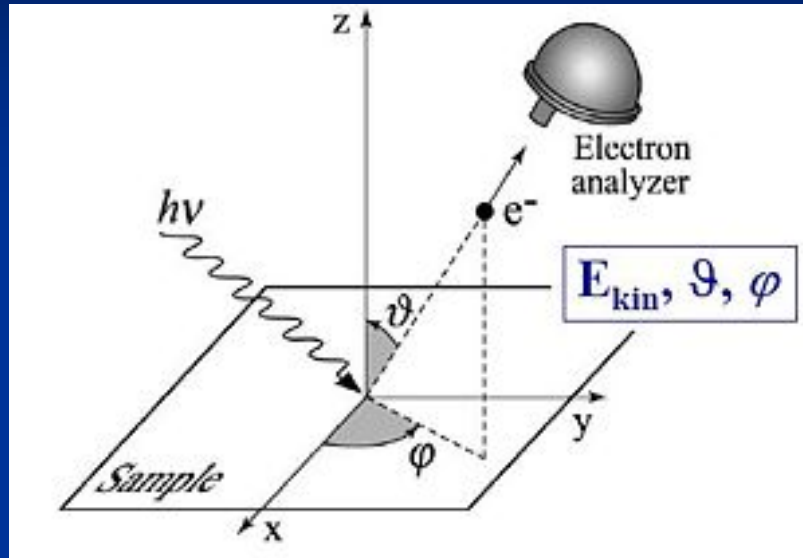
The cleaved surface structure of

I. BaFe_2As_2 (001) surface

II. SrFe_2As_2 and CaFe_2As_2 (001) surface

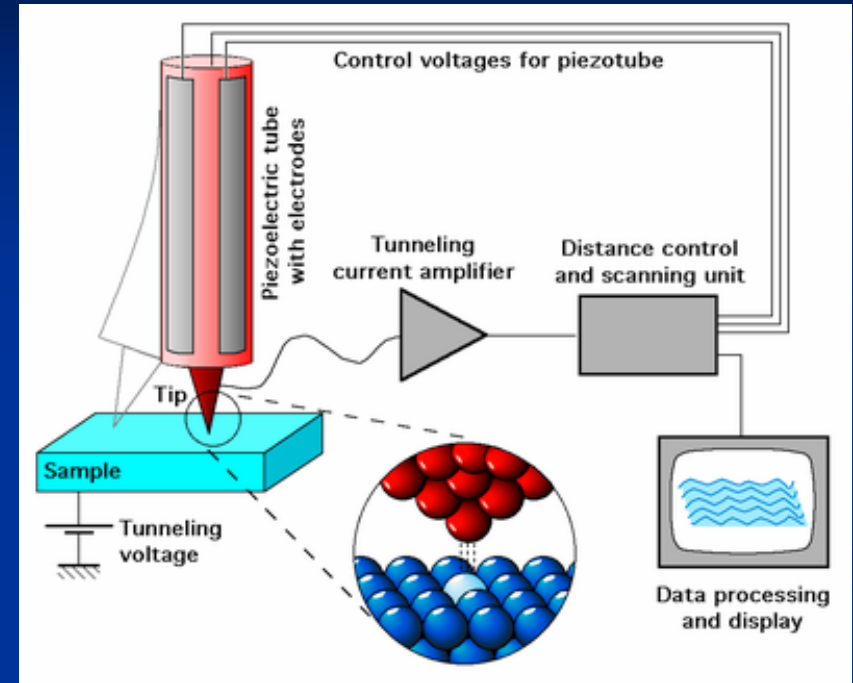
[arXiv:0909.5136](https://arxiv.org/abs/0909.5136); PRB 81, 193409 (2010).

Experiment measurement



ARPES

- ◆ directly determine the electronic structure
- ◆ surface-sensitive
- ◆ The surface electronic properties will strongly influence the detection.



STM

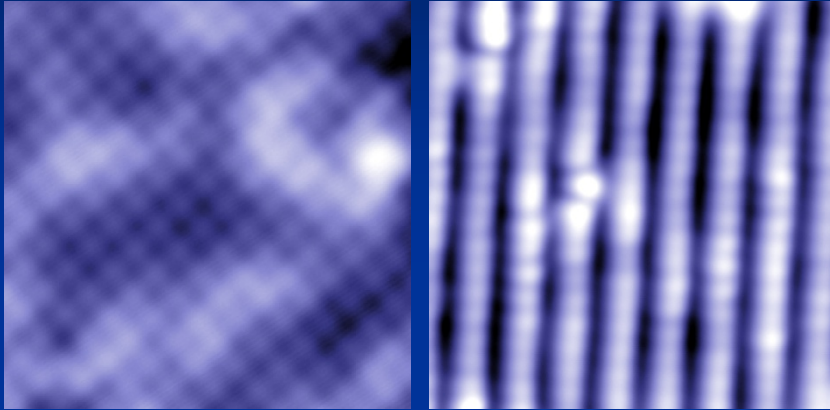
- ◆ atomic scale resolution
- ◆ simultaneously probe topography and low-energy electronic structure at surface

STM patterns of BaFe₂As₂ in experiments

20K

Cleaving temperature

120K



BaFe₂As₂

$\sqrt{2} \times \sqrt{2}$

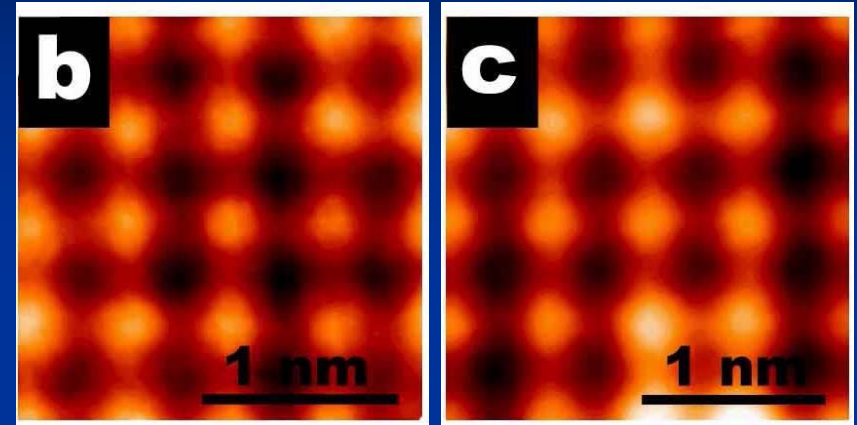
Co-doping

1×2

The STM images show that the cleaved surface is in $\sqrt{2} \times \sqrt{2}$ order for parent compound, and it will gradually evolve to 1×2 order with increasing of Co-doping.

As-termination was suggested

V.B. Nascimento et al., arXiv:0905.3194



BaFe₂As₂

$\sqrt{2} \times \sqrt{2}$

BaFe_{1.8}Co_{0.2}As₂

The STM images show $\sqrt{2} \times \sqrt{2}$ order both in parent compound and Co-doped materials.

Ba-termination was suggested

Hui Zhang et al., arxiv:0908.1710

Cleaved surface structures

1x1 structure

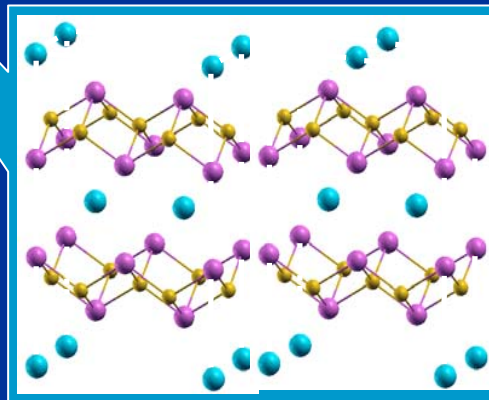
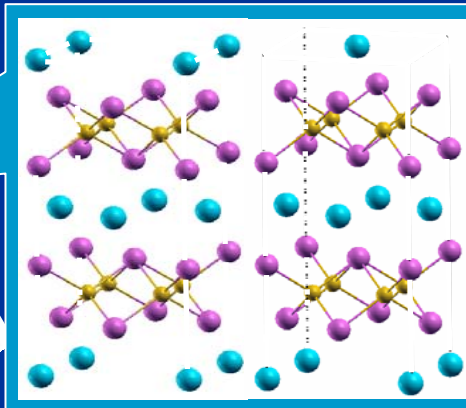
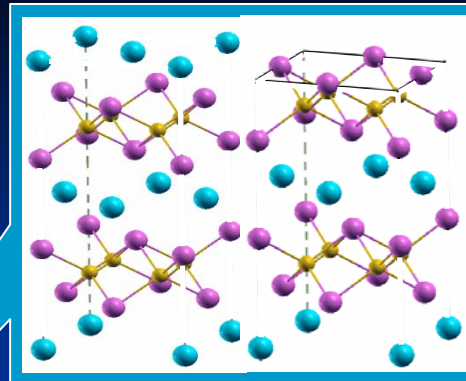
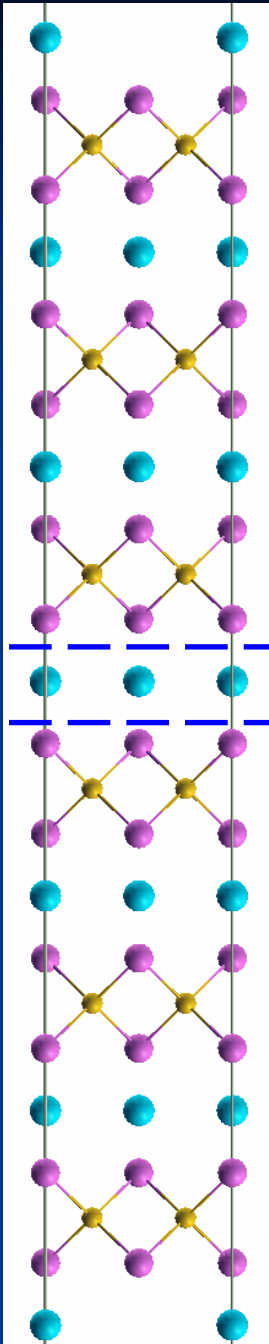
Both of the two cleaved surfaces are 1x1 structure. One side is "A"-terminated, and the other one is As-terminated.

$\sqrt{2} \times \sqrt{2}$ structure --- "A"-terminated

Half of the "A" atoms are on each exposed surfaces.

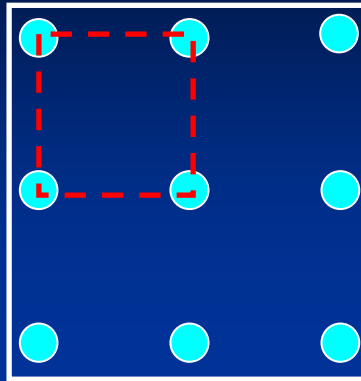
1x2 structure --- "A"-terminated

Half of the "A" atoms are on each exposed surfaces.

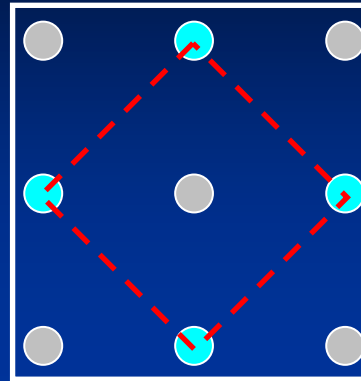




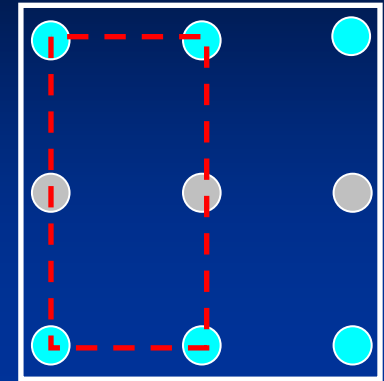
For "A"-termination



1x1



$\sqrt{2} \times \sqrt{2}$

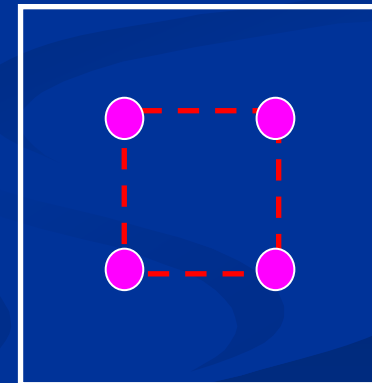


1x2

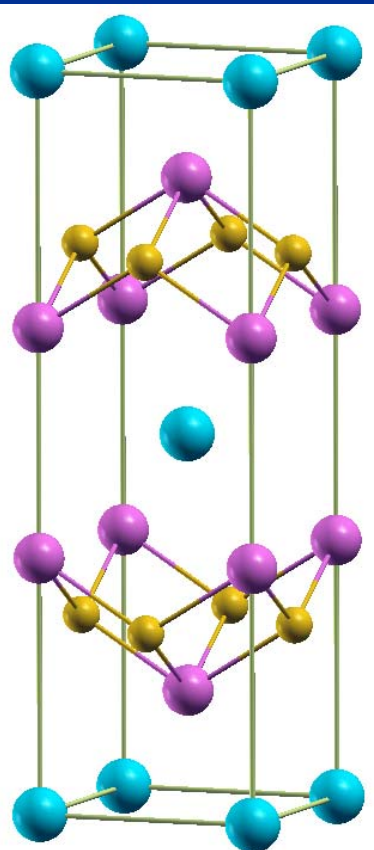
Note: in bulk both Ba atoms and As atoms sit at a square lattice (~4angs x 4angs).

For As-termination

➤ Because of **the same periodicity** with "A" atoms in bulk, the basic cell of As surface is **1x1** structure. "A" and As planes can be treated on **the same footing** for the **STM** data.



1x1

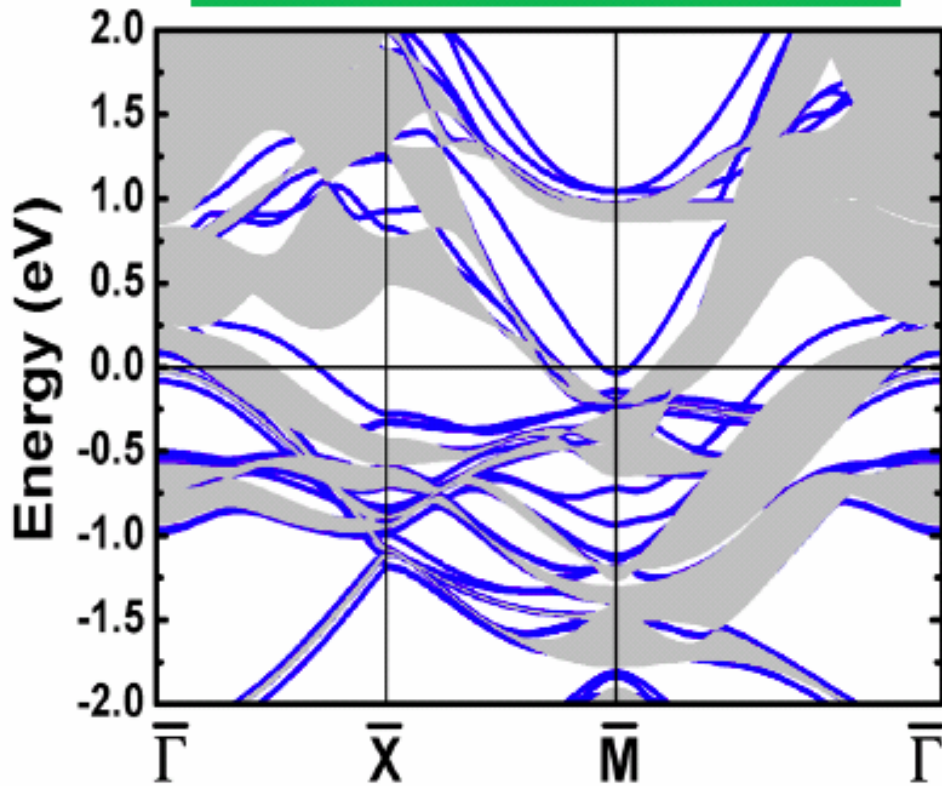


AFe ₂ As ₂ (001)	tetragonal			orthorhombic		
	($\sqrt{2} \times \sqrt{2}$)	(1x2)	(1x1)	($\sqrt{2} \times \sqrt{2}$)	(1x2)	(1x1)
BaFe ₂ As ₂	-411.6	-217.8	0	-534.8	-312.0	0
SrFe ₂ As ₂	-217.0	-167.8	0	-314.6	-219.0	0
CaFe ₂ As ₂	-34.0	-97.0	0	-185.4	-189.2	0

- For Ba122 it is ($\sqrt{2} \times \sqrt{2}$)-ordered dominantly;
- For Ca122 it is mainly (1x2)-ordered with partly ($\sqrt{2} \times \sqrt{2}$)-order coexisting;
- for Sr122 it is mainly ($\sqrt{2} \times \sqrt{2}$)-ordered with partly (1x2)-order coexisting as the energy difference between the (1x2) and ($\sqrt{2} \times \sqrt{2}$) orders becomes small and further reverse in the line of Ba, Sr, and Ca.

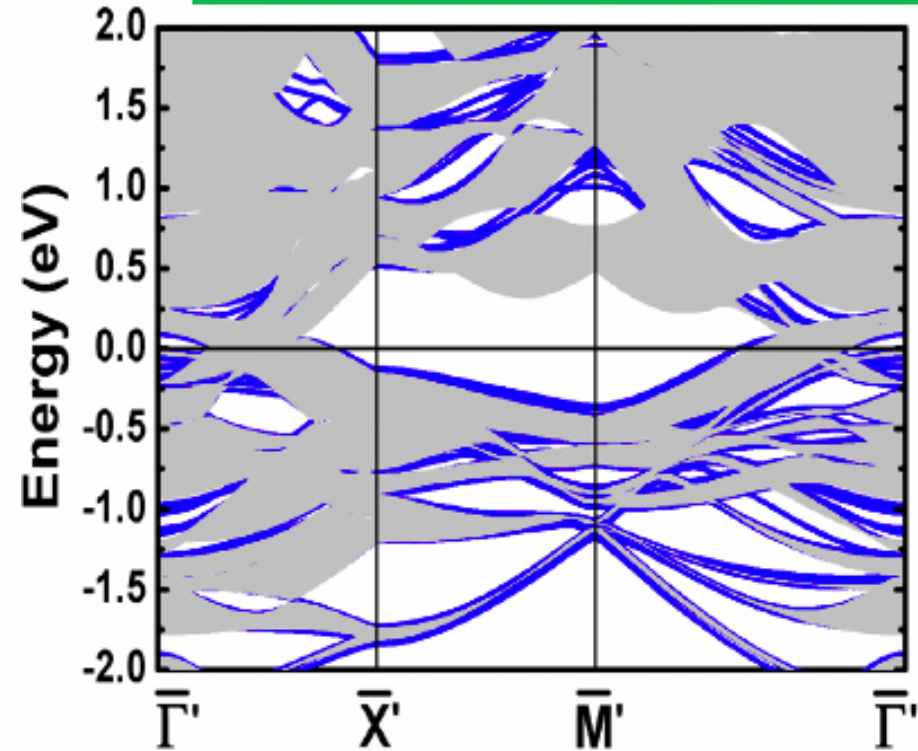
1x2-ordered surface unit cell in magnetic orthorhombic phase is 2x4

As-terminated (1x1) NM



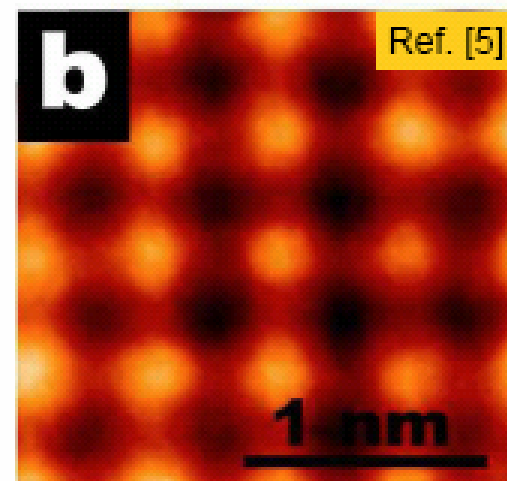
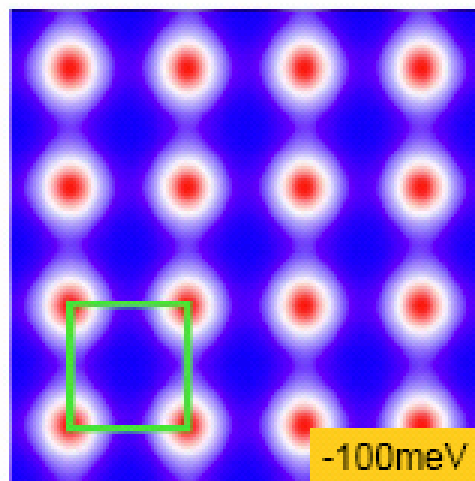
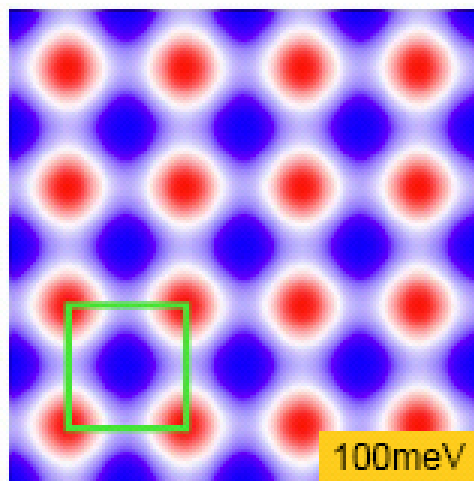
The surface state may induce a large Fermi surface sheet between Gamma and M or X

Ba-terminated ($\sqrt{2} \times \sqrt{2}$) NM

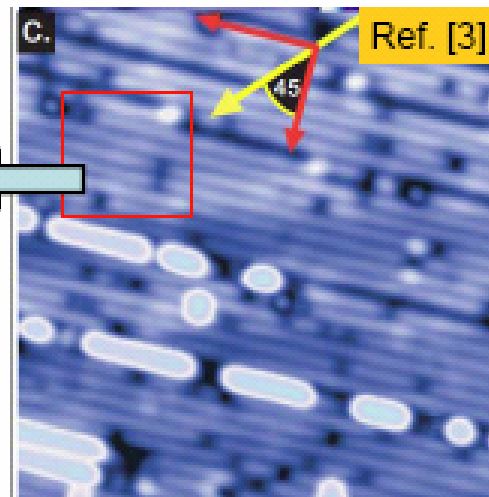
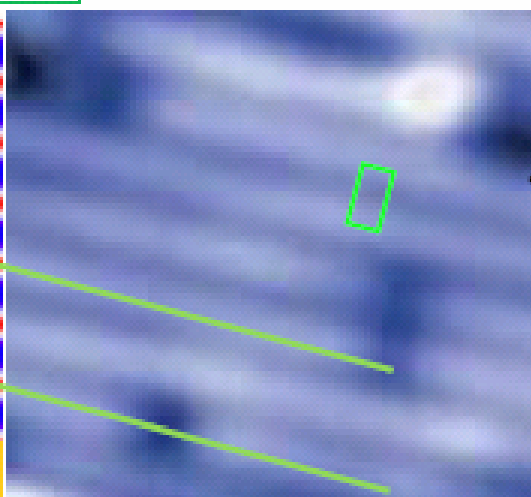
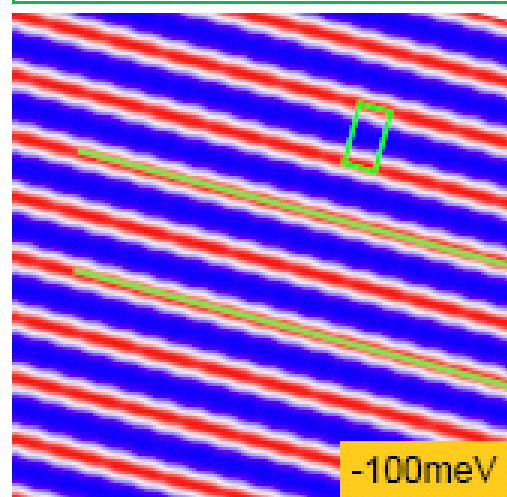


Unpolarized, no significant surface states

Ba-terminated ($\sqrt{2}\times\sqrt{2}$) NM



Sr-terminated (1x2) Col.-AFM

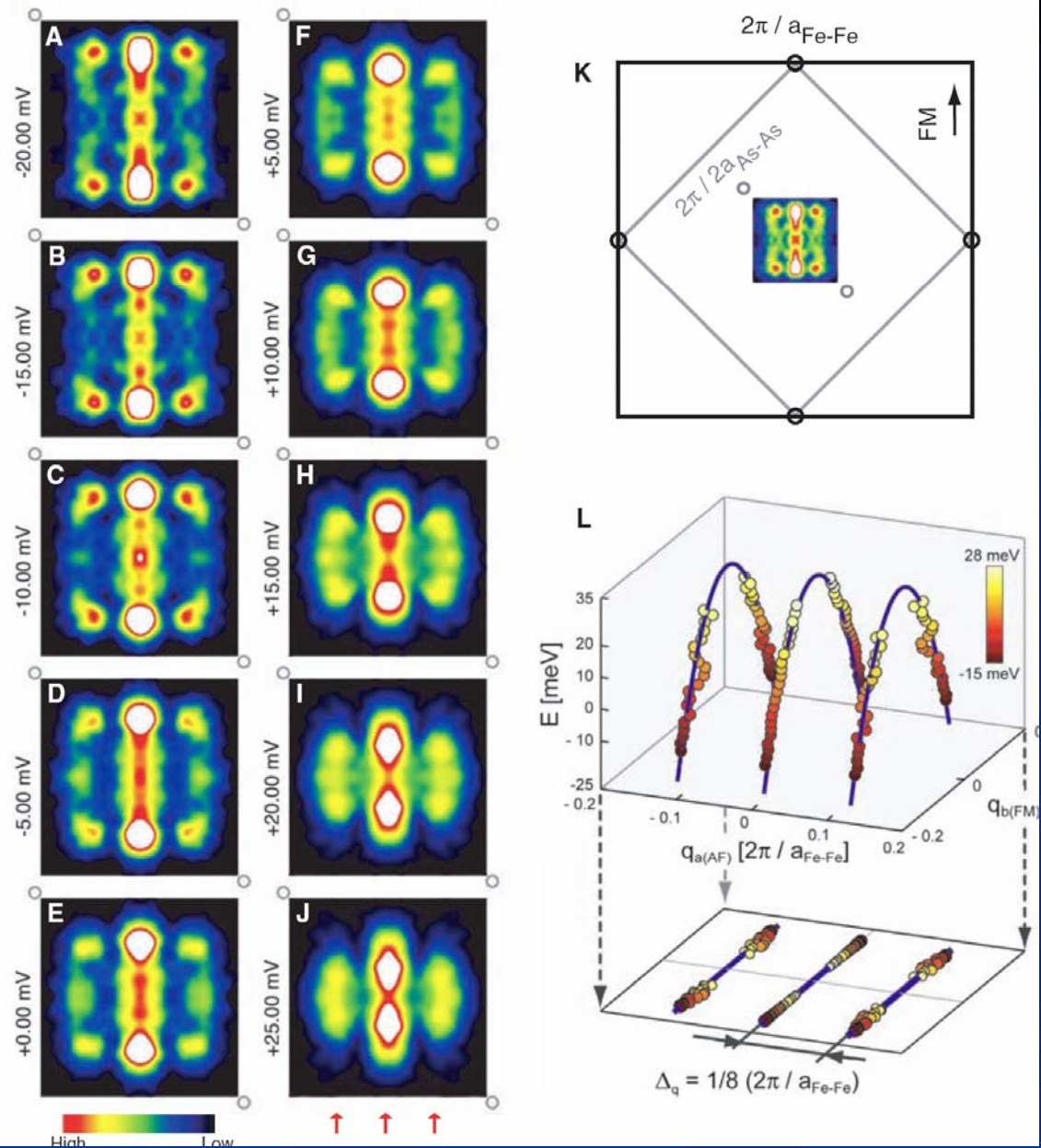


Nematic Electronic Structure in the “Parent” State of the Iron-Based Superconductor $\text{Ca}(\text{Fe}_{1-x}\text{Co}_x)_2\text{As}_2$

T.-M. Chuang,^{1,2*} M. P. Allan,^{1,3*} Jinho Lee,^{1,4} Yang Xie,¹ Ni Ni,^{5,6} S. L. Bud’ko,^{5,6}
G. S. Boebinger,² P. C. Canfield,^{5,6} J. C. Davis^{1,3,4,7†}

The mechanism of high-temperature superconductivity in the newly discovered iron-based superconductors is unresolved. We use spectroscopic imaging–scanning tunneling microscopy to study the electronic structure of a representative compound $\text{CaFe}_{1.94}\text{Co}_{0.06}\text{As}_2$ in the “parent” state from which this superconductivity emerges. Static, unidirectional electronic nanostructures of dimension eight times the inter–iron-atom distance $a_{\text{Fe-Fe}}$ and aligned along the crystal a axis are observed. In contrast, the delocalized electronic states detectable by quasiparticle interference imaging are dispersive along the b axis only and are consistent with a nematic α_2 band with an apparent band folding having wave vector $\vec{q} \cong \pm 2\pi/8a_{\text{Fe-Fe}}$ along the a axis. All these effects rotate through 90 degrees at orthorhombic twin boundaries, indicating that they are bulk properties. As none of these phenomena are expected merely due to crystal symmetry, underdoped ferropnictides may exhibit a more complex electronic nematic state than originally expected.

Fig. 3. (A to J) The Fourier transforms $g(\vec{q}, E)$ of the $g(\vec{r}, E)$ images in fig. S4 reveal the highly C_2 -symmetric structure of the QPI patterns. The data shown here are from a larger 94-nm square FOV. Six dispersing peaks are clearly visible. The two center peaks disperse in a hole-like fashion along the b axis only. Pairs of side peaks mimic their dispersion at $\vec{q} \approx \pm 1/8 (2\pi/a_{\text{Fe-Fe}})$. The open circles at two corners of each image represent the \vec{q} -space locations of the 1×2 reconstruction. Red arrows indicate the three parallel dispersion trajectories. **(K)** Overview of the different directions and length scales in \vec{q} space. The dispersing QPI vectors are short compared with the $2\pi/a_{\text{Fe-Fe}}$ box that spans all scattering vectors in the first Fe-Fe Brillouin zone (the large black box). The small gray box indicates the first As-As reciprocal unit cell. FM indicates the b axis direction along which spin correlations are ferromagnetic. **(L)** The hole-like dispersion of QPI, plotted in \vec{q}_b, \vec{q}_a, E space. Circles mark the positions of the six dispersion peaks extracted from each $g(\vec{q}, E)$ image; the blue lines are the parabolic fit for QPI. Projections to the (\vec{q}_b, \vec{q}_a) plane emphasize how unidirectional the dispersions are along the b axis. The side peaks are at $\pm 1/8 (2\pi/a_{\text{Fe-Fe}})$, suggesting an intimate relation between the unidirectional QPI modulations and unidirectional static electronic structure in Fig. 2.



We think that these observations result from 2x4 magnetic surface structure rather than the pure bulk electronic correlation effect.

Questions to address in this talk

1. Origin of a local moment around Fe atom?

Answer: The Hund's rule coupling among the five Fe-3d orbitals.

2. The mechanism underlying magnetic structures?

Answer: As(Se, Te)-bridged superexchange antiferromagnetic interactions.

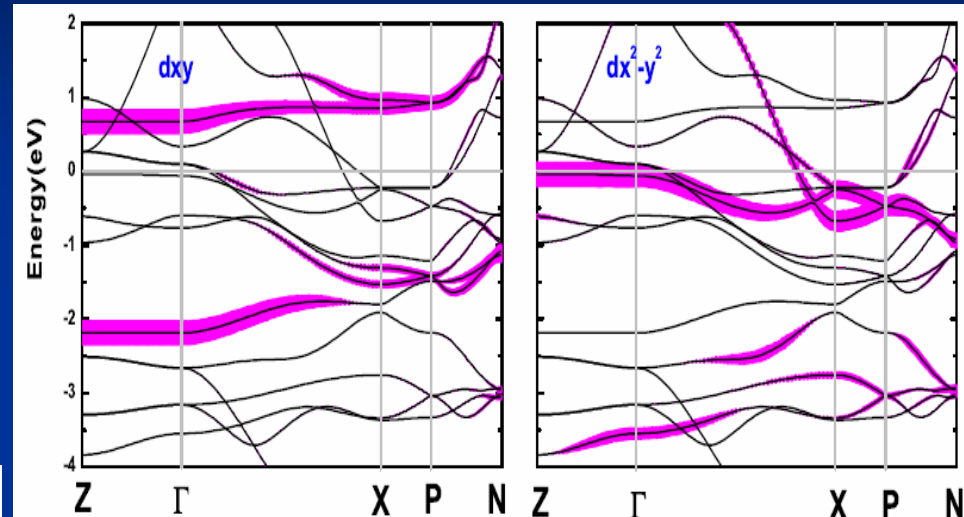
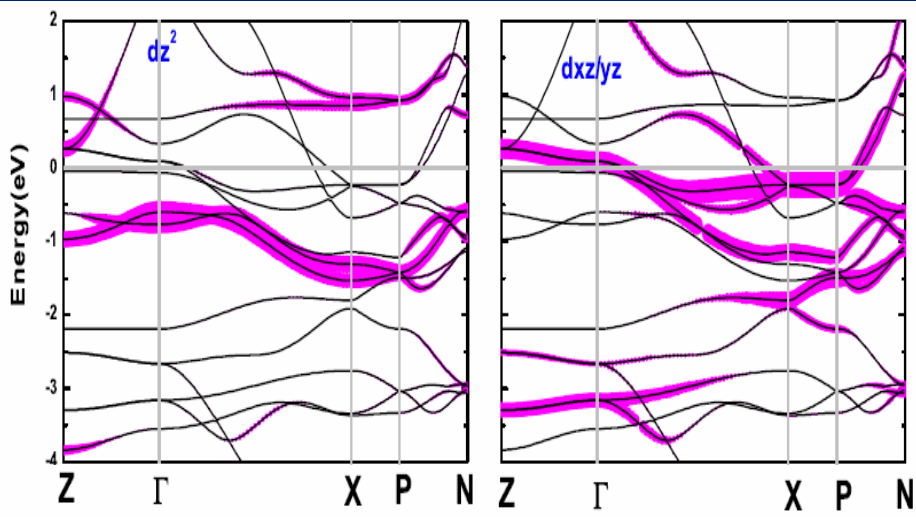
We are going to show that these two answers are universal to all the iron- pnictides or chalcogenides

Summary:

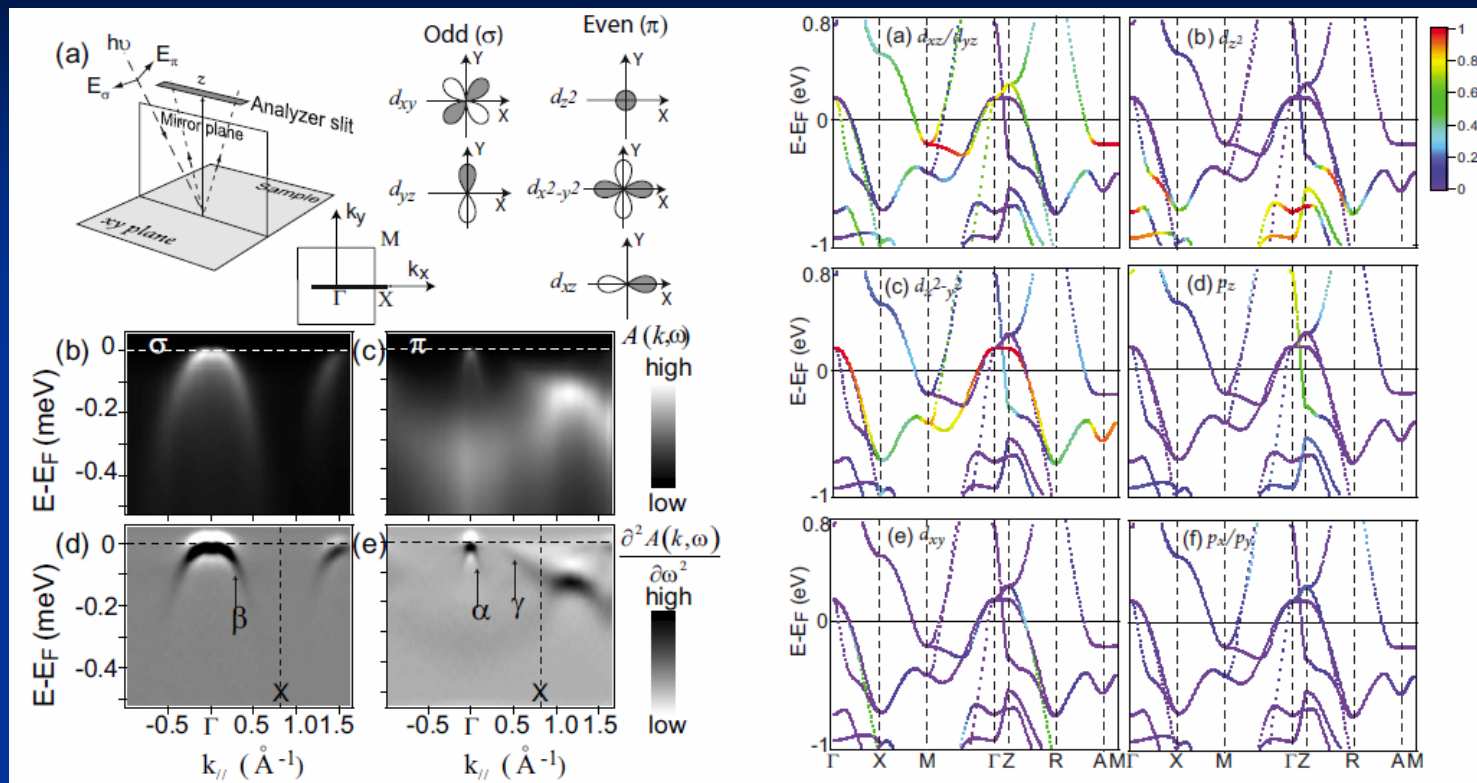
1. The parent compounds of Fe-based superconductors are quasi-2-dimensional antiferromagnetic semimetals or semiconductors;
2. The Hund's rule coupling is the dominate interaction for the formation of local moment and is important for the description of charge dynamics;
3. As(Se, Te)-bridged superexchange antiferromagnetic interactions between Fe-Fe fluctuating local moments play a substantial role in forming magnetic orders.

Thank you!

Orbital Projection and Calculated parameters

BaFe₂As₂

AFe ₂ As ₂	State	ρ		f_p		γ		χ_p	Coupling		
		hole	electron	Cal.	Exp.	Cal.	Exp.		J_1	J_2	J_z
BaFe ₂ As ₂	NM	2.54	2.54	25392	12900[108]	9.26	37[109], 16[97], 6.1 [103]	1.60	27.2	33.1	5.6
	Col	0.69	0.52	5469	4660[108]	5.68					
SrFe ₂ As ₂	NM	3.33	3.33	27386	13840[108]	7.71	6.5	1.33	18.7	31.4	7.8
	Col	0.46	0.27	6736	4750[108]	4.52					
CaFe ₂ As ₂	NM	4.21	4.21	20883		9.31	8.2	1.60	5.53	23.3	9.4
	Col	0.26	0.23	8385		2.87					

FeTe_{0.66}Se_{0.34}(NM)

F. Chen et al., PRB 81, 014526 (2010)

Near the Fermi energy,

the α band $\sim dxz/dyz$ orbitals, which should be purely dxz along the Γ -X direction

the β band $\sim dxz$ and dyz orbitals, and some dxy orbitals

the γ band $\sim dx^2-y^2$ orbital

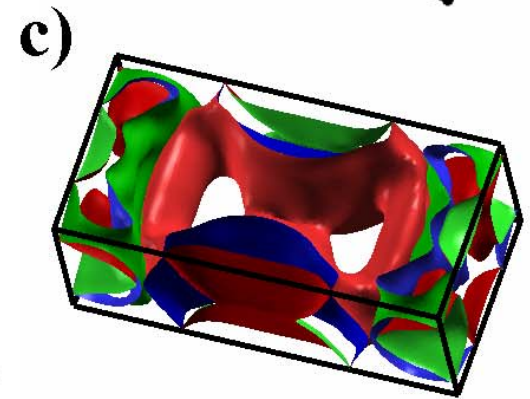
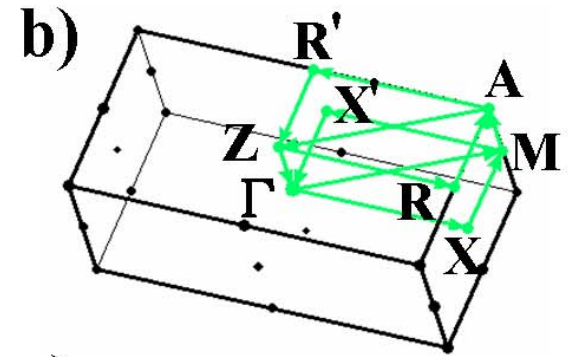
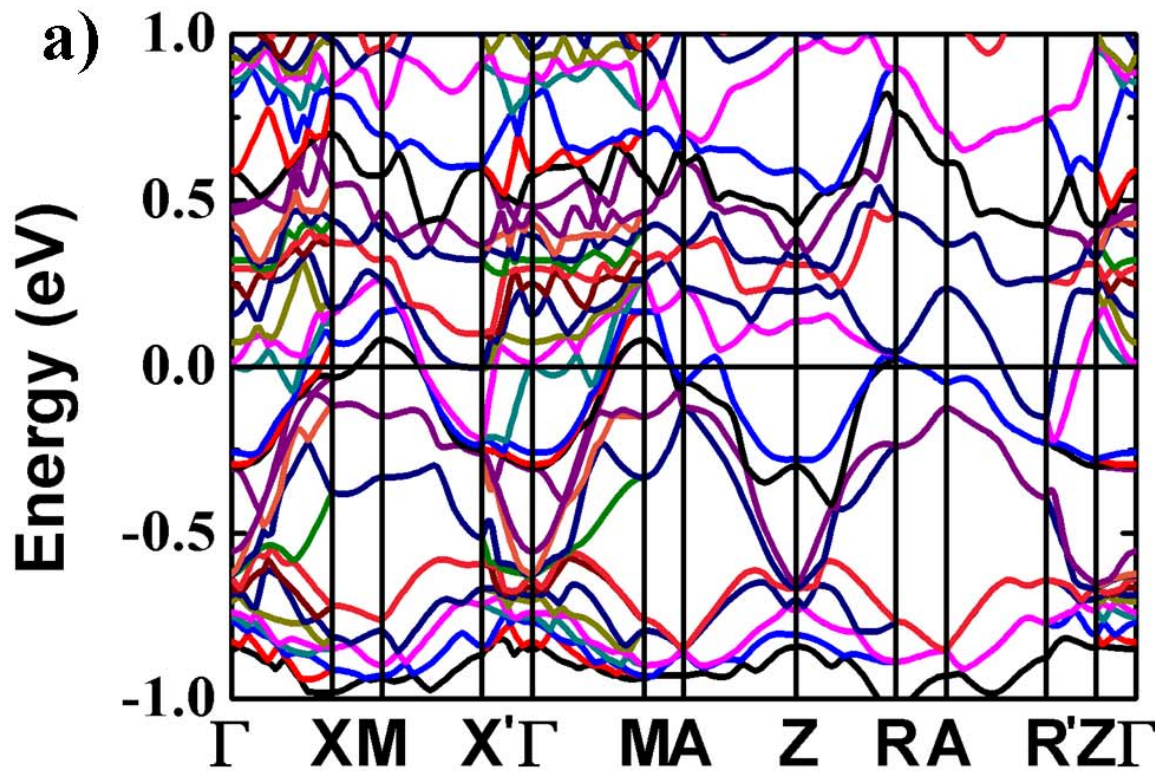
Along the Γ -Z direction,

$\sim pz$ and dx^2-y^2 orbital (even symmetry, π experimental geometry).

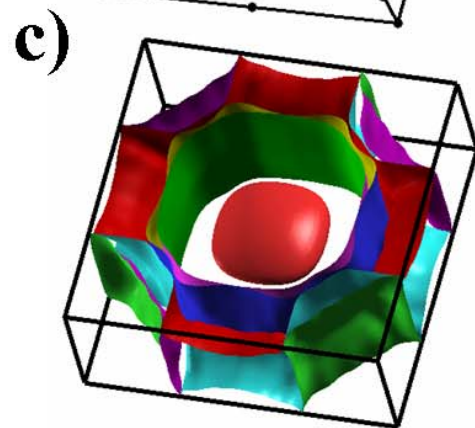
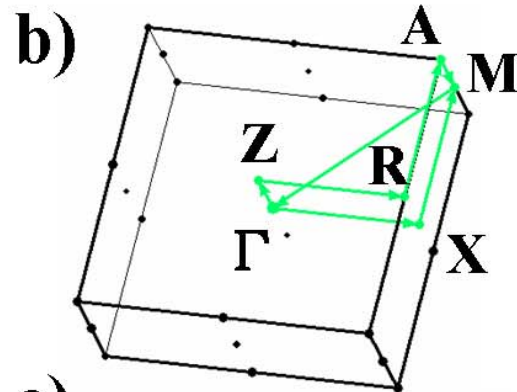
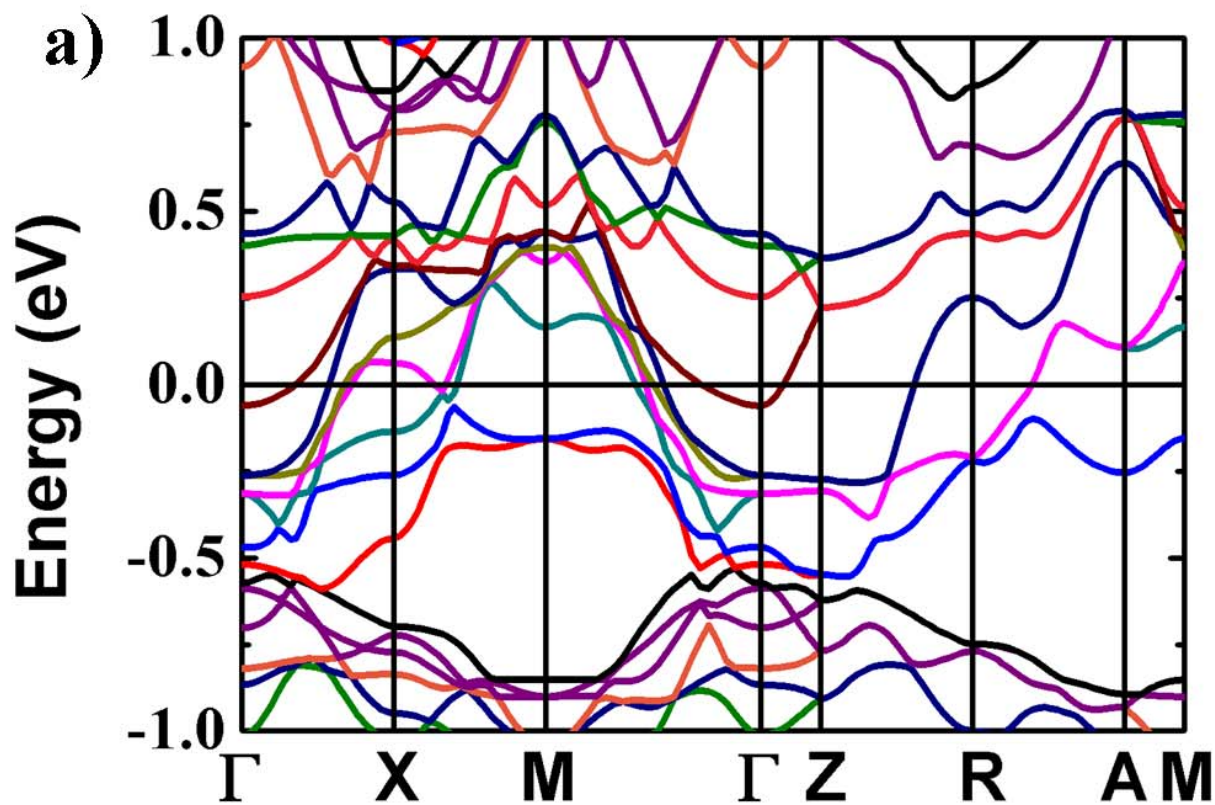
The small ellipsoidal Fermi surface near zone

$\sim (dz^2$ orbital FeAs-compounds) \rightarrow nz orbital (Te/Se)

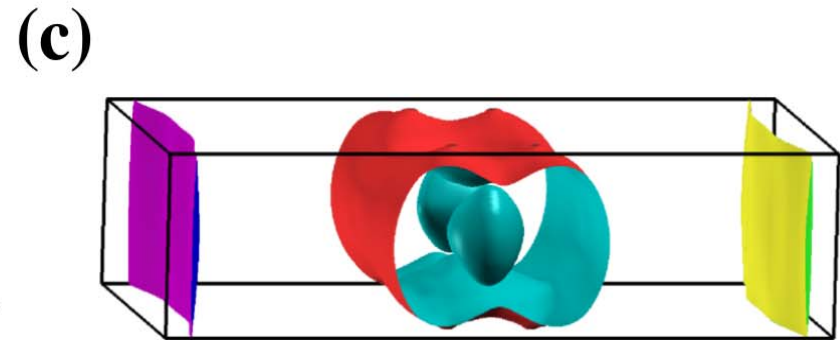
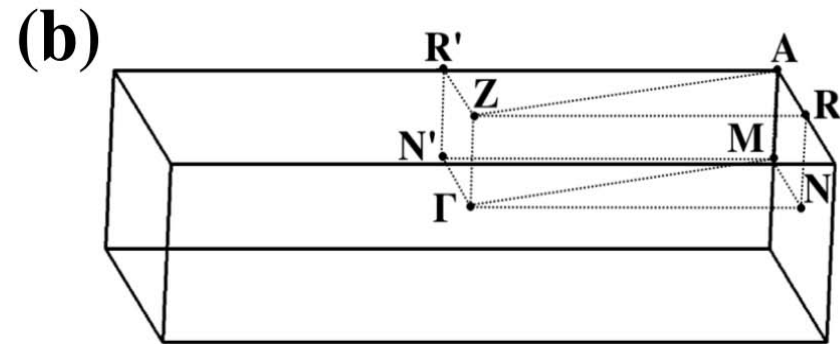
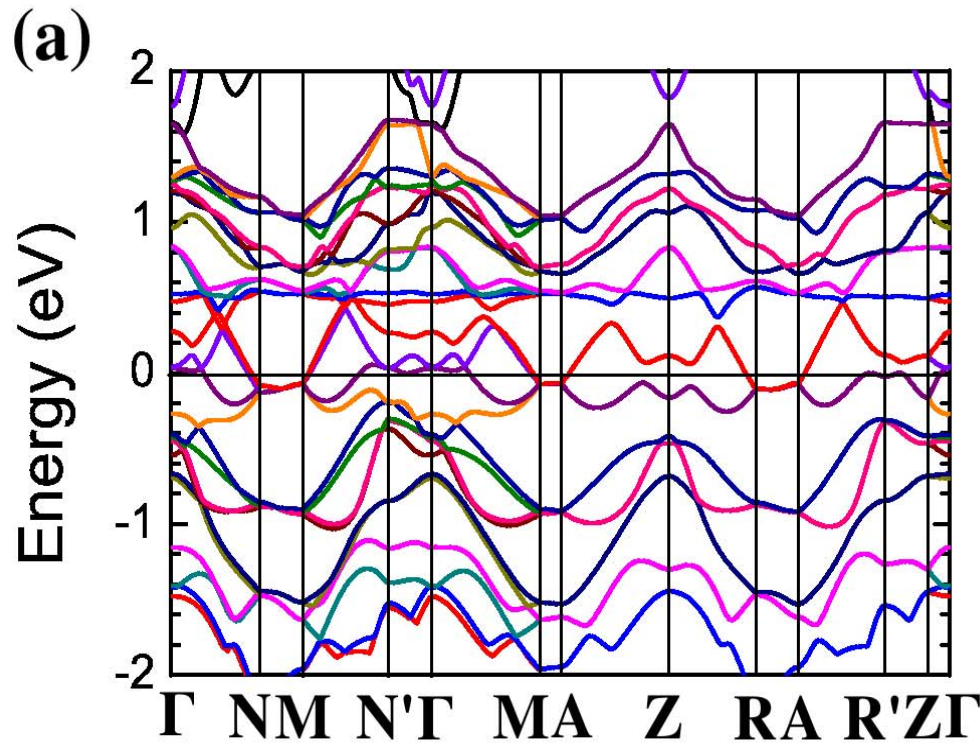
Nonmagnetic state for F-vacancies in rhombus-ordering



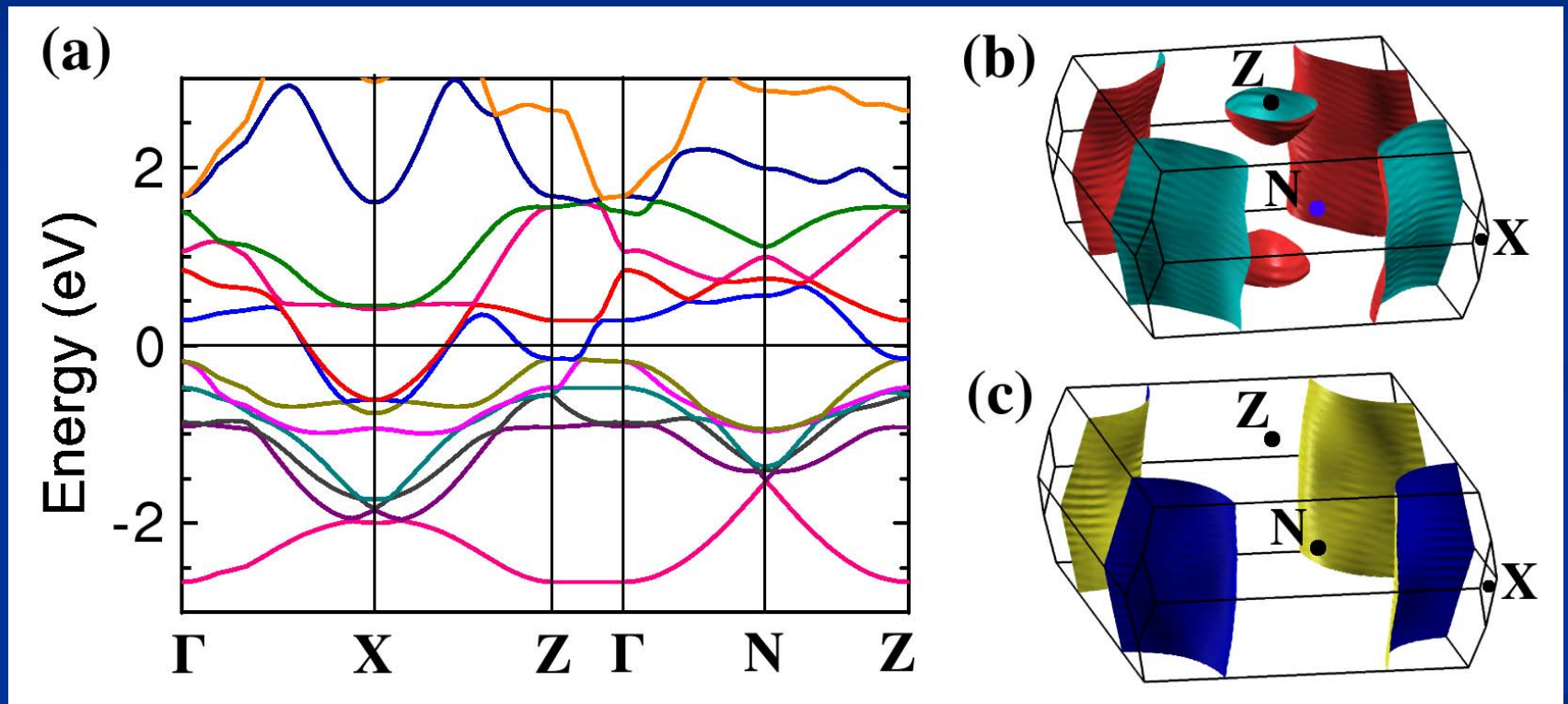
Nonmagnetic state for Fe-vacancies in square-ordering



The bi-collinear AFM of CsFe₂Se₂ in the ground state

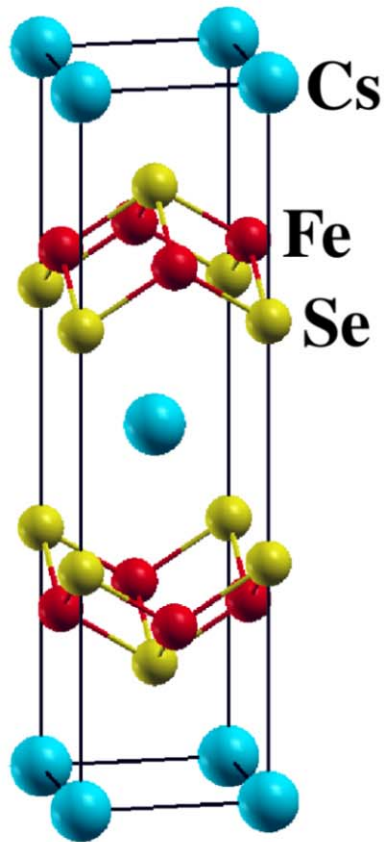


The nonmagnetic state of CsFe₂Se₂



$A\text{Fe}_2\text{Se}_2$ with ThCr_2Si_2 -type structure

(a)



(b)

